LACTOFERRIN ADSORBED ONTO BIOMIMETIC HYDROXYAPATITE: A MULTIFUNCTIONAL ANTIMICROBIAL MOLECULE

Andrea Fulgione

Dottorato in Scienze Biotecnologiche – XXVII° ciclo
Indirizzo Biotecnologie per le Produzioni Vegetali
Dottorato in Azienda
Università di Napoli Federico II

Dottorato in Scienze Biotecnologiche – XXVII° ciclo
Indirizzo Biotecnologie per le Produzioni Vegetali
Dottorato in Azienda
Università di Napoli Federico II

LACTOFERRIN ADSORBED ONTO BIOMIMETIC HYDROXYAPATITE: A MULTIFUNCTIONAL ANTIMICROBIAL MOLECULE

Andrea Fulgione

Dottorando: Andrea Fulgione

Relatore: Prof.ssa Rosanna Capparelli

Correlatore: Dott. Piero Porcaro

Coordinatore: Prof. Giovanni Sannia

Alla mia famiglia
che mi ha sostenuto e che ancora
mi sostiene durante il mio percorso di vita…

INDICE

RIASSUNTO	pag. 1
SUMMARY	pag. 7
STUDY DESIGN	pag. 8
INTRODUCTION	pag. 9
LACTOFERRIN	pag. 9
ANTIMICROBIAL ACTIVITY OF LACTOFERRIN	pag. 9
IMMUNOMODULATORY ACTIVITY OF LACTOFERRIN	pag. 10
ANTICARCINOGENIC ACTIVITY OF LACTOFERRIN	pag. 11
BIOMIMETIC HYDROXYAPATITE	pag. 12
BRIEF HISTORY OF FOOD PACKAGING	pag. 14
ANTIMICROBIALS USED IN FOOD PACKAGING	pag. 14
AIM OF THE PROJECT	pag. 17
MATERIALS AND METHODS	pag. 18
RESULTS	pag. 23
CONCLUSIONS	pag. 33
BIBLIOGRAPHY	pag. 34
PUBBLICATIONS	pag. 45
COMMUNICATIONS AND PATENT	pag. 45

RIASSUNTO

Lattoferrina

La lattoferrina (LF) è una proteina antimicrobica con un peso di circa 80 KDa, presente principalmente nel latte umano e bovino ma anche nei granuli dei neutrofili e nelle secrezioni mucose quali saliva, secrezioni nasali e bronchiali (Aisen P et al, 1972; Baker EN, 1994). E' una proteina pleiotropica che oltre alla ben documentata attività antimicrobica, mostra anche efficaci proprietà anti-infiammatoria, antiossidante ed anticarcinogenica (Baker EN, 1994; Duarte DC et al. 2011; Sato R et al. 1996). Inizialmente si pensava che l'attività antimicrobica di tale molecola fosse dovuta solo alla sua nota capacità di legare il ferro, uno dei nutrienti fondamentali per la crescita batterica ma, studi successivi hanno dimostrato che tale attività biologica dipende anche dalla carica positiva della lattoferrina che le consente di interagire con la membrana cellulare batterica - carica negativamente - determinando in tal modo la lisi della membrana stessa (Gonzalez-Chavez SA et al. 2009).

Riguardo l'attività anti-infiammatoria, diversi studi hanno evidenziato il coinvolgimento della lattoferrina nella risposta infiammatoria, mediante l'interazione della stessa con il lipopolisaccaride (LPS), componente della parete cellulare dei batteri Gram-negativi, considerato un comune agente infiammatorio. Normalmente LPS interagisce con LPS-binding protein (LBP) - proteina solubile presente nel plasma - e questo complesso LPS-LBP, mediante una serie di reazioni determina l'attivazione del fattore di trascrizione NF-kB che promuove la sintesi delle citochine pro-infiammatorie. La lattoferrina, dunque, compete con LPS-binding protein (LBP) per il legame con LPS, ostacolando cosi l'attivazione della trasduzione del segnale NF-kB, necessaria per la sintesi di citochine pro-infiammatorie e lo sviluppo, quindi, di uno stato infiammatorio (Ellison RT et al. 1988; Legrand D et al. 2005).

Studi clinici condotti nell'uomo hanno dimostrato che l'assunzione di lattoferrina può avere un effetto benefico sul decorso del cancro (Hayes TG et al. 2006). Successivi studi *in vitro* hanno evidenziato la capacità anti metastatica della lattoferrina che viene esplicata mediante le sue capacità di indurre l'apoptosi o di bloccare la transizione delle cellule tumorali dalla fase G1 ad S del loro ciclo cellulare. Inoltre è in grado, come durante l'infiammazione, di modulare la produzione di citochine nel cancro (Oztas ER et al. 2005; Varadhachary A et al. 2004; Iigo M et al. 2004; Crouch SPM et al. 1992).

Idrossiapatite

L'idrossiapatite (HA) è uno degli elementi costitutivi delle ossa, nelle quali si trova sotto forma di sali di Calcio: $CaCO_3$ (carbonato di calcio), $Ca_3(PO_4)_2$ (fosfato di calcio) e CaF_2 (fluoruro di calcio) (Clarke B, 2008). Alterazioni nel metabolismo dell'idrossiapatite possono comportare seri danni come la calcificazione delle arterie, malattia renale cronica oppure osteoporosi. Numerosi studi hanno dimostrato la capacità dell'idrossiapatite di integrarsi in strutture o supporti ossei senza subire danno o dissolversi, e questa caratteristica potrebbe renderla un valido veicolo di trasporto e rilascio di una molecola con una cinetica ben determinata (Fox K et al. 2012). Diverse ricerche hanno dimostrato la possibilità di sostituire alcuni ioni presenti nella struttura dell'idrossiapatite con altri in grado di modificare le proprietà della molecola (Thian ES et al. 2006; Porter AE et al. 2004; Patel N et al. 2002). Un esempio è rappresentato dall'idrossiapatite zinco sostituita in cui la sostituzione di parte del Calcio con lo Zinco ha determinato un significativo incremento dell' attività

antimicrobica della nuova molecola sintetizzata (Chen y et al. 2010; Rameshbabu N et al. 2007; Kim TN et al. 1998).
Inoltre è stato dimostrato che variando la concentrazione dei reagenti, la temperatura ed il tempo di reazione ed il pH, è possibile ottenere molecole di HA che presentano caratteristiche strutturali (dimensione, porosità, morfologia) e proprietà di legame differenti a seconda delle specifiche applicazioni per le quali vengono utilizzate (Walsh D et al. 2007; Villacampa A et al. 2000; Tanaka HK et al. 1989; Koutsopoulos S, 2002; Manara S et al. 2008; Palazzo B et al. 2007; Tampieri et al. 2005)
L'idrossiapatite, grazie alla elevata affinità con proteine ed altre molecole, viene impiegata anche in diversi sistemi cromatografici (Kandori K et al. 2000; Akawa T et al. 1999).
Diversi studi hanno dimostrato che la nanotecnologia può sensibilmente migliorare le risposte biologiche dell'idrossiapatite. Strutture di dimensioni minori presentano, rispetto a quelle di dimensioni maggiori, un elevato rapporto volume/superficie e, nella maggior parte dei casi, ottime capacità di interazione chimica con altre molecole. La presenza di molecole bioattive sulla superficie dei nanocristalli di HA biomimetica favorirebbe non solo i processi di osteointegrazione e/o osteoinduzione, ma stimolerebbe anche risposte cellulari specifiche (Kandori K et al. 2000; Jack KS et al. 2007).
Un'ulteriore studio ha dimostrato la stabilità dell'interazione tra i nanocristalli di idrossiapatite e la mioglobina o l'alendronato, evidenziando in tal modo la possibilità di utilizzare un biomateriale inorganico come supporto per molecole bioattive e farmaci. I materiali che presentano una composizione ed una struttura simile a quella dei sistemi biologici e che per questa peculiarità sono definiti biomimetici, sembrano funzionare principalmente come veicoli di trasporto per molecole (Roveri N et al. 2008).
L'idrossiapatite biomimetica utilizzata in questo studio risulta essere simile a quella presente nell'organismo e quindi, presenta ottime proprietà in termini di biocompatibilità, bioattività, osteoconduttività ed interazione diretta con il tessuto osseo (Roveri N and Palazzo B, 2006).

Food packaging
Il settore del food packaging può essere considerato un indicatore socio-economico della capacità di spesa di un paese e della disponibilità degli alimenti naturali rispetto a quelli trasformati (Wilson C, 2007). Le più significative innovazioni in tale settore sono avvenute tra la prima e la seconda guerra mondiale a causa della crescente esigenza di protezione dei beni militari e del cibo nelle zone di guerra.
Agli inizi del ventesimo secolo, le materie plastiche, polietilene e propilene hanno sostituito il metallo, il vetro e la carta impiegati fino a quel momento per il confezionamento e la conservazione degli alimenti. Il packaging ha il ruolo di proteggere l'alimento dalla contaminazione da parte di agenti patogeni e da fattori ambientali (ossigeno, umidità e calore), prolungando la shelf life del prodotto e preservando le caratteristiche nutrizionali ed organolettiche dello stesso. Il prolungamento della shelf life di un prodotto si ottiene mediante l'inibizione dell'attività antimicrobica ed enzimatica, il controllo della temperatura di conservazione, l'aggiunta si sostanze come sale e zucchero oppure la rimozione dell'ossigeno all'interno del sistema di confezionamento del prodotto.
Il packaging di un alimento, inoltre, fornisce informazioni in merito al prodotto che contiene come peso, indicazione di produzione, ingredienti utilizzati, e valore nutrizionale del prodotto stesso.

Nel passato i sistemi di confezionamento fungevano solo da barriere passive per la protezione dell'alimento dall'ambiente mentre il moderno sistema di "Active packaging" interagisce con l'alimento mediante il rilascio di composti ad azione antimicrobica o antiossidante (Brody A et al. 2001; Lopez-Rubio A et al. 2004).
Da diversi anni, l'utilizzo di molecole antimicrobiche nel settore alimentare si sta diffondendo sempre di più. Tali molecole antimicrobiche possono essere direttamente utilizzate come ingrediente nella produzione dell'alimento, oppure aggiunte direttamente sulla superficie dell'alimento o incorporate nel sistema di confezionamento. L'aggiunta della molecola antimicrobica all'alimento è in grado di controllare la proliferazione batterica per un breve periodo di tempo mentre l'incorporazione dell'antimicrobico nel packaging risulta garantire una protezione più duratura (Appendini P and Hotchkiss, 2002).
Esempi di molecole naturali ad attività antimicrobica sono: oli essenziali derivati da piante (ad esempio, basilico, timo, origano, cannella e rosmarino), enzimi ottenuti da animali (ad esempio, lisozima, lattoferrina), batteriocine prodotti da microbi (nisina), acidi organici (propionico, acido citrico) e polimeri naturali (chitosano) (Gutierrez J et al. 2009; Brewer R et al. 2012; Lopez-Pedemonte TJ et al. 2003, No HK et al. 2007).

SCOPO DELLA TESI

Lo scopo di questo progetto è stato la caratterizzazione biologica di un nuovo complesso molecolare, LF-HA, nato dalla combinazione della lattoferrina - proteina antimicrobica naturale -, con l'idrossiapatite biomimetica - biomateriale multifunzionale attualmente impiegato come riempitivo osseo ma che contemporaneamente potrebbe essere un valido veicolo di trasporto di una molecola. Appurate la stabilità e le proprietà biologiche della molecola, si è proceduto con l'applicazione della stessa in un sistema di confezionamento al fine di soddisfare due requisiti fondamentali:
- Sicurezza alimentare per la salvaguardia della salute umana;
- Prolungamento della shelf-life del prodotto stesso.

DISEGNO SPERIMENTALE

Lo studio è stato articolato in tre fasi:

- La prima fase, in collaborazione con il Prof. Norberto Roveri, Professore di Chimica Generale ed Inorganica presso l'Università di Bologna, ha interessato la sintesi del complesso molecolare LF-HA, le analisi spettrofotometriche e termogravimetriche per lo studio della stabilità della molecola prodotta ed infine la valutazione dell' attività antimicrobica della molecola contro alcuni dei principali patogeni alimentari (*Staphylococcus aureus*, *Listeria monocytogenes*, *Salmonella enterica* serovar Paratyphi B, *Escherichia coli*);

- La seconda fase, svolta in collaborazione con l'azienda, ha previsto lo svolgimento di ulteriori test *in vitro* che hanno consentito la stima di altre proprietà della molecola selezionata. E' stata, dapprima, valutata la citotossicità del complesso molecolare nei confronti di cellule eucariotiche (linea cellulare monocitica umanaTHP-1) mediante il test di vitalità cellulare, la determinazione della produzione di NO_2 e la determinazione dei livelli della lattato deidrogenasi (LDH). Successivamente sono state saggiate l'attività immunomodulatoria mediante la determinazione dei livelli

prodotti di alcune citochine (Tumor necrosis factor (TNF)-α, Interferone (IFN)-γ, Interleuchina (IL)-17, IL-8, IL-12, IL-6, IL-10,e IL-4) e l'attività antiossidante;

- L'ultima fase ha previsto l'impiego della molecola in un sistema di confezionamento quale la pellicola per alimenti. Dapprima sono state effettuate delle analisi microscopiche e spettrofotometriche per valutare l'effettiva deposizione della LF-HA sulla pellicola e, successivamente, mediante riscontro visivo è stata valutata la sua efficacia nel prolungare la shelf life dell'alimento selezionato.

RISULTATI

Lo studio è stato incentrato sulla caratterizzazione di un complesso molecolare LF-HA derivato dal legame di una proteina antimicrobica – lattoferrina – con un biomateriale che funge da agente veicolante - idrossiapatite biomimetica -.
L'idrossiapatite utilizzata in questo studio presenta caratteristiche (composizione, struttura, morfologia, dimensione) simili a quelle del tessuto osseo (Iafisco M et al. 2011).
La sintesi del complesso LF-HA è stata realizzata mediante solubilizzazione della lattoferrina nell'idrossiapatite biomimetica a temperatura ambiente.
Dall'analisi di adsorbimento condotta sulla molecola prodotta, è emersa l'elevata affinità iniziale della lattoferrina con l'idrossiapatite. Tale affinità è dovuta all'interazione della lattoferrina, carica positivamente, con le cariche negative dei nanocristalli di idrossiapatite. Le analisi termogravimetriche e la spettroscopia Raman hanno dimostrato la solidità del legame che si instaura tra la lattoferrina e l'idrossiapatite e la stabilità della struttura secondaria della lattoferrina legata, che risulta non significativamente modificata.
Successivamente si è proceduto con la caratterizzazione delle attività biologiche della molecola. Il test di attività antimicrobica contro alcuni dei principali patogeni alimentari (*Staphylococcus aureus*, *Listeria monocytogenes*, *Salmonella enterica* serovar Paratyphi B, *Escherichia coli*) ha evidenziato, a parità di concentrazione, una migliore performance della lattoferrina quando è legata all'idrossiapatite, rispetto a quando è nella forma nativa. Avendo il test di emolisi mostrato una attività emolitica della LF-HA alla concentrazione di 300 µg/mL pari al 10% e, presentando a tale concentrazione una capacità di inibizione della crescita batterica circa del 70%, si è deciso di considerare 300 µg/mL come concentrazione di LF-HA utile al controllo dei patogeni.
Il complesso LF-HA, nel range di concentrazioni testate, non risulta essere citotossico nei confronti di cellule THP-1, la cui vitalità non risulta essere compromessa fino a 72 h di incubazione delle stesse con la LF-HA. Gli ulteriori test condotti, inerenti la tossicità, hanno dimostrato che la molecola induce in cellule THP-1 una ridotta produzione di nitriti e di lattato deidrogenasi (LDH) - marker di danno tissutale- rispetto a quella provocata dalla stimolazione delle cellule con il lipopolisaccaride (LPS), comune agente infiammatorio. Inoltre dai test si è evinto che i livelli di nitriti ed LDH si riducono notevolmente in cellule THP-1 stimolate con LPS e poi trattate con LF-HA.
Ulteriore conferma della migliore performance della lattoferrina quando questa è legata all'idrossiapatite biomimetica deriva dal test dell'attività antiossidante; la molecola LF-HA ha mostrato un'attività antiossidante di circa otto volte maggiore rispetto alla sola lattoferrina.

Successivamente è stata saggiata l'attività immonomodulatoria della molecola. Tale analisi è stata condotta mediante la determinazione dei livelli di alcune citochine selezionate, prodotti da cellule THP-1 stimolate o non con il lipopolisaccaride (LPS) – comune agente infiammatorio-, trattate con LF-HA o Acido Acetilsalicilico (ASA) – farmaco anti-infiammatorio - oppure stimolate con LPS e trattate con LF-HA o con ASA.
Il trattamento delle cellule con LF-HA oppure ASA non ha indotto alcuna risposta infiammatoria mentre la stimolazione con LPS ha indotto una risposta infiammatoria che ha raggiunto il picco dopo 4 ore dalla stimolazione. In cellule stimulate con LPS e poi trattate con LF-HA o ASA, si verifica una riduzione delle citochine pro-infiammatorie ed un incremento della produzione di citochine anti-infiammatorie. E' possible quindi affermare che l'effetto della LF-HA è comparabile con quello dell'Acido Acetilsalicilico, comune agente anti-infiammatorio.
Terminata la valutazione delle numerose attività biologiche del complesso LF-HA si è proceduto con l'elettrodeposizione di quest'ultimo su una pellicola per alimenti. Prima di applicare tale pellicola sull'alimento, sono state condotte analisi spettrofotometriche che hanno confermato l'avvenuta elettrodeposizione del complesso molecolare sulla pellicola e la sua presenza sotto forma di coating omogeneo sulla pellicola stessa. Successivamente è stata effettuato il test per valutare se la molecola presente sulla pellicola fosse in grado di prolungare la shelf life del prodotto alimentare selezionato: una mela. I risultati, documentati fotograficamente, hanno dimostrato l'efficacia del sistema di active packaging trattato con la LF-HA rispetto a quello convenzionalmente utilizzato.

CONCLUSIONI

In seguito alla crescente richiesta da parte dei consumatori di alimenti naturali e sicuri, le autorità competenti e i ricercatori hanno indirizzato la loro attenzione verso l'individuazione di tecniche di conservazione più semplici per migliore la qualità e la sicurezza dell'alimento, preservandone al contempo le caratteristiche organolettiche e nutrizionale. In questo contesto, le molecole antimicrobiche naturali potrebbero essere uno strumento ideale per il raggiungimento di tale obiettivo date le loro caratteristiche biologiche ed il ridotto o inesistente effetto sulla salute umana (Kuorwel K et al. 2011). Le proteine antimicrobiche, da sole od opportunamente veicolate potrebbero essere un candidato ideale in quanto caratterizzate da un'efficace attività antimicrobica nei confronti di numerosi agenti patogeni, e dalla non significativa tossicità nei confronti delle cellule eucariotiche (Capparelli R et al. 2009).
Negli ultimi anni molti agenti antimicrobici naturali vengono impiegati nei sistemi di confezionamento dell'alimento o aggiunti all'alimento stesso come basilico, timo, origano e con le loro componenti principali linalolo, timolo e carvacrolo, rispettivamente, sono particolarmente adatti per essere utilizzati come conservanti negli alimenti e come potenziali alternative per gli additivi alimentari sintetici. La presenza di antimicrobici nel packaging dell'alimento oltre a prolungare la shelf life dell'alimento e quindi il decadimento qualitativo del prodotto, riducono al contempo l'insorgenza di malattie di origine alimentare associate alla contaminazione microbica (Brody AL et al. 2008). I progressi in diversi settori dell'industria alimentare, in particolare nel settore degli imballaggi, hanno portato ad un miglioramento della qualità e sicurezza degli alimenti. I nuovi progressi si sono per lo più concentrati sul controllo dell'ossidazione, della migrazione di umidità, della crescita microbica, e dei

sapori e aromi volatili (Lucera A et al. 2012). Lo studio condotto ha innanzitutto dimostrato che le attività antimicrobica ed antiossidante della lattoferrina risultano essere implementate quando la molecola è legata superficialmente ai nanocristalli di idrossiapatite. Inoltre assieme alle suddette proprietà la molecola è risultata non essere tossica nei confronti di cellule eucariotiche, ed ha mostrato anche un'efficace attività immonumodulatoria. L'applicazione di tale molecola su una pellicola per alimenti mediante elettrodeposizione ed il successivo utilizzo di tale pellicola per avvolgere e conservare delle fette di mela sbucciate ha consentito la valutazione dell'attività antiossidante della molecola nell'imballaggio preso in esame. I risultati hanno dimostrato che a parità di intervallo di tempo, la pellicola trattata con la LF-HA ha protetto l'alimento meglio di quella non trattata. In conclusione le caratteristiche di questa pellicola sono: rivestimento uniforme con LF-HA ottenuto mediante metodo di elettrodeposizione; conservabilità della pellicola trattata per almeno sei mesi a temperatura ambiente; stabile al congelamento.

SUMMARY

Lactoferrin (LF) is an iron-binding protein, belonging to transferrin family. It is found in the mucosal secretions (tears, saliva, milk, and colostrums) of the majority of mammalian species, including humans. LF is a multitask molecule: it partecipates to iron absorption and distribution, but also displays anti-inflammatory, antioxidant, anticarcinogenic, and antimicrobial properties.
Hydroxyapatite (HA) plays an important role in the formation of the bony skeleton and bone remodeling. Alteration of HA metabolism can cause serious clinical consequences, such as arterial calcification, chronic kidney disease or osteoporosis.
HA is also used in numerous bioengineering and biomedical applications - due to its bioactivity and osteoconductivity – and also as vehicle for drug targeting, bone scaffolds and implant coating materials, filler in polymeric matrices.
In this project, the biological properties (such as antimicrobial, immunomodulatory and antioxidant activities) of lactoferrin adsorbed onto biomimetic hydroxyapatatite nanocrystals (LF-HA) were evaluated. After the biological characterization, the complex LF-HA was embedded in an active packaging system (on a cling film) - by electrodeposition - to estimate the antioxidant property of this active packaging system.
Packaging protects food from external pathogen contamination and environmental factors (oxygen, moisture and heat), providing longer product shelf life and avoiding the quality decay. Shelf life prolongation is possible by controlling enzymatic and microbial activities through the control of temperature, addition of salt, or by removing oxygen. In recent years, foods preserved with natural additives have become very popular due to the great consumer awareness and concern regarding synthetic chemical additives.
The tests carried out showed the antimicrobial and antioxidant efficacy of LF-HA versus the lactoferrin alone, when tested at the same concentrations, and the effectiveness of this molecule embedded in a food packaging system.
The results obtained permit to conclude that the chemical manipulation of the lactoferrin with hydroxyapatite nanocrystals significantly improved the antimicrobial and antioxidant activities of the native molecule. The main characteristics of the food packaging system obtained by electrodeposition of LF-HA on cling film are: uniform coating with LF-HA obtained throughout a new method of electrodeposition; long lasting stability, when stored for six months or longer at room temperature before being used to protect the food; stable to deep freezing, for six months or more.

STUDY DESIGN

Lactoferrin (LF) is the most abundant naturally antimicrobial protein, more abundant than lysozyme, and it exerts its antimicrobial activity by sequestrating iron, a nutrient essential for pathogens.
Hydroxyapatite (HA) plays an important role in the formation of the bony skeleton and bone remodeling and it is used as vehicle for drug targeting, bone scaffolds and implant coating materials, filler in polymeric matrices.
The present study describes the efficacy of lactoferrin adsorbed on biomimetic hydroxyapatite nanoparticles and it use in a food packaging system. The feasibility of the project required extensive tests. In these tests the antimicrobial and antioxidant activities of the soluble form of lactoferrin were compared with those of the lactoferrin adsorbed onto biomimetic hydroxyapatatite nanocrystal (LF-HA) and embedded in a food packaging system. The antimicrobial activity was tested against several common foodborn pathogens (*Staphylococcus aureus, Listeria monocytogenes, Salmonella enterica* serovar Paratyphi B*, Escherichia coli*).
Innovation in food packaging is driven by the rapidity with which food preparation from fresh ingredients needs to be carried out; the growing demand for ready-to-eat fresh food products; globalization of food trade and the increasing request of consumers for use of naturally available antimicrobial molecules as food additivies.
All the tests carried out led to the conclusion that the chemical manipulation of the lactoferrin with hydroxyapatite nanocrystals significantly improved the antimicrobial and antioxidant activities of the native molecule.

INTRODUCTION

LACTOFERRIN

Lactoferrin (LF), first described almost 50 years ago, is an iron-binding protein. It is a member of the transferrin family, along with serum transferrin and ovotransferrin. The function of these proteins is to transfer iron and inhibit carbonic anhydrate. LF is produced by mucosal epithelial cells. It is found in the mucosal secretions (tears, saliva, milk, and colostrum) of the majority of mammalian species, including humans. It is the most abundant antimicrobial proteins; more abundant than lysozyme. The important characteristics of the molecule are the high iron-binding affinity, the ability to retain it over a wide pH range, and resistance to proteolysis (Aiden et al. 1972; Baker EN, 1994). LF is a multitask molecule: it participates to iron absorption and distribution, but also displays anti-inflammatory, antioxidant, anticarcinogenic, and antimicrobial properties (Baker EN, 1994; Rodriguez DA et al. 2005; Duarte DC et al. 2011; Drago SME, 2006; Marchetti M et al. 1999; Sato R et al. 1996). The antimicrobial activity of LF is due to its property to sequestrate iron at the site of infection and depriving microorganisms of this nutrient. In addition, the positively charged amino acids of the LF can bind to the anionic molecules of several pathogens (virus, fungi, and bacteria), causing cell lysis. Given the pharmaceutical and nutritional (nutraceutical) importance of LF, several purification methods of this protein have been developed. At present, LF is commercially purified from milk or colostrums from several domesticated mammalian species, bacterial expression systems, and transgenic plants and animals (Gonzalez-Chavez SA et al. 2009).

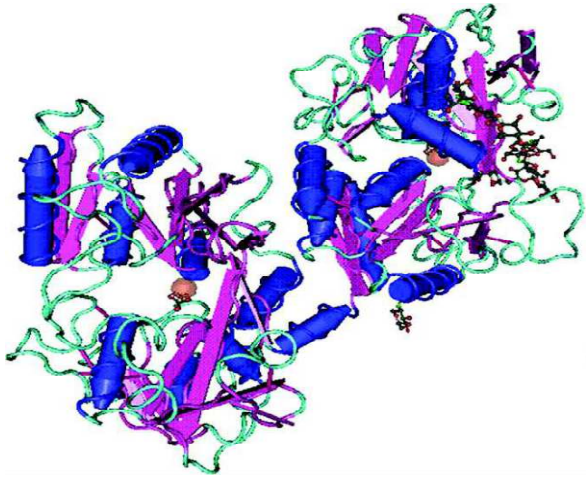

Figure 1: Three-dimensional structure of biferric bovine lactoferrin (Gonzalez-Chavez SA et al. 2009).

ANTIMICROBIAL ACTIVITY OF LACTOFERRIN

LF is active against Gram-positive and Gram-negative bacteria (Gonzalez-Chavez et al. 2009). LF is active also against strains resistant to antimicrobials (strains of *Staphylococcus aureus*, *Listeria monocytogenes*, methicillin-resistant *Klebsiella pneumoniae* and *Mycobacterium*). LF, by sequestering the iron, inhibits the bacterial growth. In addition, LF damages the external membrane of Gram-negative bacteria through an interaction with lipopolysaccharide (LPS). This interaction between LF and LPS potentiates the production of lysozyme (Ellison RT et al. 1988). *In vitro* and *in vivo* studies have shown that LF has the ability to prevent the attachment of certain bacteria to the host cell. The attachment-inhibiting mechanisms are unknown, but it

has been suggested that L-glycans bind bacterial adhesins, preventing their interaction with host cell receptors (Roseanu A et al. 2010; Wakabayashi H and Kondo I, 2010). *Pseudomonas aeruginosa* biofilm occurs frequently in in patients suffering from cystic fibrosis. Through biofilm formation, bacteria become highly resistant to host cell defence mechanisms and antibiotic treatment (Odeh R and Quinn JP, 2000; Singh PK et al. 2002; Caraher EM et al. 2007). Biofilm formation requires high levels of iron. There is evidence that LF , by chelating iron, effectively inhibit biofilm formation (Leitch EC and Willcox MD, 1999; Weinberg ED, 2004).
LF possesses antiviral activity against a broad range of viruses - RNA and DNA viruses - with and without envelope - that infect humans and animals (Van Der Strate BWA et al. 2001). LF inhibits the virus–host interaction of: the herpes simplex virus (HSV) (Andersen JH et al. 2004; Hasegawa K et al. 1994); the intracellular virus trafficking of the hepatitis B virus (HBV) (Marr AK et al. 2009; Hara K. Et al. 2002; Viani RM et al. 1999) and human cytomegalovirus (HCMV) (Beljaars L et al. 2004; Andersen JH et al. 2001). The LF can also bind directly to the hepatitis C virus (HCV) (Ikeda M et al. 1998; Ikeda M et al. 2000), feline herpes virus (FHV-1) (Sato R et al. 1996), and hepatitis G virus (HGV) (Beaumont SL et al. 2003). *In vitro* studies show that LF exerts a strong activity against HIV binding to three of the many co-receptors of HIV (Legrand D et al. 2004) and the DC-SIGN receptor (Groot F et al. 2005).

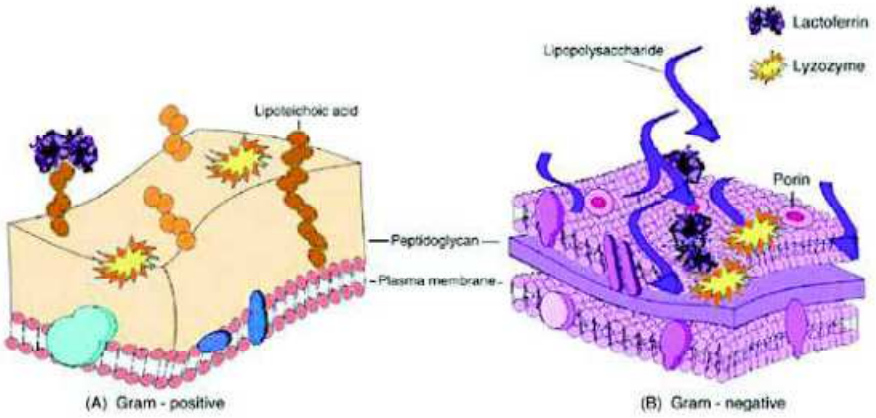

Figure 2: Mechanism of antibacterial action of lactoferrin (LF) against **(A)** Gram-positive and **(B)** Gram-negative bacteria (Gonzalez-Chavez SA et al. 2009).

IMMUNOMODULATORY ACTIVITY OF LACTOFERRIN

LF displays immunological properties that influence both innate and acquired immunities (Legrand D et al. 2006). Its relationship with the immune system is evident from the fact that people with congenital or acquired LF deficiency have recurring infections (Breton-Gorius J et al. 1980). Oral administration of LF seems to influence mucosal and systemic immune responses in mice (Sfeir RM et al. 2004). LF can modulate both specific and non-specific expression of antimicrobial proteins, pattern recognition receptors and lymphocyte movement related proteins (Wakabayashi H et al. 2006). The role that LF plays in regulating innate immune responses confirms its importance as a first line host defence mechanism against invading pathogens modulating both acute and chronic inflammation (Kruzel ML et al. 2002; Kruzel ML et al. 2006; Legrand D et al. 2005; Kane SV et al. 2003). Most intriguing is the ability of LF to induce mediators from innate immune cells that

subsequently affect the adaptive immune cell function. The positive charge of LF allows it to bind to negatively charged molecules on the surface of various cells of the immune system (Baker EN, 2005); this association can trigger signalling pathways that lead to cellular responses such as activation, differentiation and proliferation. LF can enter into the nucleus, where it can bind DNA (Swart PJ et al. 1996; Bennet RM and Davis J, 1982) and activate different signalling pathways (Oztas Yesim ER and Ozgunes N, 2005).In addition to inducing systemic immunity, LF can promote skin immunity and inhibit allergic responses. It activates the immune system against skin allergens, causing dose-dependent inhibition of Langerhans cell migration and the accumulation of dendritic cells in lymph nodes (Van Der Strate BWA et al. 2001). Leukocytes exposed to LF modulate pro-inflammatory cytokine production. Also, LF can increase - as well as decrease - TNF-α, IL-6, and IL-1β production (Kruzel ML et al. 2002; Sorimachi K et al. 1997; Zimecki M et al. 2001; Machnicki M et al. 1993; Zimecki M et al. 1999; Zimecki et al. 2003). Production of these factors is dependent upon the type of signal recognized by the immune system. At the cellular level, LF increases the number of natural killer (NK) and of CD4+ or CD8+ T cells (Haversen L et al. 2002), boosts the recruitment of polymorph nuclear cells (PMNs) in the blood (Shimuzu K et al. 1996), induces phagocytosis (Kurose I et al. 1994), and can modulate the myelopoietic process (Szuter CA et al. 1995). It is well documented that IL-12 plays an important role in driving development of helper T-cell type 1 immunity (Trinchieri G, 2003; Trinchieri G, 1995). Therefore, the role of LF in the regulation of proinflammatory cytokines and IL-12 clearly demonstrates communication between innate and adaptive immune responses.

ANTICARCINOGENIC ACTIVITY OF LACTOFERRIN

Human clinical studies show that ingestion of LF can have a beneficial effect against progression of cancer (Hayes TG et al. 2006). LF possesses anti metastatic effects and inhibits the growth of transplanted tumours (Varadhachary A et al. 2004; Iigo M et al. 2004). Similar to its role in inflammation, LF has the ability to modulate the production of cytokines in cancer. LF can induce apoptosis and arrest tumour growth in vitro; it can also block the transition from G1 to S in the cell cycle of malignant cells (Oztas Yesim ER and Ozgunes N, 2005; Crouch SPM et al. 1992). Additionally, treatment of tumours in mice with recombinant human LF (rhLF) inhibits their growth, increases the levels of anti carcinogenic cytokines such as IL-18, and activates NK cells and CD8+ T lymphocytes (Wanh WP et al. 2000; Shimamura m et al. 2004). Interestingly, human LF (hLF) and bovine LF (bLF) exert opposite effects on angiogenesis. Whereas orally administrated bovine LF inhibits angiogenesis in rats (Shimamura M et al. 2004; Norrby K et al. 2001) and tumour-induced angiogenesis in mice (Shimamura M et al. 2004), hLF exerts a specific pro-angiogenic effect (Kozu T et al. 2009). Recently, clinical trials have shown that bLF can reduce the risk of colorectal cancer (Nakajima K et al. 2001). Increasing evidence suggests that inhibition of the Akt signalling pathway might be a promising strategy for cancer treatment (Xu XX et al. 2010). In breast cancer, LF is able to limit the growth of tumour cells, and addition of exogenous LF to the culture media of breast cancer cell lines (MDA-MB-231) induced cell cycle arrest at the G1/S transition (Damiens E et al. 1999). Additionally, LF induced growth arrest and nuclear accumulation of Smad-2 in HeLa cells (Zemann N et al. 2010). The ability of bovine Lfc to induce apoptosis in THP-1 human monocytic leukemic cells has also been demonstrated (Yoo YC et al. 1997). Although the results achieved by several researchers point to a clear anti-

tumour role for LF, the mechanisms by which it exerts these effects are not fully understood. Thus, further work on this subject is required.

BIOMIMETIC HYDROXYAPATITE

During development, hydroxyapatite (HA) plays an important role in the formation of the bony skeleton and during adult life in bone remodeling (Clarke B, 2008). Alteration of HA metabolism can lead to serious clinical consequences, such as arterial calcification, chronic kidney disease or osteoporosis (Zhu D et al. 2012, Hofbauer LC et al. 2007).

Apart from its importance in normal and pathological biological processes, HA is also finding increasing use in numerous bioengineering and biomedical applications due to its bioactivity and osteoconductivity (De Groot K and Wolke J, 1998). HA is being explored as vehicle for drug targeting, transfection, bone scaffolds and implant coating materials (Uskokovic V and Uskokovic DP, 2011; Dorozhkin SV, 2012; Fox K et al. 2012), filler in polymeric matrices and self-setting bone cements (Fox K et al. 2012).

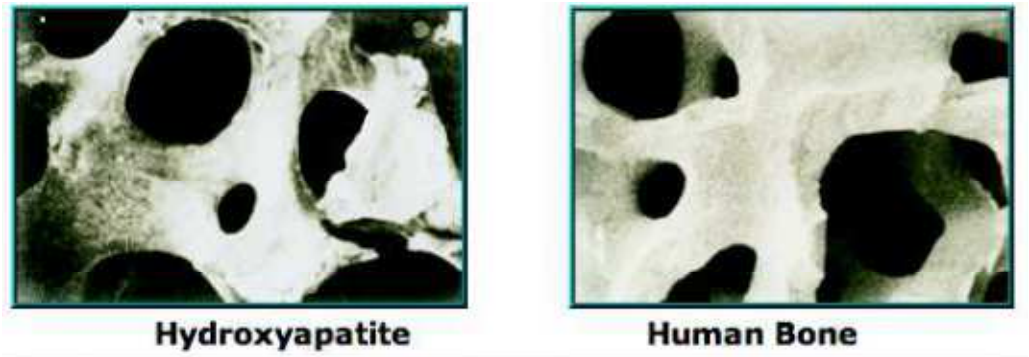

Figure 3: Image of Hydroxyapatite and Human Bone structure (http://www.muetingmedia.com/Kolberg_Ocular_Products/ocular_implants-2.html).

However, HA has the disadvantage of an extremely slow rate of bone bonding (Oonishi H et al. 1999). Furthermore, HA does not inhibit bacteria from adhering onto the bone surface, delaying the bone healing process or, worse, infection and failure of surgical operation (Darouiche RO, 2004). An alternative way to enhance bone fixation and reduce infection rate is to incorporate bone morphogenetic proteins and antibiotics into HA.

Hydroxyapatite has a crystallographic and chemical composition approaching that of the natural bone mineral (Oonishi H, 1991) and can easily accommodate substitutions by various beneficial ions. As such, there has been an increasing research interest concerning the effects of these ion substitutions. A number of studies introducing silicon-substituted HA have been reported in the literature, and this biomaterial has shown to enhance the rate and quality of bone tissue repair (Thian ES et al. 2006; Porter AE et al. 2004; Patel N et al. 2002). On the other hand, silver-substituted HA - synthesized by various groups – has been shown to reduce bacterial adhesion (Chen Y et al. 2010; Rameshbabu N et al. 2007; Kim TN et al. 1998). Though each of these ions has shown to play a significant role in the bone healing process, it is rational to synthesize a HA that exhibits enhanced bioactivity and, at the same time, possesses antibacterial property.

It is well known that HA also shows a high affinity for proteins and a wide variety of biological molecules. For example, HA is widely used for the separation of various proteins in high performance liquid chromatography systems (Kandori K et al. 2000; Akawa T et al. 1999). The interaction between proteins and different kinds of inorganic surfaces, like HA nanocrystals, carbonates and phosphate, plays an important role in many applications - including medicine, pharmacy, nanodevices, biosensors, and bioengineering (latour RA, 2008; Dee KC et al. 2003). The interaction of HA nanocrystals with myoglobin or alendronate bioconjugates indicates the possibility to use an inorganic biomaterial as a carrier for bioactive molecules and drugs. Biomimetic materials appear to function mainly as drug delivery agents (Roveri N et al. 2008). Ideal drug delivery systems should control the rate and time of release of drugs in specific conditions through the chemical–physical characteristics of the carrier material (Park K, 2007).

Designing bio-inspired materials represents a promising way for technological innovations in biomimetic materials. This approach in fact optimizes the interface between bio-inspired material and biological tissues and the release of bioactive molecules according to a tailored kinetic (Mann S, 1997; Sarikaya M and Aksay I,1995; Bensatude VB et al. 2002; Sanchez C et al. 2005; Tamerler C and Sarikaya M, 2007; Weirner S and Addadi L, 1997; Sarikaya M et al. 2003).

Chemists, biologists, physicists and engineers interested in material science are amazed to the high degree of sophistication, hierarchical organization, and adaptability that characterize natural materials. These properties - which biogenic materials have achieved through specific building principles selected by evolution - can only be possessed partially in man-made materials by present synthetic processes. Biomimetism represent important tools for the design and synthesis of innovative materials and devices (Mann S, 1997; Sarikaya M and Aksay I,1995; Bensatude VB et al. 2002; Sanchez C et al. 2005), which offer a unique approach to overcome many shortcomings in materials science (Molle P et al. 2005).

Synthetic biomimetic hydroxyapatite exhibits good properties as a biomaterial, in terms of biocompatibility, bioactivity, osteoconductivity, direct bonding to bone. Exciting applications of HA in the fields of bone tissue engineering and orthopedic therapies have already been achieved (Roveri N and Palazzo B, 2006). There are many synthetic strategies to produce HA and substituted HA, which include wet producing or hydrothermal, electrochemical and ultrasonic mobilization methods. HA with different stoichiometries and morphologies have been prepared and the effects of different synthesis conditions have been studied. The effects of varying the concentration of the reagents, the reaction temperature and time, initial pH, ageing time and the atmosphere within the reaction vessel have also been considered (Walsh D et al. 2007; Villacampa A and Garcia-Ruiz CM, 2000; Tanaka HK et al. 1989; Koutsopoulous S, 2002; Manara S et al. 2008). Dimension, porosity, morphology and surface properties are the characteristics that need to be optimized in order to adapt biomimetic HA to a specific application (Tampieri A et al. 2005; Barroug A et al. 2003). There is evidence that nanotechnology can sensibly improve the biological responses of HA. Today HA nanocrystals are constituents of bone, improving the biomaterial–bone interface. Nanostructured biomimetic materials offer much higher performances than their larger particle-sized counterparts, due to their larger surface - volume ratio and unusual chemical/electronic synergistic effects. In addition, the property of these materials to adsorb molecules on their surfaces has led to applications in affinity chromatography (Akawa T et al. 1999), waste-water remediation (Molle P et al. 2005) and drug delivery systems (Barroug A et al. 2003).

The presence of bioactive molecules on the surface of biomimetic HA nanocrystals makes them able to transfer information and selectively influence the biological environment. At present this approach represents a main challenge for innovative bone substitute materials. In this way, HA nanocrystals will not only guarantee, for instance, osteo-integration or osteo-induction enhanced properties, but also stimulate specific cellular responses at the molecular level (Kandori k et al. 2000; Jack KS et al.2007).

BRIEF HISTORY OF FOOD PACKAGING

Food packaging comprises about 65% of the $130 billion value of packaging in the United States (Brody A, 2008). At present, the value of food packaging is a valid socio-economic indicator of the country's spending ability and of the rural versus urban food availability.

This paragraph is a brief account of the innovations in food packaging. The activity in this field started in the 9th century, when the principles of bacteriology were extended to the canning process (Wilson C, 2007). However, the most significant innovations took place between the first and second world wars, under the pressure of protecting military goods and foods from extreme conditions in war zones. Aseptic packaging, cellophane, aluminum foil, modified atmosphere packaging were invented at this time. The invention of metal cans in the 1960s brought to the exponential growth of canned carbonated beverages and beer. The development of plastics, polyethylene and propylene brought to the rapid replacement of metal, glass and paperboard packaging with these new materials. More recent application - nanotechnology and sensing technologies - reflect the needs of food services and fast food transportation.

Packaging protects food from external pathogen contamination and environmental factors (oxygen, moisture and heat), extending shelf life of packaged food and preserving its initial qualities. Shelf life prolongation is attained by retarding enzymatic and microbial activity through the control of temperature, moisture, addition of salt, sugar, or by removing oxygen. A combination of two or more of these factors is also frequently used. Another major function of packaging is to provide information about weight, source, ingredients and nutritional value of the packed food.

Traditional food packages are passive barriers designed to delay the environmental adverse effects on the product. Active packaging, instead, interacts with food and the environment (Brody A et al. 2001; Lopez-Rubio A et al. 2004). Active packaging technology includes drip-absorbing pad (highly successful in poultry industry) and the selective permeation of package materials to various gases. Through coating, micro perforation, or polymer manipulation, selective permeation modifies the atmospheric concentration of gaseous compounds inside a package. Nanotechnology, acting by different means, prevents oxygen, carbon dioxide, and moisture from reaching food. Intelligent or smart packaging is intended to inform about food quality (storage temperature, food ripeness), origin and traceability (biosensors and radio frequency) (Brody A et al. 2001; Kerry JP et al. 2006). These smart devices are incorporated in package materials or attached to the inside or outside of a package.

ANTIMICROBIALS USED IN FOOD PACKAGING

The demand for minimally processed, easily prepared, and ready-to-eat fresh food products, globalization of food trade, and distribution from centralized processing place pose major challenges for food safety and quality. Food products can be subjected to contamination by bacteria and fungi. Microbial growth is a major concern

because some microorganisms (*Listeria monocytogenes, Escherichia coli* O157, *Salmonella, Campylobacter, Clostridium perfringens, Aspergillus niger*) can potentially cause foodborne illness. To prevent growth of pathogenic microorganisms in foods, heat treatment, salting, acidification, and drying have all been used in the food industry (Davidson PM and Taylor MT,2007; Farkas J, 2007). In recent years, because of the great consumer awareness and concern regarding synthetic chemical additives, foods preserved with natural additives have become very popular. To inhibit growth of undesirable microorganisms, the antimicrobials can be directly added into the product formulation, coated on its surface or incorporated into the packaging material. Direct incorporation of active agents into food results in an immediate but short-term reduction of bacterial populations, while the antimicrobial films can maintain their activity for a long period of time (Appendini P and Hotchkiss JH). Main natural compounds are essential oils derived from plants (e.g., basil, thyme, oregano, cinnamon, and rosemary), enzymes obtained from animals sources (e.g., lysozyme, lactoferrin), bacteriocins from microbial sources (nisin), organic acids (propionic, or citric acid) and naturally occurring polymers (chitosan). In this context, plant essential oils are gaining a wide interest in food industry for their potential as decontaminating agents, as they are Generally Recognized as Safe (GRAS).The active components are commonly found in the essential oil fractions and it is well established that most of them have a wide spectrum of antimicrobial activity against food-borne pathogens (Gutierrez J et al. 2008; Gutierrez J et al.2009). The antimicrobial activity of plant essential oils is due to the presence of phenolic functional groups, such as hydroxyl groups (Dorman HJD). Usually, the compounds with groups as oils of clove, oregano, rosemary, thyme, sage, and vanillin are the most effective (Skandamis PN and Nyachas GJE, 2002).

They are more inhibitory agents against Gram-positive than Gram-negative bacteria (Mangena T and Muyima NYO, 1999; Marino M et al. 2001). The use of bacteriocin producing lactic acid bacteria or their more or less purified bacteriocins has been also receiving increased interest. Bacteriocins are small bacterial peptides that show strong antimicrobial activity against closely related bacteria. Nisin is a polypeptide produced by *Lactococcus lactis* spp, approved as a food additive with GRAS status in over 50 countries worldwide. It has a relatively broad spectrum of activity against various lactic acid bacteria and other Gram-positive bacteria. Moreover, it is particularly effective against heat-resistant bacterial spores of *Clostridium botulinum* and against food-borne pathogens such as *L. mococytogenes, S. aureus,* or *B. Cereus* (Brewer R et al. 2002; Lopez-Pedemonte TJ et al. 2003; Sobrino-Lopez and Martin-Belloso O, 2006). Use of nisin in conjunction with ethylene- diaminetetra-acetic acid (EDTA) may increase the effectiveness. Moreover, the effect of nisin can be enhanced by using exposure to chelating agents, osmotic shock and freezing, because these treatments make the cell wall of Gram-negative microorganisms more permeable and therefore more susceptible to the nisin (Galvez A et al. 2007).

The enzymes represent another group of natural compounds that found application in food as valid preservatives. Lysozyme for example, is a lytic enzyme found in foods, such as milk and eggs. Lysozyme can hydrolyze β-1,4linkages between N-acetyl muramic acid and N-acetylglucosamine (Cunningham FE et al. 1991). Commercially, lysozyme has been used primarily to prevent late blowing in semi-hard cheeses, caused by *Clostridium tyrobutyricum*. It is well known that lysozyme is bactericidal against Gram-positive bacteria, whereas it is essentially ineffective against Gram-negative bacteria, owing to the presence of a lipopolysaccharide layer in the outer membrane. It has been recognized since the1960's that susceptibility of Gram-

negative bacteria to lysis by lysozyme can be increased by the use of membrane disrupting agents, such as detergents and chelators (EDTA) (Vaara M et al. 1992; Shelef L and Seiter J, 1993; Branen JK and Davidson PM, 2004). Organic acids and their salts are widely used as chemical antimicrobial agents because their efficacy is generally well understood and cost effective. The most effective organic compounds are acetic, lactic, propionic, sorbic, and benzoic acids. Their antimicrobial effect is based on the increase in proton concentration thereby lowering the external pH. Organic acids may affect the integrity of microbial cell membrane or cell macromolecules or interfere with nutrient transport and energy metabolism, causing bactericidal effect (Ricke SC, 2003). Among the natural antimicrobials, chitosan also received considerable interest for commercial applications. It has been used in medical, food, agricultural, and chemical industry, mainly due to its high biodegradability and antimicrobial properties. The biological activity of chitosan depends on its molecular weight, the degree of deacetylation and derivatization, such as degree of substitution, length, and position of a substitute in glucosamine units of chitosan, pH of chitosan solution and the target organisms (No HK et al. 2007). It is commercially produced from crab and shrimp shell wastes, with different deacetylation grades and molecular weights and, hence, it possess different functional properties, like emulsification ability, dye binding, and gelatine. Chitosan has also been documented to possess a film-forming property for use as edible film or coating, to decrease water vapor and oxygen transmission, diminish respiration rate and increase shelf life of fruit (Jiang Y and Li Y, 2001).

AIM OF THE PROJECT

In this study, lactoferrin (LF), the most abundant naturally antimicrobial protein, was adsorbed onto hydroxyapatite nanocrystals (HA), forming a new molecular complex called LF-HA.
The aim of the project was assessing the biological properties (such as antimicrobial, immunomodulatory and antioxidant activities) of LF-HA, and the efficacy of this molecule - embedded in a food package system - to extend the shelf life of packaged food, maintaining the food safety and quality properties.
Food packaging plays a crucial role in preserving the quality and safety of food during distribution and storage from farm to fork.

MATERIALS AND METHODS

Preparation of biomimetic hydroxyapatite nanocrystals

Biomimetic hydroxyapatite (HA) [$Ca_5(PO_4)_3(OH)$] nanocrystals were synthesized according to a previously reported method (Palazzo b et al. 2009). HA nanocrystals were precipitated from an aqueous solution of $(CH_3COO)_2Ca$ by slow addition (one drop per second) of an aqueous solution of H_3PO_4, keeping the pH constant at 10 by addition of $(NH_4)OH$ solution. The reaction mixture was stirred at 37°C for 24 h, then stirring was suspended and the mixture was left standing for 2 h to allow deposition of the inorganic phase. This was isolated by filtration of the mother liquor, repeatedly washed with water and freeze-dried at -60 °C under vacuum (3 mbar) for 12 hours. To produce apatites with stoichiometric Ca/P ratio (1.67), the $Ca(CH_3COO)_2$ suspension and the H_3PO_4 solution used were 83 and 50 mM, respectively.

Transmission electron microscopy

Transmission electron microscopy (TEM) investigations were carried out using a 1200 EX microscope fitted with link elemental dispersive X-ray analysis detectors and a 3010 UHR operating at 300 kV (JEOL Ltd, Tokyo, Japan). The powdered samples were ultrasonically dispersed in ultrapure water and a few droplets of the slurry were then deposited on perforated carbon foils supported on conventional copper microgrids.

Zeta potential analysis

Electrophoretic determinations were performed by a Coulter DELSA apparatus. A Coulter Delsa 440 instrument measured the electrophoretic velocities of suspended particles by measuring the Doppler shift of scattered laser light simultaneously at four different scattering angles: 7.5, 15.0, 22.5 and 30.0. The suspensions of modified HA were prepared as follows: 0.05 g $l^{-1}$of functionalized HA in 10^{-2} M KNO_3 (constant ionic strength), at spontaneous constant pH.

Determination of specific surface area

Measurements were done using a Sorpty 1750 instrument (Carlo Erba) using N_2 absorption at 77 K and the well known Brunauer, Emmett, and Teller procedure (brunauer S et al. 1938).

Adsorption of lactoferrin

LF, a 97% pure protein fraction from cow's milk, was obtained from DMW International Ltd (Veghel, Netherlands). All common high-purity chemical reagents were supplied by Sigma-Aldrich (St Louis, MO, USA). Ultrapure water (0.22 µS, 25°C) was used. Samples of adsorbed lactoferrin (LF-HA) were prepared by mixing 10 mg of HA with 1.5 mL of protein dissolved in HEPES buffer (0.01 M HEPES, 0.15 M NaCl) at pH 7.4 with different concentrations (10 mg ml^{-1}, 3 mg ml^{-1} and 1 mg ml^{-1}) in a 2 mL Eppendorf tube. The mixture was maintained in a bascule bath at 37°C for 24 hours. For the spectroscopic and thermal investigations, the solid was washed twice with ultrapure water and recovered by centrifuging at 10,000 rpm (12,700 g) for 3 minutes. Protein content was assessed by UV-Vis spectroscopy (λ= 280 nm, ε= 92000 M^{-1} cm^{-1}).The amount of adsorbed protein was determined by calculating the difference between the concentrations of the protein solutions before and after adsorption on HA nanocrystals.

Spectroscopic, thermal and morphological investigation

In order to investigate the amount of protein adsorbed onto HA after washing, thermogravimetric analysis (TGA) investigations were carried out on freeze dried samples using a Thermal Analysis SDT Q600 (TA Instruments, New Castle, DE, USA). Heating was performed under a nitrogen flow (100 ml min^{-1}) using an alumina sample holder. The temperature was increased to 120°C using a heating rate of 10°C min^{-1}, followed by an annealing of the sample at 120°C for 30 min and then the temperature was increased further to 700°C with the same temperature gradient. The weight of the samples was approximately 10 mg.

Transmission electron microscopy (TEM) investigations were carried out using a Philips CM100 instrument (Philips Electronic Instruments, Inc, NJ, US) operating at 80 kV. The powdered samples were dispersed in water and a few droplets of the slurry were deposited on holey-carbon foils supported on conventional copper microgrids.

The FT-Raman spectra were recorded by a Bruker MultiRAM spectrometer equipped with a Ge-diode detector (Bruker Optik GmbH, Ettlingen, DE). The excitation source was a Nd^{3+} -YAG laser (1064 nm) with a power on the sample of about 100 mW, the spectral resolution was 4 cm^{-1} and the number of scans for each spectrum was 5000. The curve fitting analysis was performed by means of a GPL software (Fityk 0.9.0 by Marcin Wojdyr) on the original spectra after baseline correction in the 1750 – 1525 cm^{-1} range, using the Levenberg–Marquardt algorithm. In order to fit the vibrational bands, some parameters should be fixed or constrained within reasonable limits: the number and the positions of bands, their shape and their full-width at half maximum. The information to fix the number and the position of the component peaks comes from the second derivative spectra, smoothed with a 5-point Savitsky–Golay function. The peak profiles used in the curve fitting procedures were described as linear combination of Lorentian and Gaussian functions (Jun S et al. 2004).

The content of secondary structure was calculated from the area of the individually assigned bands and expressed as a fraction of the total area of the bands whose maxima were comprised between 1645 and 1690 cm^{-1}. The β-turn content was calculated from the area of the band at about 1688–1690 cm^{-1}. The β-sheet, unordered structure and α-helix contents were calculated from the areas of the bands at about 1675, 1663 and 1658–1650 cm^{-1}, respectively. The assignments of Raman marker bands of side-chains in the range 1550–1640 cm^{-1} were deduced from the literature (Domenech J et al. 2007).

Bacteria

The study included the following species: *Staphylococcus aureus*, *Listeria monocytogenes*, *Salmonella enterica* serovar Paratyphi B, *Escherichia coli*. Isolates were obtained from patients hospitalized at the Medical School, University of Naples. All bacteria were characterized using Biolog MicroStation™ System/MicroLog™ (User's guide version 5.2.01, Biolog, Hayward, CA, USA) and specimens were confirmed by polymerase chain reaction assay of the genes Hsp 60 *(S. aureus)*, Mono A (*L. monocytogenes*), invA (*S. enterica serovar Paratyphi B*), Stx1 (*E. coli*) (Blaiotta g et al. 2004; Bubert A et al. 1999; Chiu CH and Ou CT, 1996; Janezic KJ et al. 2013). *Staphylococcus aureus*, *Listeria monocytogenes*, *Salmonella enterica serovar Paratyphi B* and *Escherichia coli* were grown as described elsewhere (Capparelli R et al. 2009).

Antibacterial activity
The bacteria (10^6 CFU/ well), in exponential phase, were distributed in triplicate into plates, mixed with a series of dilutions of LF-HA (300–500 µg/ml), and incubated at 37°C for 18 hours. The minimal concentration of LF-HA causing growth inhibition was determined by measuring absorbance at 600 nm using a microplate reader (Model 680, Bio-Rad Hercules, CA, USA) (Capparelli R et al. 2012).

Hemolytic activity
LF-HA was tested for its hemolytic activity using murine red blood cells. The hemolytic activity was measured according to the formula:
$OD_{peptide} - OD_{negative\ control} / OD_{positive\ control} - OD_{negative\ control} \times 100$
where the negative control (0% hemolysis) was represented by erythrocytes suspended in saline while the positive control (100% hemolysis) was represented by erythrocytes lysed with 1% Triton X-100.

Cell culture
A human acute monocytic leukemia cell line (THP-1, American Tissue Culture Collection, Rockville, MD, USA) were cultured in complete medium consisting of Roswell Park Memorial Institute medium, 10% fetal bovine serum, 100 IU/mL penicillin, and 100 µg/mL streptomycin (all from Gibco, Paisley, Scotland).

Trials of cytotoxicity

Trypan Blue test
THP-1 cell (10^6 cells/ well) grown in RPMI medium without antibiotics, were seeded on 24-well plates (Falcon, Milan). Cell adhesion was induced with phorbol myristate acetate (PMA; 2 µg/mL; 12 h). Then, they were incubated first with LF-HA (300–500 µg/mL for 24, 48, and 72 hours), then with 1% trypsin (1.5 ml/well at 37°C for 3 min) and finally with complete medium (3 ml/well). The whole mixture was transferred into a test tube and centrifuged (3 min at 1000 g). The pellet was resuspended in 1 ml RPMI medium . 10 µl of cell suspension were mixed with 10 µl of Trypan blue and the percentage of viability determined using the formula: N° viable cells / (N° non viable cells + N° viable cells) x 100.

Nitrite production
THP-1 cells adhesion (10^6/well) was induced with phorbol myristate acetate (2 µg/ml; 12 h) and then stimulated for 24, 48 or 72 hours with Lipopolysaccharides (LPS;10 µg/ml), LF-HA (300–500 µg/mL) or with a combination of both. Nitrite accumulation (NO_2^-, µmol/10^6 cells) in the medium was determined by the Griess reaction (Cardile V et al. 2004).

LDH Assay
A lactate dehydrogenase (LDH) assay was performed using a CytoTox 96® Non-Radio cytotoxicity assay kit (Promega, Madison, WI, USA) at 2, 4, and 24 hours.

Antioxidant activity of LF-HA
The antioxidant activity of LF-HA was assessed in water-soluble fraction using ABTS method. The ABTS assay was based on the reduction of the $ABTS^{\cdot+}$ radical action by the antioxidants present in the sample. A solution constituited by 7.4 mM ABTS (5ml) mixed to 140 mM $K_2S_2O_8$ (88 µl) was prepared and stabilized for 12h at 4°C in the

dark. This mixture was then diluited by mixing $ABTS^{\cdot+}$ solution with ethanol (1:88) to obtain an absorbance of 0.70 ± 10 units at 734 nmusing spectrophotometer. LF-HA (100 µl at 300 µg/mL) was allowed to react with 1 ml of diluited $ABTS^{\cdot+}$ solution for 2.5 min and then the absorbance was taken at 734 nm using a spectrophotometer against a blank constituited by $ABTS^{\cdot+}$ solution added with 100 µl of ethanol. The standard curve was linear between 0 and 20 µM Trolox. All the replicates of sample were analyzed in triplicate and the results were expressed as mmol/L (Re R et al. 1999).

Enzyme-linked immunosorbent assay (ELISA) of inflammatory activity

THP-1 cells (10^6 cells/ well) were grown in RPMI medium without antibiotics, and cell adhesion was induced with phorbol myristate acetate (PMA; 2 µg/mL; 12 h). After the cells were stimulated with lipopolysaccharide (LPS; 10 µg/mL) for one hour. The THP-1 cells stimulated or not with LPS were then treated with LF-HA (300 µg/mL) or acetylsalicylic acid (ASA; 300 µg/mL) for 2, 4, and 24 hours. Tumor necrosis factor (TNF)-α, interferon (IFN)-γ, interleukin (IL)-17, IL-8, IL-12, IL-6, IL-10, and IL-4 levels were assayed by enzyme-linked immunosorbent assay as reported elsewhere (Rozalska B and Wadstrom T, 1993).

Electrochemically-assisted deposition of LF-HA

Electrochemically-assisted deposition (ELD) was carried out in a two-electrode electrochemical cell. Working electrode, cathode, was made, from 10 x 20 mm^2 cling film, while a platinum sheet is used like a counter electrode (anode). During the tests, prior to deposition, platinum sheet were cleaned by a standard protocol: it was ultrasonically cleaned in cold acetone and then in distilled water to remove impurities. The electrochemistry system was controlled by Keitley Model 2000 Multimeter and Keitley Model 6220 Dc Current Source . In preparing the electrolyte, proper amount of Ca $(CH_3COO)_2$ and H_3PO_4 were dissolved separately in distilled water to make two different solutions: the first one with 42 mM of $[Ca^{2+}]$ and the second with 25 mM of $[PO_4^{3-}]$ (Lelli M et al. 2010; Roveri N et al. 2003; Karunakar K et al. 2006). These two solutions were mixed in the same measure. During the electrochemical process the ion migration to the cathode takes place and a basic environment near the work electrode forms, favoring contemporary both the HA crystallization and the hydroxyapatite coating formation on the same electrode (Lelli M et al. 2010; Falini g et al. 2004). During electrolytic deposition, the electrochemical cell with the electrolyte mixture was kept at room temperature and a constant current of 34 mA was applied. Biomimetic coatings of hydroxyapatite nanocrystals functionalized with LF, have been performed by electrochemically-assisted deposition process on cling film. HA coating deposition followed by an electrochemically assisted co-deposition of LF onto it (method labelled as “two steps” electrodeposition) were carried out. In the first step only the calcium acetate and phosphoric acid solutions have been inserted into the cell, allowing the HA coating deposition, and in the second step the protein LF solution has been added to the solution to obtain a final concentration of LF-HA ranging between 100 µg/mL to 500 µg/mL. LF-HA electrodeposition on the working electrode have been carried out for different electrodeposited time (3, 5, 7 and 9 min).

Morphological characterization
Scanning Electron Microscopy (SEM) observation were carried out by a SEM (Philips - 515) using secondary electrons at 25Kv and various magnifications using secondary electrons at 5 voltage and 2000X. The specimens were mounted on aluminium stubs using carbon tape and they were covered with a gold coating, 10nm thick, using a coating unit.

Fourier Transform Infrared Spectroscopy (FTIR)
Infrared Microscopy Spectral data were recorded by a Perkin-Elmer Spectrum One Fourier Transform Infrared Spectrometer (FT-IR) equipped with a Perkin-Elmer Autoimage microscope. The spatial resolution was 100 x 100 μm^2 and the spectral resolution was 4 cm^{-1}. This spatial resolution was chosen in order to optimize the signal to noise ratio. The spectra were related to the surface of the sample. Specific areas of interest were identified by a microscope television camera and for each ones an IR image was acquired using a liquid nitrogen cooled, 16-pixel mercury cadmium telluride (MCT-A) line detector at a 25 µm/pixel resolution.
Baseline (polynomial line fit), smoothing of hydroxyapatite normalization were performed in all cases. The correlation maps allow to evidence the chemical topographic distribution of a selected spectrum on the analyzed area. According to a colorimetric scale, the white colour corresponds to a zone with maximum absorption, while the dark-blue colour refers to a zone in which the corresponding absorption band is absent (Hernandez-Hernandez A et al. 2008).

Active packaging trial
Apples (cultivar Stark) were peeled, immersed in water (to avoid their rapid oxidation caused by air exposure, cut into four slices, which were rapidly wrapped in cling film pretreated or not with LF-HA and kept for 1 week at room temperature. The level of oxidation of the slices was then documented by photography.

RESULTS

Synthetic biomimetic hydroxyapatite nanocrystals

The HA nanocrystals used in the present study have composition, structure, morphology, dimension and surface reactivity very close to those of bone nanocrystals, which had already been approved for *in vivo* use (Thian ES et al. 2013). Figure 4A is a transmission electron microscopy image of the synthesized HA nanocrystals. It reveals the planar acicular morphology, typical of the HA nano-crystals of human bone (Figure 4B). The crystals have a plate-like morphology (length and width about 110 ± 5 nm and 20 ± 3 nm, respectively, and a thickness of about 8 ± 2 nm). The presence of 5% phosphate anions substituted by carbonate anions produces a pseudo amorphous layer without crystalline order on the surface of the nanocrystals. The amorphous surface of nanocrystals is responsible for the zeta potential of –20.5±1.5 mV observed when - as in Figure 4 - HA nanocrystals are shown at physiological pH 7.4. The high reactivity of HA nanocrystals is ascribed to their amorphous surface, together with the their high surface area (about 110 m^2/g), which is only slightly lower than that of biological nanocrystals (120 m^2/g).

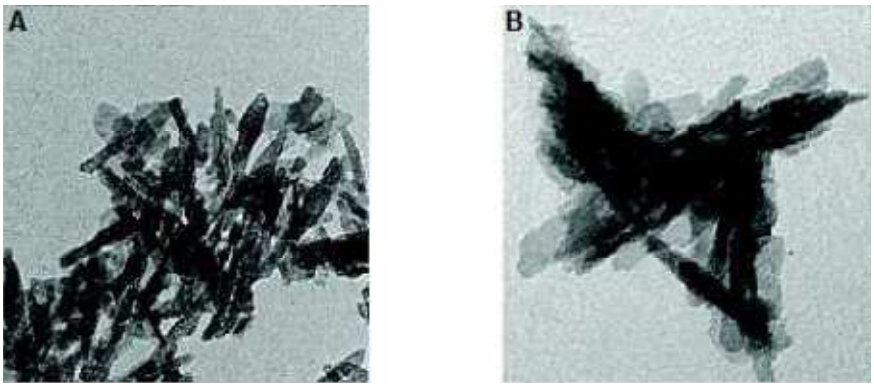

Figure 4: A) Transmission electron microscopy (TEM) image of a synthetic hydroxyapatite nanocrystal with a planar acicular morphology mimicking the bone biogenic hydroxyapatite nanocrystals; **B)** TEM image of bone hydroxyapatite nanocrystals.

Interaction of lactoferrin with hydroxyapatite nanocrystals

Synthetic biomimetic HA nanocrystals were surface-functionalized at pH 7.4 by different amounts of lactoferrin molecules using the method reported by Iafisco et al (Iafisco M et al. 2011). Isotherm LF adsorption onto biomimetic HA nanocrystals at pH 7.4 is reported in Figure 5, where the adsorbed amount (LF concentration expressed in mg/m^2) is plotted against the protein concentration after adsorption (LF concentration expressed in mg/mL). The plot is characterized by an initial slope, indicating high protein affinity for the HA surface.

The increase in LF concentration in the buffer solution enhances the surface coverage until it is complete. The absorption-saturation yields a plateau value corresponding to the maximum amount of LF surface immobilization of about 1mg/m^2.

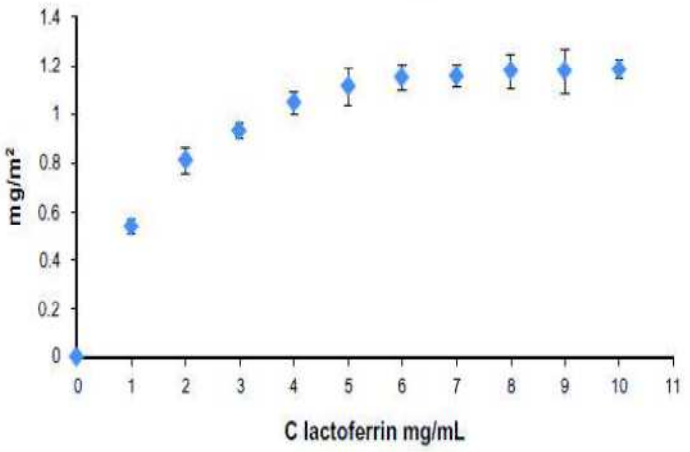

Figure 5: Adsorption isotherm of lactoferrin on biomimetic hydroxyapatite nanocrystals at pH 7.4. The adsorbed lactoferrin is plotted against the protein concentration after adsorption.

The isoelectric point of LF is 8.5, and it thus has a net positive charge below the isoelectric point (Pan F et al. 2008). The analysis of the surface electrostatic potential of LF at pH 7.4 allowed the study of the interaction of LF with HA nanocrystals in terms of electrostatic interactions. The basically positive electrostatic surface potential of LF at pH 7.4 allows the strong interaction with the slightly negative HA nanocrystals (zeta potential of –20.5 ± 1.5 mV) and avoids the protein-protein interaction. This electrostatic interaction leads to formation of an LF monolayer coated onto the HA nanocrystals. The HA morphology and the nanodimension do not appreciably affect the conformation of the absorbed LF. At pH 7.4, the LF covering the HA nanocrystals was only slightly unfolded, with a small fraction of the alpha-helix structure being converted into turn while the beta-sheet content remained almost unchanged (Iafisco M et al. 2011).
In order to investigate the amount of protein adsorbed onto HA after washing, thermogravimetric analysis (TGA) was carried out on freeze-dried samples. Thermogravimetric curves of HA and protein-coated HAs obtained at three different surface coverage conditions (protein starting concentrations: 10 mg ml^{-1}, 3 mg ml^{-1} and 1 mg ml^{-1}) at pH 7.4 of the LF solutions are reported in Figure 6.

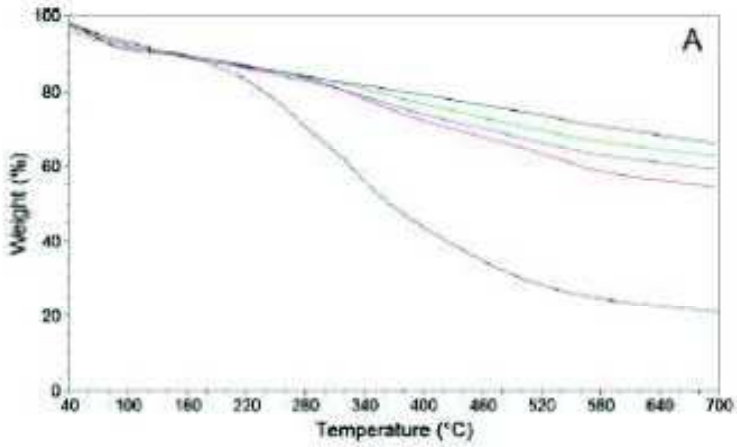

Figure 6: TGA curves of HA (black, solid), LF (black, dash) and HA–LF at three different surface coverage conditions (protein starting concentration: 10 mg ml-1 (red), 3 mg ml-1 (blue) and 1 mg ml^{-1} (green) at pH 7.4.

The TGA curve of pure LF showed two weight losses, the first from room temperature to 120°C ascribable to the loss of the adsorbed water and the second from 120 to 700°C due to the thermal degradation (Chen PH et al. 2008).
The percentage amount of adsorbed LF was calculated by using eqn:

$$LF\% = 100 - (\Delta w\%_{LF} - \Delta w\%_{LF\text{-}HA}) \times \frac{100}{(\Delta w\%_{LF} - \Delta w\%_{HA})}$$

where D$w\%_{LF}$, D$w\%_{HA}$ and D$w\%_{LF\text{-}HA}$ are the percentage weight losses in the range 120–700° C of pure LF, pure HA and LF-HA conjugates, respectively. The weight percentage of LF adsorbed onto HA was significantly higher in agreement with the affinity of the protein (K_{LF}) calculated by the theoretical models.
The TEM images of the washed HA nanocrystals coupled with LF (Figure 7B) showed that they are bigger and more spherical than the unfunctionalized ones (Figure 7A) as a result of the layer of protein covering their surfaces. The uncoated crystals displayed a flat and round shape with a diameter of about 15 nm (Figure 7), while the functionalized ones at pH 7.4, showed spheres with a diameter of about 30 nm. The increase of about 15 nm in dimension could be in agreement with a monolayer of LF adsorbed in an end-on way.

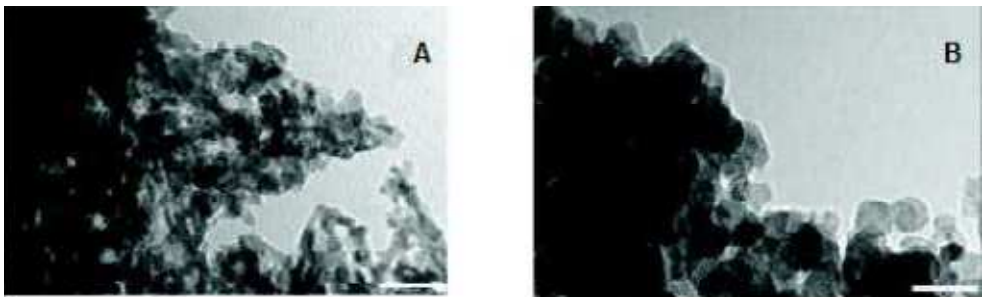

Figure 7: TEM images of synthetic biomimetic hydroxyapatite nanocrystals: **A)** uncoated and **B)** coated with LFat pH 7.4. Scale bars are 50 nm.

FT-Raman spectroscopy established that the secondary structure of LF was poorly affected by adsorption on HA nanocrystals (Figure 8): the curve fitting method showed that the protein slightly unfolded after adsorption and, as a matter of fact, a small fraction of the α-helix structure converted into turn, while the β-sheet content remained almost unchanged.

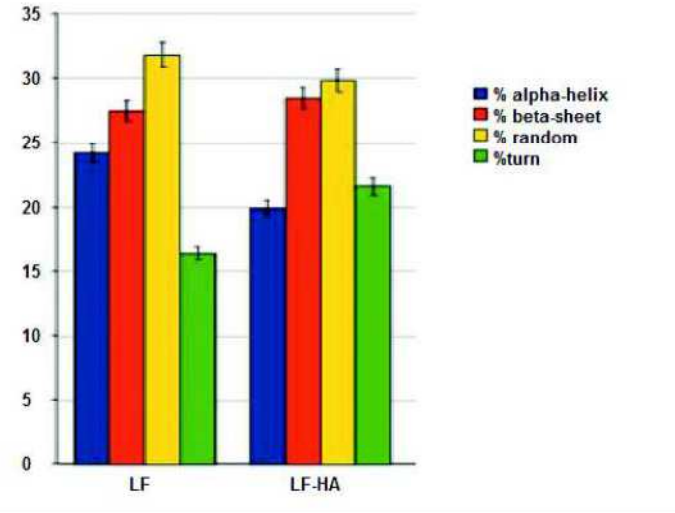

Figure 8: Secondary structure composition after the band fitting procedure on the amide I Raman band. Associated error: 4%, as proposed by other authors (Tinti A et al. 2008).

Nanohybrid composite made of biomimetic HA nanocrystals surface - covered of 1mg/m^2 (LF-HA) were used to test their biological activity.

Antimicrobial and hemolytic activities

Synthetic biomimetic HA nanocrystals surface-functionalized with LF were tested for their antibacterial activity against *S. aureus*, *L. monocytogenes*, *S. enterica* serovar Paratyphi B, and *E. coli.* LF molecules delivered by the biomimetic HA nanocrystals were active against both Gram-positive and Gram-negative bacteria. LF molecules effectiveness depend on LF-HA concentration. The antimicrobial activity of LF-HA and LF is shown at different concentrations (300–500 µg/mL) in Table 1. The antimicrobial activity of LF-HA at a concentration of 300 µg/mL is higher than that of unconiugated LF. The LF-HA nanohybrid composite at a concentration of 300 µg/mL had low hemolytic activity (10%).

Table 1: Antimicrobial activity of unconiugated LF versus LF-HA.

Bacteria	**LF 300µg/ml**	**LF 350µg/ml**	**LF 400µg/ml**	**LF 450µg/ml**	**LF 500µg/ml**
Staphylococcus Aureus	28%	30%	36%	40%	42%
Listeria monocytogenes	22%	26%	30%	37%	40%
Salmonella paratyphi B	23%	28%	31%	35%	41%
Escherechia coli	25%	31%	36%	42%	48%
Bacteria	**LF-HA 300µg/ml**	**LF-HA 350µg/ml**	**LF-HA 400µg/ml**	**LF-HA 450µg/ml**	**LF-HA 500µg/ml**
Staphylococcus Aureus	61%	65%	70%	77%	80%
Listeria monocytogenes	60%	63%	70%	75%	80%
Salmonella paratyphi B	63%	66%	71%	78%	81%
Escherechia coli	65%	68%	72%	75%	78%

Cytotoxic activity and antioxidant capacity

LF-HA was slightly cytotoxic when tested in the THP-1 cell line at concentrations of 300–500 µg/mL. The THP-1 cells remained viable for up to 72 hours (Table 2). In addition, LF-HA induced low production of NO_2 in THP-1 cells. Production of NO_2 was reduced in cells stimulated with lipopolysaccharide and then treated with LF-HA compared with control cells (stimulated only with lipopolysaccharide) (Table 3). The LDH enzyme released by THP-1 cells was used as the endpoint for the study of cellular toxicity (Figure 9). LF-HA induced low production of LDH in THP-1 cells. Release of LDH into the medium is a sign of necrotic cell death (Awad WA et al. 2012), and production of LDH was reduced in cells stimulated with lipopolysaccharide (10 µg/mL) and then treated with LF-HA compared with the positive control provided by the kit (Figure 9). The antioxidant properties of HA and LF alone or combined in the hybrid LF-HA composites was evaluated using the ABTS test (HA, 14,632 mmol/L; LF, 2,605 mmol/L; LF-HA, 15,294 mmol/L). A small increase in antioxidant activity was found in the LF-HA composite (Table 4).

Table 2: Cell viability analysis of THP-1 cells treated with LF-HA (300-500 µg/ml).

Time (h)	THP-1	THP-1 + LF-HA 300µg/ml	THP-1 + LF-HA 350µg/ml	THP-1 + LF-HA 400µg/ml	THP-1 + LF-HA 450µg/ml	THP-1 + LF-HA 500µg/ml
24	99%	90%	76%	71%	70%	67%
48	96%	86%	74%	70%	67%	64%
72	90%	80%	72%	68%	65%	62%

Table 3: NO_2 production in: untreated THP-1 cells for 24, 48, or 72 hours; THP-1 cells stimulated with LPS (10 µg/mL) for 24, 48, or 72 hours; THP-1 cells treated with LF-HA (300-500 µg/mL) for 24, 48, or 72 hours; THP-1 cells stimulated with LPS (10 µg/mL) and then treated with LF-HA (300-500 µg/mL) for 24, 48, or 72 hours.

	Time (h)		
Conditions	**24**	**48**	**72**
THP-1	0,596 ± 0.02µmol	0,760 ± 0.08µmol	0,996 ± 0.04µmol
THP-1 + LPS	3,910 ± 0.01µmol	4,415 ± 0.22µmol	5,312 ± 0.04µmol
LF-HA 300µg/ml	1,120 ± 0.04µmol	1,520 ± 0.25µmol	1,720 ± 0.04µmol
LF-HA 350µg/ml	1,140 ± 0.03µmol	1,449 ± 0.12µmol	1,740 ± 0.05µmol
LF-HA 400µg/ml	1,175 ± 0.10µmol	1,775 ± 0.16µmol	1,875 ± 0.04µmol
LF-HA 450µg/ml	1,250 ± 0.04µmol	1,655 ± 0.07µmol	1,958 ± 0.04µmol
LF-HA 500µg/ml	1,278 ± 0.04µmol	1,878 ± 0.09µmol	1,968 ± 0.16µmol
LPS+ LF-HA 300µg/ml	1,814 ± 0.12µmol	1,940 ± 0.01µmol	1,991 ± 0.25µmol
LPS+ LF-HA 350µg/ml	1,775 ± 0.04µmol	1,970 ± 0.04µmol	2,075 ± 0.10µmol
LPS + LF-HA 400µg/ml	1,950 ± 0.01µmol	1,980 ± 0.03µmol	2,190 ± 0.02µmol
LPS + LF-HA 450µg/ml	2,159 ± 0.11µmol	2,359 ± 0.07µmol	2,431 ± 0.20µmol
LPS + LF-HA 500µg/ml	2,250 ± 0.17µmol	2,395 ± 0.14µmol	2,249 ± 0.18µmol

Table 4: Antioxidant activity of hydroxyapatite (HA), lactoferrin (LF) and lactoferrin adsorbed onto hydroxyapatite (LF-HA).

	Concentration (µg/mL)
Molecule	**300**
HA	14,632 mmol/L
LF	2,605 mmol/L
LF-HA	15,294 mmol/L

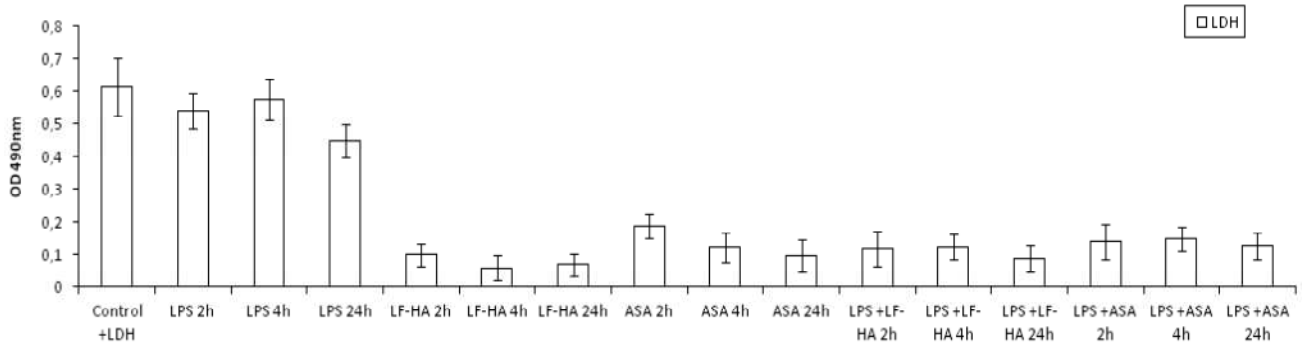

Figure 9: LDH production in: THP-1 cells stimulated with LPS (10 µg/mL) for 2, 4, or 24 hours; THP-1 cells treated with LF-HA (300 µg/mL) or ASA (300 µg/mL) for 2, 4, or 24 hours; THP-1 cells stimulated with LPS (10 µg/mL) and then treated with LF-HA (300 µg/mL) or ASA (300 µg/mL) for 2, 4, or 24 hours. Positive control: control plus LDH provided by the kit.

Immunomodulatory activity

We also investigated the immunomodulatory activity of LF-HA in THP-1 cells stimulated by lipopolysaccharide. For this purpose, the performance of selected cytokines, including TNF-α, IFN-γ, IL-17, IL-4, IL-12, IL-8, IL-6, and IL-10, was evaluated by enzyme-linked immunosorbent assay. Cytokines can be considered as an important parameter for defining inflammation (Gould IM and Bal AM, 2013). Treatment of THP-1 cells with acetylsalicylic acid (ASA) or LF-HA did not induce any significant inflammatory response, and levels of TNF-α, IFN-γ, IL-17, IL-4, IL-6, IL-10, IL-12, and IL-8 appeared to be low. After stimulation of THP-1 cells by lipopolysaccharide, an increase in levels of pro-inflammatory cytokines, i.e. TNF-α, IFN-γ, IL-6, and IL-17, was observed, with a peak after 4 hours (Figure 10). After treatment of lipopolysaccharide-stimulated THP-1 cells with LF-HA, the levels of pro-inflammatory cytokines decreased, while the levels of others, such as IL-4, IL-10, IL-12, and IL-8, showed an increase, reaching a peak at 4 hours. On treating lipopolysaccharide-stimulated THP-1 cells with acetylsalicylic acid, there was a decrease in TNF-α, IFN-γ, IL-6, and IL-17 levels and an increase in IL-4, IL-10, IL-12, and IL-8 levels (Figure 10). Moreover, THP-1 cells were treated with lipopolysaccharide, the supernatant was collected at 2, 4, 6, 8, 12, and 24 hours, and TNF-α and IL-6, early cytokines to be produced, were quantified. These cytokines

showed a high level of expression for up to 8 hours (data not shown). In THP-1 cells stimulated with lipopolysaccharide and treated with LF-HA, TNF-α, and IL-6 levels started to decrease 4 hours after treatment. In the presence of lipopolysaccharide, LF-HA specifically inhibits the release of pro-inflammatory cytokines and increases the secretion of anti-inflammatory cytokines. LF-HA down regulates the synthesis of proinflammatory cytokines due to its ability to bind lipopolysaccharide through the LF domain. Therefore, LF-HA competes with lipopolysaccharide-binding protein for binding to lipopolysaccharide and blocks transport of endotoxins to mCD14, which is expressed on the surface of macrophages. By binding lipopolysaccharide, LF-HA prevents activation of NF-kB and consequently the production of pro-inflammatory cytokines (Haversen L et al. 2002).
Finally, we can conclude that the expression of TNF-α and IL-6 in THP-1 cells stimulated with lipopolysaccharide and then treated with acetylsalicylic acid is comparable with the levels obtained in cells stimulated with lipopolysaccharide and then treated with LF-HA. Further tests have shown that LF-HA down regulates the level of other pro-inflammatory cytokines and that it also acts as immunomodulatory agent. The effects of LF-HA appeared to be comparable with those of acetylsalicylic acid, a well known anti-inflammatory drug (Figure 10).

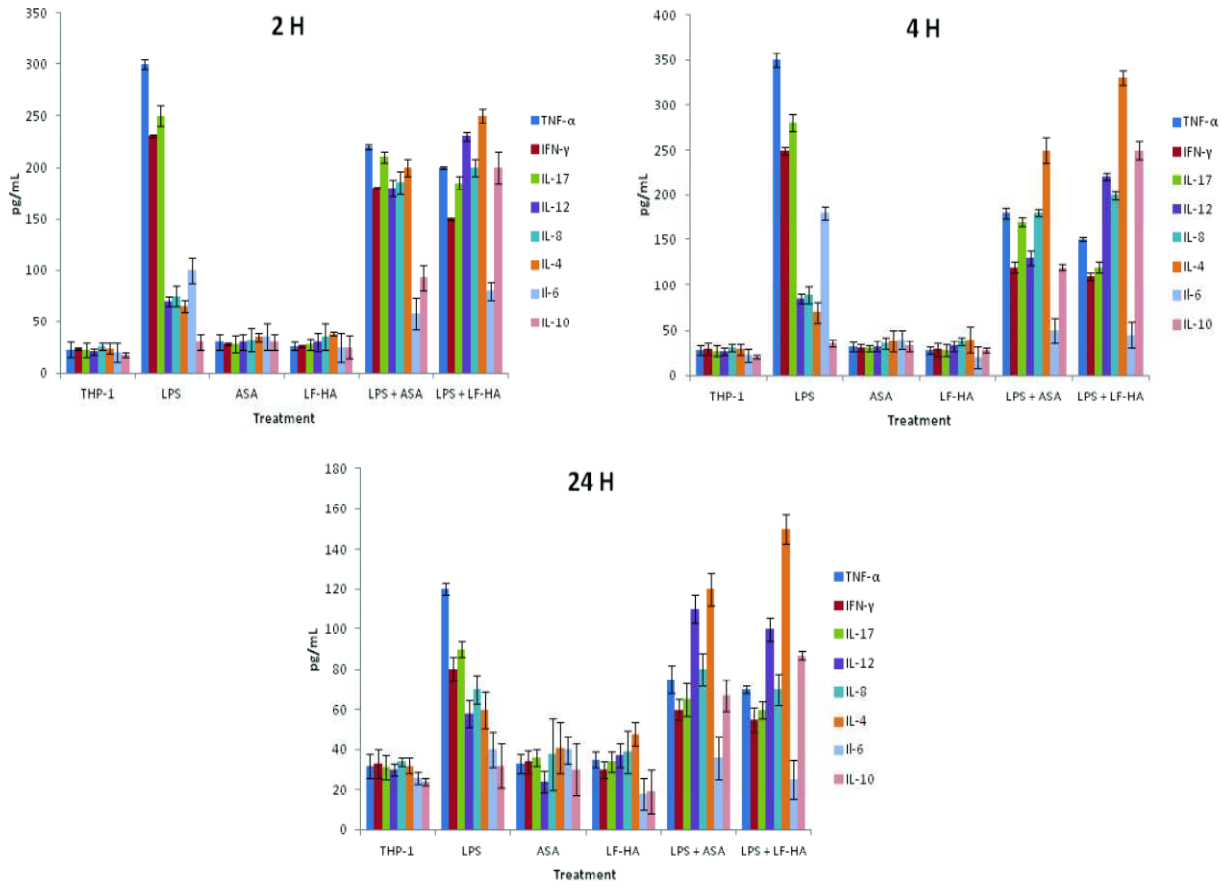

Figure 10: IFN-γ, TNF-α, IL-17, IL-4, IL-12, IL-8, IL-6, and IL-10 levels of: untreated THP-1 cells; THP-1 cells stimulated with LPS (10 µg/mL) for 2, 4, or 24 hours; THP-1 cells treated with LF-HA (300 µg/mL) or ASA (300 µg/mL) for 2, 4, or 24 hours; THP-1 cells stimulated with LPS (10 µg/mL) and then treated with LF-HA (300 µg/mL) or ASA (300 µg/mL) for 2, 4, or 24 hours. Negative control: THP-1 cells in Roswell Park Memorial Institute medium. Results from the representative experiments are presented as the mean ± standard deviation.

Electrochemically-assisted deposition (ELD) of LF-HA

Electrochemically-assisted deposition (ELD) has been utilized by a two-electrode electrochemical cell alimented a constant current of 34 mA and kept at room temperature to obtain LF-HA coatings on the working electrode, cathode, constituted of 10 x 20 mm^2 cling film, using different electrodeposited time (3, 5, 7 and 9 minutes).

Different coatings have been obtained using an electrolytes water solution prepared mixing in the same measure a solution of Ca^{2+} 42 mM and a solution of PO_4^{3-} 25 mM. To this electrolytic solution was added LF to a final concentration of LF-HA ranging between 100 µg/mL to 500 µg/mL. This range included the LF-HA concentration of 300 µg/mL, with optimal antimicrobial, immonomodulatory and anti-oxidant activities.

According to the "two step" electro deposition method, the first step consisted in coating the cling film with an electrolytic solution of calcium and phosphates ions, the second step consisted in the addition of different concentrations of LF. Using the "two steps" method of electro deposition, the LF-HA coatings results uniform on the whole cling film surface. Figure 11 is an SEM image of LF-HA coating at 300 µg/mL, prepared by the "two step" method.

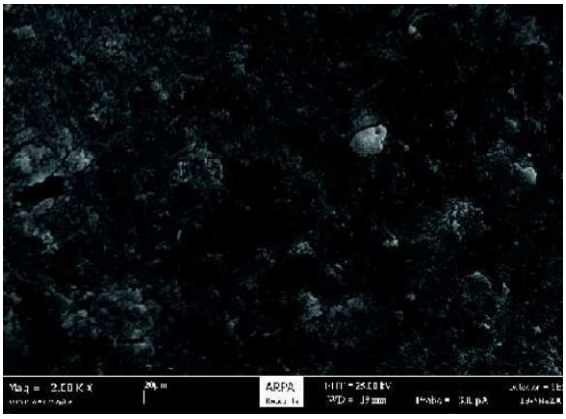

Figure 11: SEM image of LF-HA homogeneous coating obtained by two step method.

In order to map the spatial distribution on the cling film surface and evaluate the interaction between the protein and inorganic components, FT-IR micro spectroscopy was used. Figure 12 shows representative spectra of selected areas of the cling film prepared by "two step" method at four different times of electro deposition (3, 5, 7 and 9 minutes) compared with those of LF and HA alone after 5 minutes of ELD. The representative bands of LF (1651, 1458 and 1443 cm^{-1}) are no longer detectable after 3 minutes of ELD, while the nanocrystals of HA maintain a low degree of crystalline structure, as shown by the broadening of the band at 1040 cm^{-1}. After 9 minutes of ELD, LF is no more detectable, presumably because it did deposit onto HA nanocrystals.

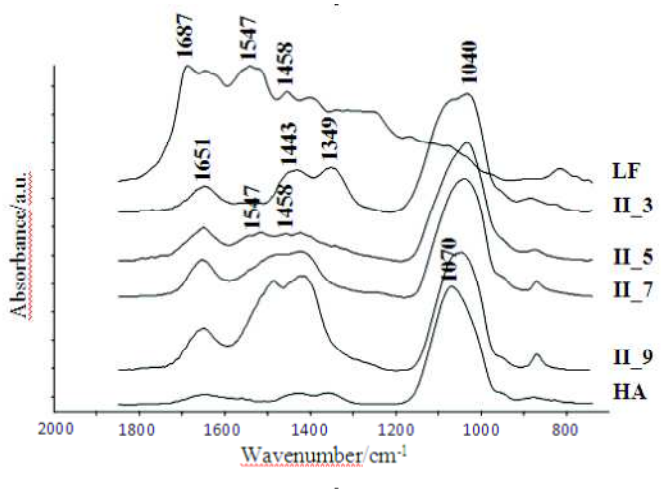

Figure 12: Representative spectra of the coatings obtained by the "two step" method of ELD according to four different times (**II_3** refers to 3 minute of ELD, **II_5** refers to 5 minutes of ELD, **II_7** refers to 7 minutes of ELD and **II_9** refers to 9 minutes of ELD) compared with those of pure lactoferrine (**LF**) and the hydroxyapatite after 5 minutes of ELD (**HA**) in the range 1800-700 cm^{-1}.

The correlation maps (Figure 13) obtained by loading the spectrum II_9 in the chemical map relative to 9'of ELD (1000 × 2700 µm) allow to evidence the chemical topographic distribution of a selected spectrum on the analyzed area. According to a colorimetric scale, the white colour corresponds to a zone with maximum absorption, while the dark-blue colour refers to a zone in which the corresponding absorption band is absent (Manara S et al. 2008); pointing-out that the coating is homogeneously distributed on all the cling film.

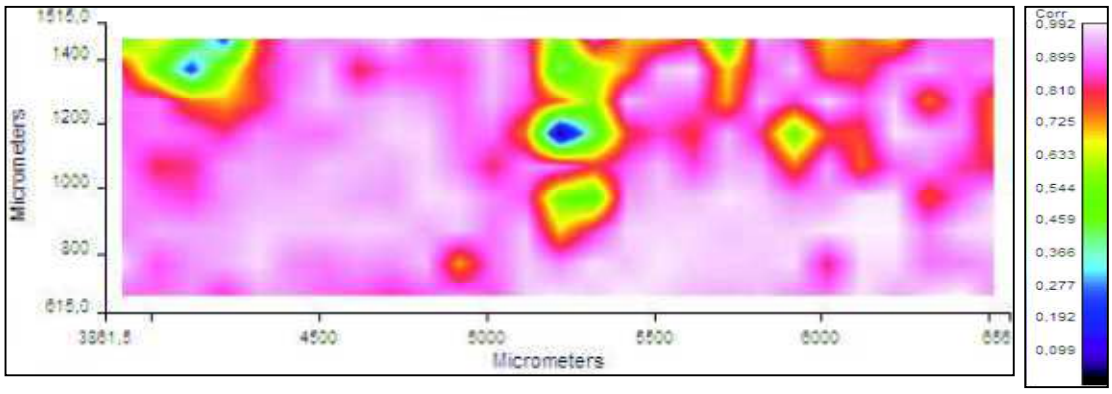

Figure 13: Correlation map obtained by loading the spectrum II_9 in the chemical map of the sample relative to 9'of ELD in the range 1800- 900 cm^{-1}.

Next we tested the efficacy of the cling film as active packaging on apples, the fruit characterised by a high tendency to oxidation. For this purpose, the apple was peeled and wrapped in untreated and LF-HA-treated cling film and stored at room temperature for one week. The LF-HA-treated cling film protected the apple from oxidation more efficiently (Figure 14).

Figure 14: Level of oxidation of the slices wrapped in **A)** untreated cling film and **B)** LF-HA treated cling film.

CONCLUSIONS

Consumers demand safe natural products. This drives the search of food authorities and researchers for mild preservation techniques to improve quality and safety without causing nutritional and organoleptic losses. In this context natural compounds are gaining a great interest from research and industry, due to the potential to provide quality and safety benefits, with a reduced impact on human health (Kuorwel KK et al. 2011). The antimicrobial proteins, in their natural form alone or combined with other molecules, could represent a solution to this problem. Antimicrobial molecules are characterized by a broad spectrum of activity against Gram-positive and Gram-negative bacteria and have a low level of toxicity in eukaryotic cells (Capparelli R et al. 2009).

In recent years, in fact, an increasing interest has emerged in the development of various forms of food packaging systems: many natural antimicrobial agents incorporated into or coated on synthetic polymer-based packaging materials have demonstrated a significant and a large spectrum of antimicrobial activity. Thus, natural antimicrobial agents such as basil, thyme, and oregano with their main components linalool, thymol, and carvacrol, respectively, are well suited to be utilized as preservatives in foods and as potential alternatives for synthetic food additives. Packaging materials containing antimicrobial molecules demonstrate a potential for applications in packaging systems that could prolong food shelf life and reduce the risk of food-borne illness associated with microbial contamination.

Prolonging the food shelf life represents a constant challenge for food industry. The challenge consists on protecting food against pathogens colonization and the natural decay of food constituents (in particular, the most liable constituents, lipids and proteins), in accordance with an evolving legislation (Brody AL et al. 2008).

The advances in different sectors of food industry, especially in the packaging sector, have led to improved food quality and safety. The new advances have mostly focused on delaying oxidation and controlling moisture migration, microbial growth, respiration rates, and volatile flavors and aromas.

Nanotechnology has the potential of greatly influencing the packaging sector. Nanoscale innovations in the forms of pathogen detection, active packaging, and barrier formation are poised to elevate food packaging to new heights (Lucera A et al. 2012).

The development of active systems has promoted great changes in food technology, since it can improve sensorial characteristics and extend the shelf life of foods.

The present work has demonstrated the several important properties of lactoferrin adsorbed onto hydroxyapatite nanocristals - a new complex molecule - such as antibacterial, immunomodulatory, and antioxidant activities, and its use as coating for cling film. The main characteristics of this cling film are: uniform coating with LF-HA obtained throughout a new method of electrodeposition; long lasting stability, when stored for six months or longer at room temperature before being used to protect the food; stable to deep freezing, for six months or more.

BIBLIOGRAPHY

Aisen P, Leibman A. “Lactoferrin and transferrin: a comparative study“. Biochim. Biophys. Acta .1972; 257: 314–323.

Akawa T, Kobayashi M, Yoshida M, Matsushima K, Minoshima H, Sugimura H, Kanno T, Horiuchi J. “Improved liquid chromatographic separation of different proteins by designing functional surfaces of cattle bone-originated apatite“. J. Chromatogr. 1999; 862: 217 -220.

Andersen JH, Jenssen H, Sandvik K, Gutteberg TJ. “Anti-HSV activity of lactoferrin and lactoferricin is dependent on the presence of heparan sulphate at the cell surface“. J. Med. Virol. 2004; 74: 262–271.

Andersen JH, Osbakk SA, Vorland LH, Traavik T, Gutteberg TJ. “Lactoferrin and cyclic lactoferricin inhibit the entry of human cytomegalovirus into human fibroblasts“. Antiviral Res. 2001; 51: 141–149.

Appendini P, Hotchkiss JH. “Review of antimicrobial food packaging“. Innov Food. Sci. Emerg.Technol. 2002; 3(2): 113–126.

Awad WA, Aschenbach JR, Zentek J. “Cytotoxicity and metabolic stress induced by deoxynivalenol in the porcine intestinal IPEC-J2 cell line“. J. Anim. Physiol. Anim. Nutr. 2012; 96: 709–716.

Baker EN, Baker HM. “Lactoferrin molecular structure, binding properties and dynamics of lactoferrin“. Cell Mol. Life Sci. 2005; 62: 2531–2539.

Baker EN. “Structure and reactivity of transferrins“. Adv. Inorg. Chem. 1994; 41: 389–463.

Barroug A, Kuhn LT, Gerstenfeld LC, Glimcher MJ. “Interactions of cisplatin with calcium phosphate nanoparticles: in vitro controlled adsorption and release“. J. Orthop. Res. 2003; 22: 703 -708.

Beaumont SL, Maggs DJ, Clarke HE. “Effects of bovine lactoferrin on in vitro replication of feline herpesvirus“. Vet. Ophthalmol. 2003; 6: 245–250.

Beljaars L, Van Der Strate BW, Bakker HI. “Inhibition of cytomegalovirus infection by lactoferrin in vitro and in vivo“. Antiviral Res. 2004; 63: 197–208.

Bennett RM, Davis J. “Lactoferrin interacts with deoxyribonucleic acid: a preferential reactivity with double-stranded DNA and dissociation of DNA-anti-DNA complex“. J. Lab. Clin. Med. 1982; 99: 127–138.

Bensatude-Vincent B, Arribart H, Boulligand Y, Sanchez C. “Chemists and the school of nature“. New J. Chem. 2002; 26: 1 -5.

Blaiotta G, Ercolini D, Pennacchia C, Fusco V, Casaburi A, Pepe O, Villani F. “PCR detection of staphylococcal enterotoxin genes in Staphylococcus spp. strains isolated from meat and dairy products. Evidence for new variants of seG and sel in *S. aureus* AB-8802“. J. Appl. Microbiol. 2004; 97: 719–730.

Branen JK, Davidson PM. “Enhancement of nisin, lysozyme, and monolaurin antimicrobial activities by ethylene diamine tetraaceticacid and lactoferrin“. Int. J. Food Microbiol. 2004; 90: 63–67.

Breton-Gorius J, Mason D, Buriot D, Vilde JL, Griscelli C. “Lactoferrin deficiency as a consequence of a lack of specific granules in neutrophils from a patient with recurrent infections. Detection by immunoperoxidase staining for lactoferrin and cytochemical electron microscopy“. Am. J. Pathol. 1980; 99: 413–428.

Brewer R, Adams MR, Park SF. “Enhanced inactivation of Listeria monocytogenes by nisin in the presence of ethanol“. Lett. Appl. Microbiol. 2002; 34: 18–21.

Brody A, Strupinsky ER, Kline LR. “Odor removers“. In: Brody A, Strupinsky ER, Kline LR, editors. Active packaging for food applications. Lancaster, Pa.: Technomic Publishing Company, Inc. 2001; pp.107–117.
Brody A. “Packaging by the numbers“. Food Tech. 2008; 62(2): 89–91.
Brody AL, Bugusu B, Han JH, Sand CK, Mchugh TH. “Scientific status summary. Innovative food packaging solutions“. J. Food Sci. 2008; 73(8): r107-116.
Brunauer S, Emmett PH, Teller E. “Adsorption of gases in multimolecular layers“. J. Am. Chem. Soc. 1938; 60: 309–319.
Bubert A, Hein I, Rauch M, Lehner A, Yoon B, Goebel W, Wagner M. “Detection and differentiation of Listeria spp. by a single reaction based on multiplex PCR“. Appl. Environ. Microbiol. 1999; 65: 4688–4692.
Capparelli R, De Chiara F, Nocerino N, Montella RC, Iannaccone M, Fulgione A, Romanelli A, Avitabile C, Blaiotta G, Capuano F. “New perspectives for natural antimicrobial peptides: application as antinflammatory drugs in a murine model“. BMC Immunol. 2012; 13: 61.
Capparelli R, Romanelli A, Iannaccone M, Nocerino N, Ripa R, Pensato S, Pedone C, Iannelli D. “Synergistic antibacterial and anti-inflammatory activity of temporin A and modified temporin B in vivo“. PLoS One. 2009; 4: e7191.
Caraher EM, Gumulapurapu K, Taggart CC, Murphy P, McClean S, Callaghan M. “The effect of recombinant human lactoferrin on growth and the antibiotic susceptibility of the cystic fibrosis pathogen Burkholderia cepacia complex when cultured planktonically or as biofilms“. Antimicrob. Chemother. 2007; 60: 546–554.
Cardile V, Proietti L, Panico A, Lombardo L. “Nitric oxide production in fluoro-edenite treated mouse monocyte-macrophage cultures“. Oncol. Rep. 2004; 12(6): 1209-1215.
Chen PH, Tseng YH, Mou Y, Tsai YL, Guo SM, Huang SJ, Yu SS, Chan JC. “Adsorption of a statherin peptide fragment on the surface of nanocrystallites of hydroxyapatite“. J. Am. Chem. Soc. 2008; 130: 2862–2868
Chen Y, Zheng X, Xie Y, Ji H, Ding C, Li H, Dai K. “Silver release from silver-containing hydroxyapatite coatings“. Surf. Coat. Tech. 2010; 205: 1892–1896.
Chiu CH, Ou JT. “Rapid identification of Salmonella serovars in feces by specific detection of virulence genes, invA and spvC, by an enrichment broth culture-multiplex PCR combination assay“. J. Clin. Microbiol. 1996; 34: 2619–2622.
Clarke B. “Normal bone anatomy and physiology“. Clin. J. Am. Soc. Nephrol. 2008; 3:S131-139.
Crouch SPM, Slate KJ, Fletcher J. “Regulation of cytokine release from mononuclear cells by the iron-binding protein lactoferrin“. Blood. 1992; 80: 235–240.
Cunningham FE, Proctor VA, Goetsch SJ. “Egg white lysozyme as food preservative: an overview“. Worlds Poult. Sci. J. 1991; 47: 141–163.
Damiens E, Yazidi I, Mazurier J, Duthile I, Spik G, Boilly-Marer Y. “Lactoferrin inhibits G1 cyclin-dependent kinases during growth arrest of human breast carcinoma cells“. J. Cell. Biochem. 1999; 74: 486–498.
Darouiche RO. “Treatment of infections associated with surgical implants“. Infect. Dis. Clin. Pract. 2004; 12: 258–259.
Davidson PM, Taylor MT. “Chemical preservatives and natural antimicrobial compounds“. In: Doyle P, Beuchat LR, Montville TJ, editors. Food microbiology: fundamentals and frontiers. Washington, D.C. American Society for Microbiology Press. 2007; pp. 713–734.
De Groot K, Wolke J. “Calcium phosphate coatings for medical implants“. Proc. Instn. Mech. Eng. 1998; 212H:137–147.

Dee KC, Puleo DA, Bizios R. “An Introduction to Tissue Biomaterial Interactions“. Wiley-Liss, Hoboken, NJ, USA; 2003.
Domenech J, Tinti A, Torreggiani A. “Biopolymer Research Trends“ (Ed:T.S. Nemeth), Nova Science Publishers, New York, 2007; pp. 11.
Dorman HJD, Deans SG. “Antimicrobial agents from plants: antibacterial activity of plant volatile oils“. J. Appl. Microbiol. 2000; 88(2): 308–16.
Dorozhkin SV. “Nanodimensional and nanocrystalline calcium orthophosphates“. Am. J. Biomed. Eng. 2012; 2: 48-97.
Drago SME. “Actividad es antibacterianas de la lactoferrina“. Enferm. Infecc. Microbiol. 2006; 26: 58–63.
Duarte DC, Nicolau A, Teixeira JA, Rodrigues LR. “The effect of bovine milk lactoferrin on human breast cancer cell lines“. J. Dairy Sci. 2011; 94: 66–76.
Ellison RT, Giehl TJ, Laforce FM. “Damage of the membrane of enteric Gram negative bacteria by lactoferrin and transferring“. Infect. Immun. 1988; 56: 2774–2781.
Falini G, Fermani S, Foresti E, Parma B, Rubini K, Sidoti MC, Roveri N. “Films of self-assembled purely helical type I collagen molecule“. J. Mater. Sci. 2004; 14: 2297 - 2302.
Farkas J. “Physical methods of food preservation“. In: Doyle P, Beuchat LR, Montville TJ, editors. Food microbiology: fundamentals and frontiers. Washington, D.C.: American Society for Microbiology Press. 2007; pp. 685–705.
Fox K, Tran PA, Tran N. “Recent advances in research application of nanophase hydroxyapatite“. Chem. Phys. Chem. 2012; 13: 2495-2506.
Gálvez A, Abriouel H, López RL, Omar NB. “Bacteriocin-basedstrategiesfor food biopreservation“. Int.J.Food Microbiol. 2007; 120: 51–70.
Gonzalez-Chavez SA, Arevalo-Gallegos S, Rascon-Cruz Q. “Lactoferrin: structure, function and applications“. Int. J. Antimicrob. Agents 2009; 33: 301.e1–301.e8.
Gould IM, Bal AM. New antibiotic agents in the pipeline and how they can help overcome microbial resistance. Virulence. 2013; 4: 185–191.
Groot F, Geijtenbeek TB, Sanders RW, Baldwin CE, Sanchez-Hernandez M, Floris R, van Kooyk Y, de Jong EC, Berkhout B. “Lactoferrin prevents dendritic cell mediated human immunodeficiency virus type 1 transmission by blocking the DC-SIGN–gp120 interaction“. J. Virol. 2005; 79: 3009–3015.
Gutierrez J, Barry-Ryan C, Bourke P. “Antimicrobial activity of plant essential oils using food model media: efficacy, synergistic potential and interactions with food components“. Food Microbiol. 2009; 26(2): 142–150.
Gutierrez J, Barry-Ryan C, Bourke P. “The antimicrobial efficacy of plant essential oil combinations and interactions with food ingredients“. Int. J. Food Microbiol. 2008; 124(1): 91–97.
Hara K, Ikeda M, Saito S, Matsumoto S, Numata K, Kato N, Tanaka K, Sekihara H. “Lactoferrin inhibits hepatitis B virus infection in cultured human hepatocytes“. Hepatol. Res. 2002; 24: 228.
Hasegawa K, Motsuchi W, Tanaka S, Dosako S. “Inhibition with lactoferrin of in vitro infection with human herpes virus“. J. Med. Sci. Biol. (Jpn). 1994; 47: 73–85.
Haversen L, Ohlsson BG, Hahn-Zoric MG, Hanson LA, Mattsby-Baltzer I. “Lactoferrin down-regulates the LPS-induced cytokine production in monocytic cells via NF-kappa B“. Cell. Immunol. 2002; 220: 83–95.
Hayes TG, Falchook GF, Varadhachary GR, Smith DP, Davis LD, Dhingra HM, Hayes BP, Varadhachary A. “Phase I trial of oral talactoferrin alfa in refractory solid tumors“. Invest. New Drugs. 2006; 24: 233–240.

Hernandez-Hernandez A, Rodrıguez-Navarro AB, Gomez-Morales J, Jimenez-Lopez C, Nys Y, Garcıa-Ruiz JM. "Influence of model globular proteins with different isoelectric points on the precipitation of calcium carbonate". Cryst.Growth Des. 2008; 8: 1495–1502.
Hofbauer LC, Brueck CC, Shanahan CM, Schoppet M, Dobnig H. "Vascular calcification and osteoporosis e from clinical observation towards molecular understanding". Osteoporos Int. 2007; 18: 251e9.
Iafisco M, Di Foggia M, Bonora S, Prat M, Roveri N. "Adsorption and spectroscopic characterization of lactoferrin on hydroxyapatite nanocrystals". Dalton Trans. 2011; 40: 820–827.
Iigo M, Shimamura M, Matsuda E, Fujita K, Nomoto H, Satoh J, Kojima S, Moore MA, Tsuda H. "Orally administered bovine lactoferrin induces caspase-1 and interleukin-18 in the mouse intestinal mucosa: a possible explanation for inhibition of carcinogenesis and metastasis". Cytokine. 2004; 25: 36–44.
Ikeda M, Nozakia A, Sugiyama K, Tanaka T, Naganuma A, Tanaka K, Sekihara H, Shimotohno K, Saito M, Kato N. "Characterization of antiviral activity of lactoferrin against hepatitis C virus infection in human cultured cells". Virus Res. 2000; 66: 51–63.
Ikeda M, Sugiyama K, Tanaka T, Tanaka K, Sekiharab H, Shimotohno K, Kato N. Lactoferrin markedly inhibits hepatitis C virus infection in cultured human hepatocytes". Biochem. Biophys. Res. Commun. 1998; 245: 549–553.
Jack KS, Vizcarra TG, Trau M. "Characterization and surface properties of amino-acid-modified carbonate-containing hydroxyapatite particles". Langmuir. 2007; 23: 12233 -12242.
Janezic KJ, Ferry B, Hendricks EW, Janiga BA, Johnson T, Murphy S, Roberts ME, Scott SM, Theisen AN, Hung KF, Daniel SL. "Phenotypic and genotypic characterization of Escherichia coli isolated from untreated surface waters. Open Microbiol. J. 2013; 7: 9–19.
Jiang Y, Li Y. "Effects of chitosan coating on postharvest life and quality of longan fruit". Food Chem. 2001; 73: 139–143.
Jun S, Hong Y, Imamura H, Ha BY, Bechhoefer J, Chen P. "Self-Assembly of the Ionic Peptide EAK16: The Effect of Charge Distributions on Self-Assembly". Biophys. J. 2004; 87: 1249–1259.
Kandori K, Fudo A, Ishikawa T. "Adsorption of myoglobin onto various synthetic hydroxyapatite particles". Phys. Chem. Chem. Phys. 2000; 2: 2015 -2020.
Kane SV, Sandborn WJ, Rufo PA, Zholudev A, Boone J, Lyerly D, Camilleri M, Hanauer SB. "Fecal lactoferrin is a sensitive and specific marker in identifying intestinal inflammation". Am. J. Gastroenterol. 2003; 98: 1309–1314.
Karunakar K, Priya A, Bryan MA, Persikov AV, Mohs A, Wang YH, Brodsky B. "Self-association of collagen triple helix peptides into higher order structures". J. Biol. Chem. 2006; 281: 33283 –33290.
Kerry JP, O'Grady MN,Hogan SA. "Past, current and potential utilization of active and intelligent packaging systems for meat and muscle-based products: a review". Meat Sci. 2006; 74: 113–130.
Kim TN, Feng QL, Kim JO, Wu J, Wang H, Chen GC, Cui FZ. "Antimicrobial effects of metal ions (Ag^{+}, Cu^{2+}, Zn^{2+}) in hydroxyapatite". J. Mater. Sci. Mater. Med. 1998; 9: 129–134.
Koutsopoulos S. "Synthesis and characterization of hydroxyapatite crystals: a review study on the analytical methods". J. Biomed. Mater. Res. 2002; 62: 600 -612.

Kozu T, Iinuma G, Ohashi Y, Saito Y, Akasu T, Saito D, Alexander DB, Iigo M, Kakizoe T, Tsuda H. “Effect of orally administered bovine lactoferrin on the growth of adenomatous colorectal polyps in a randomized, placebo-controlled clinical trial Takahiro Kozu“. Cancer Prev. Res. 2009; 2: 975–983.
Kruzel ML, Bacsi A, Choudhury B, Sur S, Boldogh I. “Lactoferrin decreases pollen antigen-induced allergic airway inflammation in a murine model of asthma“. Immunology. 2006; 119: 159–166.
Kruzel ML, Harari Y, Mailman D, Actor JK, Zimecki M. “Differential effects of prophylactic, concurrent and therapeutic lactoferrin treatment on LPS-induced inflammatory responses in mice“. Clin. Exp. Immunol. 2002; 130: 25–31.
Kuorwel KK, Cran MJ, Sonneveld K, Miltz J, Bigger SW. “Essential Oils and Their Principal Constituents as Antimicrobial Agents for Synthetic Packaging Films”. J. Food Sci. 2011; 76(9): R164-177.
Kurose I, Yamada T, Wolf R, Granger DN. “P-selectin-dependent leukocyte recruitment and intestinal mucosal injury induced by lactoferrin“. J. Leuckoc. Biol. 1994; 55: 771–777.
Latour RA. “In the biomaterials field, its study is fundamental: to learn more about the biomineralization process in vivo, but also to test the material performance in the biological environment“. Biointerphases. 2008; 3: FC2–FC12.
Legrand D, Elass E, Carpentier M, Mazurier J. “Interaction of lactoferrin with cells involved in immune function“. Biochem. Cell Biol. 2006; 84: 282–290.
Legrand D, Elass E, Carpentier M, Mazurier J. “Lactoferrin: a modulator of immune and inflammatory responses“. Cell Mol. Life Sci. 2005; 62: 2549–2559.
Legrand D, Vigie´ K, Said EA, Elass E, Masson M, Slomianny MC, Carpentier M, Briand JP, Mazurier J, Hovanessian AG. “Surface nucleolin participates in both the binding and endocytosis of lactoferrin in target cells“. Eur. J. Biochem. 2004; 271: 303–317.
Leitch EC, Willcox MD. “Lactoferrin increases the susceptibility of S. epidermidis biofilms to lysozyme and vancomycin“. Curr. Eye Res. 1999; 19: 12–19.
Lelli M, Foltran I, Foresti E, Martinez-Fernandez J, Torres-Raya C, Varela-Feria FM, Roveri N. “Biomorphic silicon carbide coated with an electrodeposition of nanostructured hydroxyapatite/collagen as biomimetic bone filler and scaffold“. Adv. Biomater. 2010;12 (8): 348B – 355B.
Lopez-Pedemonte TJ, Roig-Sagues AX, Trujillo AJ, Capellas M, Guamis B. “Inactivation of sporesof Bacillus cereus in cheese by high hydrostatic pressure with the addition of nisin or lysozyme“. J. Dairy Sci. 2003; 86: 3075–3081.
Lopez-Rubio A, Almenar E, Hernandez-Munoz P, Lagaron JM, Catala R, Gavara R. “Overview of active polymer-based packaging technologies for food applications“. Food. Rev. Int. 2004; 20(4): 357–387.
Lucera A, Costa C, Conte A, Del Nobile MA. “Food applications of natural antimicrobial compounds“. Front. Microbiol. 2012; 3: 287
Machnicki M, Zimecki M, Zagulski T. “Lactoferrin regulates the release of tumor necrosis factor alpha and interleukin in vivo“. Int. J. Exp. Pathol. 1993; 74: 433–439.
Manara S, Paolucci F, Palazzo B, Marcaccio M, Foresti E,Tosi G, Sabbatini S, Sabatino P, Altankov G, Roveri N. “Electrochemically-assisted deposition of biomimetic hydroxyapatite–collagen coatings on titanium plate“. Inorg. Chim. Acta 2008; 361: 1634 - 45.
Mangena T and Muyima NYO. “Comparative evaluation of the antimicrobial activities of essential oils of Artemisiaafra, Pteroniaincana and Rosemarinus officinalis on selected bacteria and yeast strains“. Lett. Appl. Microbiol.1999; 28: 291–296.

Mann S. “Biomimetic materials chemistry”. Wiley-VCH, Weinheim; 1997.
Marchetti M, Superti F, Ammendolia MG, Rossi P, Valenti P, Seganti L. “Inhibition of poliovirus type 1 infection by iron-, manganese-, and zinc-saturated lactoferrin“. Med. Microbiol. Immunol. (Berl). 1999; 187: 199–204.
Marino M, Bersani C, Comi G. “Impedance measurement to study a ntimicrobial activity of essential oils from Lamiaceae and Compositae“. Int. J. Food Microbiol. 2001; 67: 187–195.
Marr AK, Jenssen H, Roshan Moniri M, Hancock REW, Panté N. “Bovine lactoferrin and lactoferricin interfere with intracellular trafficking of Herpes simplex virus-1“. Biochimie. 2009; 91: 160–164.
Molle P, Lienard A, Gramsik A, Iwema A, Kabbabi A. “Apatite as an interesting seed to remove phosphorus from wastewater in constructed wetlands“. Water Sci. Technol. 2005; 51: 193-203.
Nakajima K, Kanno Y, Nakamura M, Gao XD, Kawamura A, Itoh F, Ishisaki A. “Bovine milk lactoferrin induces synthesis of the angiogenic factors VEGF and FGF2 in osteoblasts via the p44/p42 MAP kinase pathway“. BioMetals. 2011; 23: 1–10.
No HK, Meyers SP, Prinyawiwatkul W, Xu Z. “Application of chitosan for improvement of quality and shelf life of foods: a review“. J. Food Sci.2007; 72: 100–187.
Norrby K, Mattsby-Baltzer I, Innocenti M, Tuneberg S. “Orally administered bovine lactoferrin systemically inhibits VEGF-mediated angiogenesis in the rat“. Int. J. Cancer.2001; 91: 236–240.
Odeh R, Quinn JP. “Problem pulmonary pathogens: Pseudomonas aeruinosa“. Semin. Respir. Crit. Care Med. 200; 21: 331–339.
Oonishi H, Hench LL, Wilson J, Sugihara F, Tsuji E, Kushitani S, Iwaki H. “Comparative bone growth behavior in granules of bioceramic materials of various sizes“. J. Biomed. Mater. Res. 1999; 44: 31–43.
Oonishi H. “Orthopaedic applications of hydroxyapatite“. Biomaterials. 1991; 12: 171–178.
Öztaş YE, Özgüneş N. “Lactoferrin: a multifunctional protein“. Adv. Mol. Med. 2005; 1: 149–154.
Palazzo B, Iafisco M, Laforgia M, Margiotta N, Natile G, Bianchi CL, Walsh D, Mann S, Roveri N. “Biomimetic hydroxyapatite-drug nanocrystals as potential bone substitutes with antitumor drug delivery properties“. Adv. Funct. Mater. 2007; 17: 2180 -2188.
Palazzo B, Walsh D, Iafisco M, Foresti E, Bertinetti L, Martra G, Bianchi CL, Cappelletti G, Roveri N. “Amino acid synergetic effect on structure, morphology and surface properties of biomimetic apatite nanocrystals“. Acta Biomater. 2009; 5: 1241–1252.
Pan F, Zhao X, Waigh TA, Lu JR, Miano F. “Interfacial adsorption and denaturization of human milk and recombinant rice lactoferrin“. Biointerphases. 2008; 3: FB36–FB47.
Park K. “Nanotecnology: what it can do for drug delivery? “ J. Control. Release 2007; 120: 1 -3.
Patel N, Best SM, Bonfield W, Gibson IR, Hing KA, Damien E, Revell PA. “A comparative study on the in vivo behavior of hydroxyapatite and silicon substituted hydroxyapatite granules“. J. Mater. Sci. Mater. Med. 2002; 13: 1199–1206.
Porter AE, Patel N, Skepper JN, Best SM, Bonfield W. “Effect of sintered silicate-substituted hydroxyapatite on remodelling processes at the bone-implant interface“. Biomaterials. 2004; 25: 3303–3314.

Rameshbabu N, Kumar TSS, Prabhakar TG, Sastry VS, Murty KVGK, Rao KP. "Antibacterial nanosized silver substituted hydroxyapatite: synthesis and characterization". J. Biomed. Mater. Res. 2007; 80A :581–591.
Re R, Pellegrini N, Proteggente A, Pannala A, Min Y, Rice-Evans C. "Antioxidant activity applying an improved abts radical cation decolorization assay". Free Radic. Biol. Med. 1999; pp. 1231–1237.
Ricke SC. "Perspectives on the use of organic acid and short chain fatty acid as antimicrobials". Poult. Sci.2003; 82: 632–639.
Rodríguez DA, Vázquez L, Ramos G. "Actividad Antimicrobiana de la lactoferrina: Mecanismos and aplicaciones clinic as potenciales". Rev. Latinoam. Microbiol. 2005; 47; 102–111.
Roseanu P, Florian M, Condei D, Cristea M. " Antibacterial activity of lactoferrin and lactoferricin against oral Streptococci". Rom. Biotechnol. Lett. 2010; 15: 5788–5792.
Roveri N, Palazzo B, Iafisco M. "The role of biomimetism in developing nanostructured inorganic matrices for drug delivery". Expert. Opin. Drug. Deliv. 2008; 5: 861–877.
Roveri N, Palazzo B. "Tissue, cell and organ engineering". Wiley-VCH, Weinheim; 2006.
Roveri N,Falini G, Sidoti MC,Tampieri A, Landi E, Sandri M and Parma B. "Biologically inspired growth of hydroxyapatite nanocrystals inside self-assembled collagen fibers". Mater. Sci. Eng. 2003; 23, 441:- 446.
Rozalska B and Wadstrom T. "Interferon-γ, interleukin-1 and tumor necrosis factor-α synthesis during experimental murine staphylococcal infection". FEMS Immunol. Med. Microbiol. 1993; 7: 145-152.
Sanchez C, Hervé Arribart H, Guille MMG. "Biomimetism and bioinspiration as tools for the design of innovative materials and systems". Nat. Mater. 2005; 4: 277 -288.
Sarikaya M, Aksay I. Biomimetics. "Design and processing of materials". Washington Univ Seattle Dept of Materials Science and Engineering; 1995.
Sarikaya M, Tamerler C, Jen AKY, Schulten K, Baneyx F. "Molecular biomimetics: nanotechnology through biology". Nat. Mater. 2003; 2: 577 -585.
Sato R, Inanami O, Tanaka Y, Takase SE, Naito Y. "Oral administration of bovine lactoferrin for treatment of intractable stomatitis in feline immunodeficiency virus (FIV)-positive and (FIV)-negative cats". Am. J. Vet. Res. 1996; 57: 1443–1446.
Sfeir RM, Dubarry M, Boyaka PN, Rautureau M, Tome D. "The mode of oral bovine lactoferrin administration influences mucosal and systemic immune responses in mice". J. Nutr. 2004; 134: 403–409.
Shelef L, Seiter J. "Indirect antimicrobials" . *Antimicrobials in Food*, 2nd Edn. Eds P.M. Davidson and A.L. Braner (NewYork,NY: Marcel Dekker). 1993; pp. 544–555.
Shimamura M, Yamamoto Y, Ashino H, Oikawa T, Hazato T, Tsuda H, Ligo M, "Bovine lactoferrin inhibits tumor-induced angiogenesis". Int. J. Cancer. 2004; 111: 111–116.
Shimizu K, Matsuzawa H, Okada K, Tazume S, Dosako S, Kawasaki Y, Hashimoto K, Koga Y. "Lactoferrin-mediated protection of the host from murine cytomegalovirus infection by T-cell-dependent augmentation of natural killer cell activity". Arch. Virol. 1996; 141: 1875–1889.
Singh PK, Parsek MR, Greenberg EP, Welsh MJ. "A component of innate immunity prevents bacterial biofilm development". Nature. 2002; 417: 552–555.
Skandamis PN, Nyachas GJE. "Preservation of fresh meat with active and modified atmosphere packaging conditions". Int. J. Food Microbiol. 2002; 79: 35–45.

Sobrino-Lopez A, Martin-Belloso O. “Enhancing inactivation of Staphylococcus aureus in skim milk by combining high-intensity pulsed electric fields and nisin“. J. FoodProt. 2006; 69: 345–353.
Sorimachi K, Akimoto K, Hattori Y, Ieiri T, Niwa A. “Activation of macrophages by lactoferrin: secretion of TNF-alpha, IL-8 and NO“. Biochem. Mol. Biol. Int. 1997; 3: 79–87.
Swart PJ, Kuipers ME, Smit C, Pauwels R, De Béthune MP, De Clercq E, Meijer DFK, Huisman JG. “Antiviral effects of milk proteins: acylation results in polyanionic compounds with potent activity against human immunodeficiency virus types 1 and 2 in vitro“. AIDS Res. Hum. Retroviruses. 1996; 12: 769–775.
Szuter CA, Kaminska T, Kandefer SM. “Phagocytosis-enhancing effect of lactoferrin on bovine peripheral blood monocytes in vitro and in vivo“. Arch. Vet. 1995; 35: 63–71.
Tamerler C, Sarikaya M. “Molecular biomimetics: utilizing nature’s molecular ways in practical engineering“. Acta Biomater. 2007; 3: 289 -299.
Tampieri A, Celotti G, Landi E. “From biomimetic apatites to biologically inspired composites“. Anal. Bioanal. Chem. 2005; 381: 568 -576.
Tanaka HK, Miyajima K, Nakagaki M, Shimabayashi S. “Interactions of aspartic acid, alanine and lysine with hydroxyapatite“. Chem. Pharm. Bull. 1989; 37: 2897 -2901.
Thian ES, Huang J, Best SM, Barber ZH, Brooks RA, Rushton N, Bonfield W. “The response of osteoblasts to nanocrystalline silicon-substituted hydroxyapatite thin films“. Biomaterials. 2006; 27: 2692–2698.
Thian ES, Konishi T, Kawanobe Y, Lim PN, Choong C, Ho B, Aizawa M. “Zinc-substituted hydroxyapatite: a biomaterial with enhanced bioactivity and antibacterial properties“. J. Mater. Sci. Mater. Med. 2013; 24: 437–445.
Tinti A. Di Foggia M, Taddei P, Torreggiani A, Dettin M and Fagnano C. “Vibrational study of auto-assembling oligopeptides for biomedical applications“. J. Raman Spectrosc. 2008; 39: 250–259.
Trinchieri G. “Interleukin-12 and the regulation of innate resistance and adaptive immunity“. Nat. Rev. Immunol. 2003; 3: 133–146.
Trinchieri G. “Interleukin-12: a proinflammatory cytokine with immunoregulatory functions that bridge innate resistance and antigen-specific adaptive immunity“. Annu. Rev. Immunol. 1995; 13: 251–276.
Uskokovic V, Uskokovic DP. “Nanosized hydroxyapatite and other calcium phosphates: chemistry of formation and application as drug and gene delivery agents“. J. Biomed. Mat. Res. 2011; 96B: 152-191.
Vaara M. “Agents that increase the permeability of the outer membrane“. Microbiol. Rev. 1992; 56: 395–411.
Van Der Strate BWA, Belijaars L, Molema G, Harmsen MC, Meijer DFK. “Antiviral activities of lactoferrin“. Antiviral Res. 2001; 52: 225–239.
Varadhachary A, Wolf JS, Petrak K, O'Malley BW Jr, Spadaro M, Curcio C, Forni G, Pericle F. “Oral lactoferrin inhibits growth of established tumors and potentiates conventional chemotherapy“. Int. J. Cancer. 2004; 111: 398–403.
Viani RM, Gutteberg TJ, Lathey JL, Spector SA. “Lactoferrin inhibits HIV-1 replication in vitro and exhibits synergy when combined with zidovudine“. AIDS. 1999; 13: 1273–1274.
Villacampa A, García-Ruiz JM. “Synthesis of a new hydroxyapatite-silica composite material“. J. Cryst. Growth. 2000; 211: 111 -115.
Wakabayashi H, Kondo I. “Periodontitis, periodontopathic bacteria and lactoferrin“. BioMetals. 2010; 23: 419–424.

Wakabayashi H, Takakura N, Yamauchi K, Yoshitaka T. “Modulation of immunerelated gene expression in small intestine of mice by oral administration of lactoferrin“. Clin. Vaccine Immunol. 2006; 13: 239–245.
Walsh D, Arcelli L, Swinerd V, Fletcher J, Mann S. “Aerosol-mediated fabrication of porous thin films using ultrasonic nebulization“. Chem. Mater. 2007; 19: 503 -508.
Wang WP, Ligo M, Sato J, Sekine K, Adachi I, Tsuda H. “Activation of mucosal intestinal immunity in tumor-bearing mice by lactoferrin“. J. Cancer Res. (Jpn). 2000; 91: 1022–1027.
Weinberg ED. “Suppression of bacterial biofilm formation by iron limitation“. Med. Hypotheses. 2004; 63: 863–865.
Weiner S, Addadi L. “Strategies in mineralized biological materials“. J. Mater. Chem. 1997; 7: 689 -702.
Wilson C. “Frontiers of intelligent and active packaging for fruits and vegetables“. Boca Raton, Fla: CRC Press. 2007; p. 360.
Xu XX, Jiang HR, Li HB, Zhang TN, Zhou Q, Liu N. “Apoptosis of stomach cancer cell SGC-7901 and regulation of Akt signaling way induced by bovine lactoferrin“. J. Dairy Sci. 2010; 93: 2344–2350.
Yoo YC, Watanabe R, Koike Y, Mitobe M, Shimazaki K, Watanabe S, Azuma I. “Apoptosis in human leukemic cells induced by lactoferricin, a bovine milk protein-derived peptide: involvement of reactive oxygen species“. Biochem. Biophys. Res. Commun. 1997; 237: 624–628.
Zemann N, Klein P, Wetzel E, Huettinger F, Huettinger M. “Lactoferrin induces growth arrest and nuclear accumulation of Smad-2 in HeLa cells“. Biochimie 2010; 92: 880–884.
Zhu D, Mackenzie NCW, Farquharson C, MacRae VE. “Mechanisms and clinical consequences of vascular calcification“. Front. Endocrinol. 2012; 3:95.
Zimecki M, Dawiskiba J, Zawirska B, Krawczyk Z, Kruzel M. “Bovine lactoferrin decreases histopathological changes in the liver and regulates cytokine production by splenocytes of obstructive jaundiced rats“. Inflamm. Res. 2003; 52: 305–310.
Zimecki M, Spiegel K, Wlaszczyk A, Kubler A, Kruzel ML. “Lactoferrin increases the output of neutrophil precursors and attenuates the spontaneous production of TNF-alpha and IL-6 by peripheral blood cells“. Arch. Immunol. Ther. Exp. (Warsz). 1999; 47: 113–118.
Zimecki M, Wlaszczyk A, Wojciechowski R, Dawiskiba J, Kruzel M. “Lactoferrin regulates the immune responses in post-surgical patients“. Arch. Immunol. Ther. Exp. 2001; 49: 325–333.

LABORATORIES

Dates (from-to)	07/02/2015 – to date
Occupation or position held	PhD Student
Main activities	Data analyses of biological characterization of lactoferrin adsorbed onto hydroxyapatite and its application as food packaging system
Name and address of employer	Immunology laboratory – University of Naples "Federico II"
Dates (from-to)	08/01/2015 – 06/02/2015
Occupation or position held	Visiting PhD Student
Main activities	Bacterial genome sequencing
Name and address of employer	SEQUENTIA BIOTECH SL
Dates (from-to)	15/11/2014 – 07/01/2015
Occupation or position held	PhD Student
Main activities	Application of lactoferrin adsorbed onto hydroxyapatite nanocrystal in food packaging system and data analyses
Name and address of employer	Immunology laboratory – University of Naples "Federico II"
Dates (from-to)	11/11/2014 – 14/11/2014
Occupation or position held	Visiting PhD Student
Main activities	Application of lactoferrin adsorbed onto hydroxyapatite nanocrystal in food packaging system
Name and address of employer	Chemical Center Srl – Castello D'argile (Bologna)

Dates (from-to)	04/09/2013 – 10/11/2014
Occupation or position held	PhD Student
Main activities	Biological characterization of lactoferrin adsorbed onto hydroxyapatite and its application as food packaging system
Name and address of employer	Immunology laboratory – University of Naples “Federico II”

Dates (from-to)	10/07/2013 – 03/09/2013
Occupation or position held	Visiting PhD Student
Main activities	Influence of different concentration of allergen Ara h 2 in dessert matrix on exctraction method and immunogenicity
Name and address of employer	Institute of Inflammation and Repair, Manchester Institute of Biotechnology, University of Manchester

Dates (from-to)	01/03/2012 – 09/07/2013
Occupation or position held	PhD Student
Main activities	Biological characterization of lactoferrin adsorbed onto hydroxyapatite
Name and address of employer	Immunology laboratory – University of Naples “Federico II”

PUBBLICATIONS

Nocerino N, **Fulgione A**, Iannaccone M, Tomasetta L, Ianniello F, Martora F, Lelli M, Roveri N, Capuano F, Capparelli R. Biological activity of lactoferrin-functionalized biomimetic hydroxyapatite nanocrystals. Int J Nanomedicine. 2014 Mar 5;9:1175-84. doi: 10.2147/IJN.S55060;

Avitabile C, Capparelli R, Rigano MM, **Fulgione A**, Barone A, Pedone C and Romanelli A. Antimicrobial peptides from plants: stabilization of the γ core of a tomato defensin by intramolecular disulfide bond. J Pept Sci. 2013 Apr;19(4):240-5. doi: 10.1002/psc.2479;

Rigano MM, Romanelli A, **Fulgione A**, Nocerino N, D'Agostino N, Avitabile C, Frusciante L, Barone A, Capuano F, Capparelli R. A novel synthetic peptide from a tomato defensin exhibits antibacterial activities against Helicobacter pylori. J Pept Sci. 2012 Dec;18(12):755-62. doi: 10.1002/psc.2462;

Capparelli R, De Chiara F, Nocerino N, Montella RC, Iannaccone M, **Fulgione A**, Romanelli A, Avitabile C, Blaiotta G, Capuano F. New perspectives for natural antimicrobial peptides: application as antinflammatory drugs in a murine model. BMC Immunol. 2012 Nov 17;13:61. doi: 10.1186/1471-2172-13-61.

COMMUNICATIONS AND PATENT

Rigano MM, Romanelli A**, Fulgione A**, Nocerino N, D'Agostino N, Avitabile C, Barone A, Capparelli R. Identification, synthesis and antibacterial activity of a novel antimicrobial peptide from tomato. Federazione Italiana della Vita. 12th Congress. September 24-27, 2012;

Rigano MM, Romanelli A, **Fulgione A**, Nocerino N, D'Agostino N, Avitabile C, Barone A, Capparelli R. A novel antimicrobial peptide from a tomato defensins exhibits antibacterial activities. Annual Congress of the Italian Society of Agricultural Gentics. Perugia (Italy) September 17-20, 2012;

Rigano MM, Romanelli A, **Fulgione A**, Nocerino N, D'Agostino N, Avitabile C, Barone A, Capparelli R. Identification, synthesis and characterization of a novel antimicrobial peptide from Solanum lycopersicum. 13th Naples Workshop on Bioactive Peptides. Naples (Italy) June 7-10, 2012;

Fiori M, Nocerino N, Capparelli R, **Fulgione A**, Van Der Jagt M, Medaglia C, Marchetti M, Roveri N, Mercuri R, Lelli M, Rinaldi F. Preparing antibacterial polymer e.g. polypropylene used to prepare antibacterial product e.g. computer keyboard involves adding solution/dispersion of zinc to a solution/dispersion of monomer in solvent and polymerizing. Patent Number(s): US2014296442-A1 ; CA2825299-A1 ; WO2014155156-A1.

International Journal of Nanomedicine

Dovepress

open access to scientific and medical research

Open Access Full Text Article

ORIGINAL RESEARCH

Biological activity of lactoferrin-functionalized biomimetic hydroxyapatite nanocrystals

Nunzia Nocerino[1]
Andrea Fulgione[1]
Marco Iannaccone[1]
Laura Tomasetta[1]
Flora Ianniello[1]
Francesca Martora[1]
Marco Lelli[2]
Norberto Roveri[2]
Federico Capuano[3]
Rosanna Capparelli[1]

[1]Department of Agriculture Special Biotechnology Center Federico II, CeBIOTEC Biotechnology, University of Naples Federico II, Naples, [2]Department of Chemistry, G Ciamician, Alma Mater Studiorum, University of Bologna, Bologna, [3]Department of Food Inspection IZS ME, Naples, Italy

Correspondence: Rosanna Capparelli
Department of Agriculture Special Biotechnology Center Federico II, CeBIOTEC Biotechnology, University of Naples, Federico II, Via Università 100, Portici 80055, Naples, Italy
Tel +39 08 1253 9274
Fax +39 08 1776 2886
Email capparel@unina.it

Abstract: The emergence of bacterial strains resistant to antibiotics is a general public health problem. Progress in developing new molecules with antimicrobial properties has been made. In this study, we evaluated the biological activity of a hybrid nanocomposite composed of synthetic biomimetic hydroxyapatite surface-functionalized by lactoferrin (LF-HA). We evaluated the antimicrobial, anti-inflammatory, and antioxidant properties of LF-HA and found that the composite was active against both Gram-positive and Gram-negative bacteria, and that it modulated proinflammatory and anti-inflammatory responses and enhanced antioxidant properties as compared with LF alone. These results indicate the possibility of using LF-HA as an antimicrobial system and biomimetic hydroxyapatite as a candidate for innovative biomedical applications.

Keywords: lactoferrin, hydroxyapatite nanocrystals, biomimetism, biological activity, drug delivery

Introduction

The widespread use of antibiotics has generated bacterial strains resistant to multiple antibiotics, sometimes resulting in very low therapeutic efficiency. For this reason, the demand for new antibiotics has been constant for almost 10 years.[1] Antimicrobial peptides or proteins represent a source of "natural antibiotics", and have been found in a wide range of organisms (bacteria, plants, insects, amphibians, and mammals) where they play an important role in defense.[2–6] Lactoferrin (LF) is an antimicrobial protein that was first identified in bovine milk and later in neutrophil granules, as well as in mucosal secretions, such as saliva and the nasal and bronchial secretions of various mammalian species, including man, goat, horse, and rodents.[7,8] LF is a nonheme glycoprotein with a molecular weight of about 80 kDa and is a part of the transferrin protein family, so is one of the proteins capable of binding and transferrin Fe^{3+} ions in serum. LF has good iron-binding affinity and is the only transferrin with the ability to retain this metal over a wide pH range.[9,10] LF also exhibits good resistance to proteolysis by trypsin and trypsin-like enzymes, and the level of resistance is proportional to the degree of iron saturation. At physiological pH, the LF molecule has a net positive charge and its distribution in various tissues makes it a multifunctional protein. LF is involved in several physiological functions, including regulation of iron absorption in the bowel, the immune response, participation in antioxidant, anticarcinogenic, and anti-inflammatory activity, and antimicrobial infection.[7]

submit your manuscript | www.dovepress.com
Dovepress
http://dx.doi.org/10.2147/IJN.S55060

The antimicrobial activity of LF is mostly due to two mechanisms. The first is the ability of LF to chelate iron with the microorganisms that require this metal, thereby depriving them of the source of this nutrient.[11] The second mechanism is related to the ability of LF to interact with the cell membrane on some bacteria, leading to changes in permeability and causing lysis, with the release of lipopolysaccharide from the outer membrane of Gram-negative bacteria.[7] It has been shown that LF can be synthesized de novo during certain bacterial infections, and this finding supports the idea that LF has an important role in defending its host; in fact, LF can act via iron deprivation or direct antimicrobial activity.[8,12] Thermal analysis characterization of LF has been well reported in the literature,[13,14] demonstrating that iron bound to LF confers more resistance to thermal denaturation, as well as to proteolytic protein digestion.

Interaction between proteins and different kinds of inorganic surfaces, like hydroxyapatite (HA) nanocrystals, biogenic silica, carbonates, and phosphate, plays an important role in many applications, including medicine, pharmacy, nanodevices, biosensors, and bioengineering.[15,16] Interesting research results concern the interaction with myoglobin or alendronate bioconjugates to check the ability of an inorganic biomaterial as a carrier for bioactive molecules and drugs. Biomimetic materials appear to be function mainly as drug delivery agents.[17]

Biomimetic HA crystals can be synthesized as non-stoichiometric carbonated HA crystals with a length of about 100 nm, a width of 20–30 nm, and a thickness of 3–6 nm, resembling the nanoscale-dimensioned plate-shaped morphology of bone crystals. Biomimetic HA crystals need to be synthesized in nanoscale dimensions, but with specific physicochemical properties, including a plate-shaped morphology, a low degree of crystallinity, a nonstoichiometric composition, surface crystalline disorder, and presence of carbonate ions in the crystal lattice. It is well known that HA shows a high affinity for proteins and a wide variety of biological molecules; for example, HA is widely used for the separation of various proteins in high performance liquid chromatography systems.[18,19] LF is adsorbed onto biomimetic HA nanocrystals at two different pH values (7.4 and 9.0). The positive electrostatic surface potential of LF at pH 7.4 allows strong surface interaction with the slightly negative HA nanocrystals and avoids protein-protein interaction, leading to formation of a coating protein monolayer. The nanosized HA does not appreciably affect the conformation of the adsorbed protein. Using Fourier transform-Raman and Fourier transform infrared (FT-IR), we found that, after adsorption, the protein was only slightly unfolded with a small fraction of the alpha-helix structure being converted into turn, while the beta-sheet content remained almost unchanged. The bioactive surface of HA functionalized with LF could be utilized to improve the material performance towards the biological environment for biomedical applications.[20–22]

A main challenge for innovative materials is the use of biomimetic HA nanocrystals surface-functionalized with bioactive molecules which can transfer information and operate specifically in the biological environment. In this work, we evaluated the biological activity and properties of biomimetic HA nanocrystals surface-functionalized with lactoferrin (LF-HA). This molecule shows good antimicrobial, immunomodulatory, and antioxidant properties, and our results indicate that LF-HA is an excellent candidate for overcoming antibiotic resistance.

Materials and methods

Preparation of biomimetic HA nanocrystals

Biomimetic HA [$Ca_5(PO_4)_3(OH)$] nanocrystals were synthesized according to a previously reported method.[23] Biomimetic HA nanocrystals were precipitated from an aqueous solution of $(CH_3COO)_2Ca$ (75 mM) by slow addition (one drop per second) of an aqueous solution of H_3PO_4 (50 mM), keeping the pH constant at 10 by addition of $(NH_4)OH$ solution.

Adsorption of LF

LF, a 97% pure protein fraction from cow's milk, was obtained from DMW International Ltd (Veghel, the Netherlands). All common high-purity chemical reagents were supplied by Sigma-Aldrich (St Louis, MO, USA). Ultrapure water (0.22 mS, 25°C) was used. Samples of adsorbed lactoferrin (LF-HA) were prepared by mixing 10 mg of HA with 1.5 mL of protein dissolved in HEPES buffer (0.01 M HEPES, 0.15 M NaCl) at pH 7.4 or in Tris buffer (0.01 M Tris, 0.15 M NaCl) at pH 9.0, with different concentrations (ranging from 0.1 to 10 mg/mL) in a 2 mL Eppendorf tube. The mixture was maintained in a bascule bath at 37°C for 24 hours. For the spectroscopic and thermal investigations, the solid was washed twice with ultrapure water and recovered by centrifuging at 10,000 rpm (12,700 g) for 3 minutes. The amount of adsorbed protein was determined by calculating the difference between the concentrations of the protein solutions before and after adsorption on HA nanocrystals.

Bacteria

The study included the following species: *Staphylococcus aureus A170*, *Listeria monocytogenes*, *Salmonella enterica* serovar Paratyphi, and *Escherichia coli*. Isolates were obtained from patients hospitalized at the Medical School, University of Naples. All bacteria were characterized using Biolog MicroStation™ System/MicroLog™ (User's guide version 5.2.01, Biolog, Hayward, CA, USA) and specimens were confirmed by polymerase chain reaction assay of the genes *Hsp 60* (*S. aureus*), *Mono A* (*L. monocytogenes*), *invA* (*S. enterica* serovar Paratyphi B), and *Stx1* (*E. coli*).[24–27] The bacteria were grown as described elsewhere.[5]

Antibacterial activity

The bacteria were distributed in triplicate into plates (60 µL per well), mixed with a series of dilutions of LF-HA (300–500 µg/mL, 40 µL per well), and incubated at 37°C for 20 hours. The minimal concentration of LF-HA causing 100% growth inhibition (MIC_{100}) was determined by measuring absorbance at 600 nm using a microplate reader (Model 680, Bio-Rad Hercules, CA, USA).[6]

Hemolytic activity

LF-HA was tested for its hemolytic activity using murine red blood cells. The hemolytic activity was measured according to the formula:

$$OD_{peptide} - OD_{negative\ control}/OD_{positive\ control} - OD_{negative\ control} \times 100$$

where the negative control (0% hemolysis) was represented by erythrocytes suspended in saline while the positive control (100% hemolysis) was represented by erythrocytes lysed with 1% Triton X-100.[6] The LC_{50} value was calculated as described elsewhere.[6]

Cell culture and trials of cytotoxicity

A human acute monocytic leukemia cell line (THP-1, American Tissue Culture Collection, Rockville, MD, USA) were cultured in complete medium consisting of Roswell Park Memorial Institute medium, 10% fetal bovine serum, 100 IU/mL penicillin, and 100 µg/mL streptomycin (all from Gibco, Paisley, Scotland). Cell adhesion was induced with phorbol myristate acetate (2 µg/mL per well). Cell viability and nitrite production were evaluated as described in another publication[6] at LF-HA concentrations of 300–500 µg/mL for 24, 48, and 72 hours. A lactate dehydrogenase (LDH) assay was performed using a CytoTox 96® Non-Radio cytotoxicity assay kit (Promega, Madison, WI, USA) at 2, 4, and 24 hours.

Antioxidant activity of LF-HA

The antioxidant activity of LF-HA was assessed as previously described.[28]

Enzyme-linked immunosorbent assay of inflammatory activity

THP-1 cells (10^6 cells per well) were stimulated with lipopolysaccharide 10 µg/mL for one hour. The THP-1 cells stimulated or not with lipopolysaccharide 10 µg/mL were then treated with LF-HA or acetylsalicylic acid 300 µg/mL for 2, 4, and 24 hours. Tumor necrosis factor (TNF)-α, interferon (IFN)-γ, interleukin (IL)-17, IL-8, IL-12, IL-6, IL-10, and IL-4 levels were assayed by enzyme-linked immunosorbent assay as reported elsewhere.[29]

Chemical analysis

Calcium and phosphorus content was determined by inductively coupled plasma-optical emission spectrometry (Liberty 200, Varian, Clayton South, Australia). HA and functionalized HA nanocrystals were dissolved in 1 wt% ultrapure nitric acid. The following analytical wavelengths were chosen: 422 nm for calcium and 213 nm for phosphorus.

Electron microscopy

Transmission electron microscopy investigations were carried out using a 1200 EX microscope fitted with link elemental dispersive X-ray analysis detectors and a 3010 UHR operating at 300 kV (JEOL Ltd, Tokyo, Japan). The powdered samples were ultrasonically dispersed in ultrapure water and a few droplets of the slurry were then deposited on perforated carbon foils supported on conventional copper microgrids. Scanning electron microscopy observations were carried out using an 840A microscope (JEOL Ltd). The specimens were mounted on aluminum stubs using carbon tape and covered with a coating of Au-Pd approximately 10 nm thick using a coating unit (Polaron Sputter Coater E5100, Polaron Equipment, Watford, UK).

X-ray diffraction analysis

X-ray diffraction powder patterns were collected using Analytical X'Pert Pro equipped with an X'Celerator detector powder diffractometer with Cu Ka radiation generated at 40 kV and 40 mA.

The degree of HA crystallinity was calculated according to the formula:

$$\text{Crystallinity} = 100 \times C/(A + C)$$

where C is the area of the peaks in the diffraction pattern ("the crystalline area") and A is the area between the peaks and the background ("the amorphous area").[30]

Determination of specific surface area

Measurements were done using a Sorpty 1750 instrument (Carlo Erba) using N_2 absorption at 77 K and the well known Brunauer, Emmett, and Teller procedure.[31]

X-ray photoelectron spectroscopy analysis

X-ray photoelectron spectroscopy measurements were performed using an M-Probe (Surface Science Instruments, Mountain View, CA, USA) equipped with a monochromatic Al Kα source (1,486.6 eV) with a spot size of 200 × 750 μm and a pass energy of 25 eV, providing a resolution of 0.74 eV. This equipment has a fixed degree of surface sensitivity due to the collection of photoelectrons at a fixed take-off electron emission angle of b=0° (relative to normal sample) between the X-ray axis and the electron analyzer axis (f=71° fixed, non variable). Surface analysis can be performed with a sampling volume that extends from the surface to a maximum depth of 40–50 Å. The accuracy of the reported binding energies was estimated to be ±0.2 eV. The quantitative data were also checked for accuracy and reproduced several times (at least ten times for each sample) and the percentage error was estimated to be ±1%.

Fourier transform and attenuated total reflectance infrared spectroscopy

Infrared spectra were recorded on a Nicolet 380 FT-IR spectrometer (Thermo Scientific, Baltimore, MD, USA) equipped with a commercial attenuated total reflectance accessory. The FT-IR spectra were recorded from 4,000 to 400 cm^{-1} at 2 cm^{-1} resolution using an IFS 66v/S spectrometer (Bruker Corporation, Karlsruhe, Germany) and KBr pellets. Spectra were collected by averaging 256 scans at 4 cm^{-1} resolution.

Analysis of zeta potential

Electrophoretic determinations were performed using DELSA apparatus (Beckman Coulter Inc., Pasadena, CA, USA). A DELSA 440 instrument was used to determine the electrophoretic velocity of the suspended particles by measuring the Doppler shift of scattered laser light simultaneously at four different scattering angles, ie, 7.5°, 15.0°, 22.5°, and 30.0°. Suspensions of HA were prepared as follows: 0.05 g/L of HA in 10^{-2} M KNO_3 (constant ionic strength) at a spontaneous constant pH.

Results

Synthetic biomimetic HA nanocrystals

In this study, we analyzed the antimicrobial, anti-inflammatory, and antioxidant activity of LF delivered by synthetic biomimetic HA nanocrystals. Biomimetic HA nanocrystals were synthesized as previously reported,[23] with a carbonate content of 5%±2%, resembling that of bone HA where the carbonate content ranges from 4 wt% to 8 wt%.

The FTIR spectrum for the synthesized biomimetic HA (Figure 1A) not only reveals the characteristic adsorption bands of phosphates at 1,034 cm^{-1} and 1,100 cm^{-1}, but also the adsorption bands due to the presence of carbonate. A small adsorption band at 880 cm^{-1} was utilized to evaluate the percent carbonate content in HA, and adsorption bands at 1,466 cm^{-1}, 1,422 cm^{-1}, and 1,545 cm^{-1} and was consistent with carbonate type A (hydroxyl site)-substituted and type B (phosphate site)-substituted HA nanocrystals, the latter closely resembling the prevalent type B carbonate substitution in the HA found in human bone (Figure 1B).[32]

In Figure 2A, a transmission electron microscopy image of the synthesized HA nanocrystals reveals their planar acicular morphology, which closely resembles that of HA nanocrystals in bone (Figure 2C). The crystals have a plate-like morphology (length and width about 110±5 nm and 20±3 nm, respectively, and a thickness of about 8±2 nm). The main crystal dimension is elongated towards the crystallographic c-axis, as derived by the orientation of fringes 0.34 nm apart and related to the (002) planes (Figure 2B). It is important to observe how the fringes related to the (002) crystallographic planes are homogeneously extended in the whole crystal core up to near the surface neighboring the crystal. The surface surrounding the nanocrystal appears to be amorphous without a defined crystallographic order. This finding is confirmed by a nearly stoichiometric calcium/phosphorus molar ratio of 1:7 as determined by chemical analysis in bulk and a surface calcium/phosphorus molar ratio of 1:3 when determined by X-ray photoelectron spectroscopy analysis. The presence of 5% phosphate anions substituted by carbonate anions produces a pseudoamorphous layer without crystalline order on the surface of the nanocrystals. The amorphous surface is responsible for the zeta potential of –20.5±1.5 mV shown by the HA nanocrystals at physiological pH (7.4). The high reactivity of the HA nanocrystals is ascribed to these findings, together with the high specific surface area of about 110 m^2/g, which is only slightly lower than the value of 120 m^2/g obtained for biological nanocrystals.

The powder X-ray diffraction pattern for the synthesized HA nanocrystals reported in Figure 3A shows the

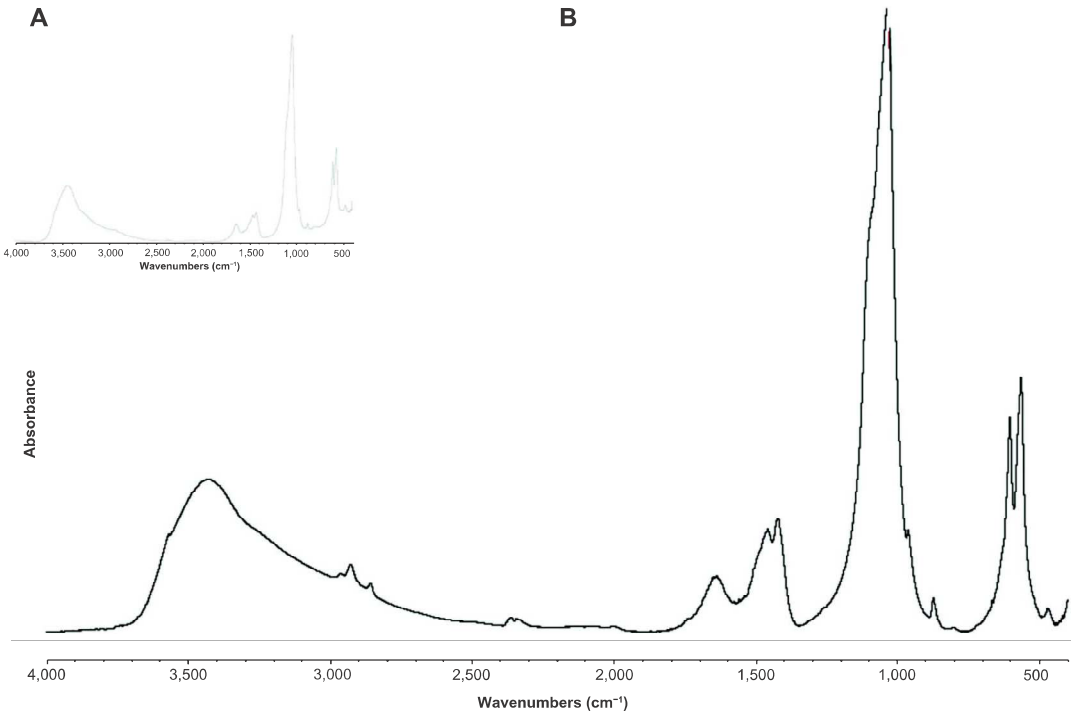

Figure 1 Fourier transform infrared spectrum of the synthesized biomimetic HA nanocrystals revealing absorption bands due to phosphate groups at 1,034 cm^{-1} and 1,100 cm^{-1} and absorption bands due to carbonate groups, ie, a small band at 880 cm^{-1} and others at 1,466 cm^{-1}, 1,422 cm^{-1}, and 1,545 cm^{-1}, which are consistent with type A and type B, respectively, carbonate-substituted hydroxyapatite (**B**) and closely resemble natural hydroxyapatite in human bone (**A**).

characteristic diffraction maxima for HA single phase (JCPDS 9-32). The diffraction pattern of the synthesized HA shows poorly defined diffraction maxima, indicating a relatively low degree of crystallinity. In Figure 3B, the X-ray diffraction pattern of deproteinated bone HA is reported for comparison. The degree of synthetic HA crystallinity[30] was calculated according to the method described by Sherman,[30] obtaining a value of 45%, which is increased in respect to the value of 28% determined from the X-ray diffraction pattern of natural apatite in deproteinated bone.

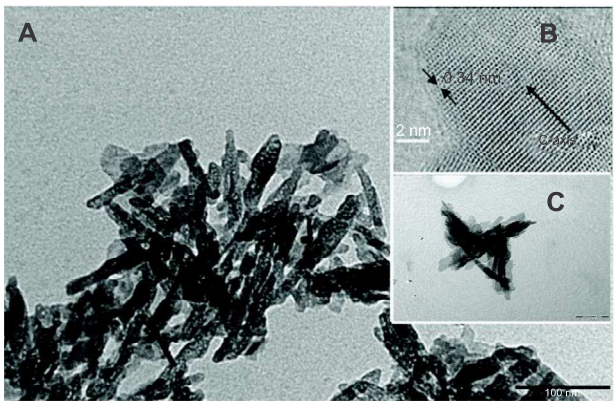

Figure 2 (**A**) Transmission electron microscopy (TEM) image of a synthetic hydroxyapatite nanocrystal with a planar acicular morphology mimicking the bone biogenic hydroxyapatite nanocrystals. (**B**) High-resolution image of a single carbonate hydroxyapatite nanocrystal with the c crystallographic axis parallel to the main crystal dimension and orthogonal to the fringes related to the (002) crystallographic planes. The arrows show the order present in the hydroxyapatite crystal. High resolution TEM image shows how it is possible to observe the regular packing present into the crystal. (**C**) TEM image of bone hydroxyapatite nanocrystals.

Preparation and characterization of LF-coated HA

Synthetic biomimetic HA nanocrystals were surface-functionalized at pH 7.4 by different amounts of lactoferrin molecules using the method reported by Iafisco et al.[20] Isotherm LF adsorption onto biomimetic HA nanocrystals at pH 7.4 is reported in Figure 4, where the adsorbed amount (C Lactoferrin, in mg/m^2) is plotted against the protein concentration after adsorption (C Lactoferrin in mg/mL). The plot is characterized by an initial slope, indicating high protein affinity for the HA surface.

The increase in LF concentration in the buffer solution enhances the surface coverage until it is complete. The absorption-saturation yields a plateau value corresponding to the maximum amount of LF surface immobilization of about 0.8 mg/m^2. The isoelectric point of LF is 8.5, and it thus has a net positive charge below the isoelectric point.[33] At pH 7.4, the positive electrostatic surface potential of

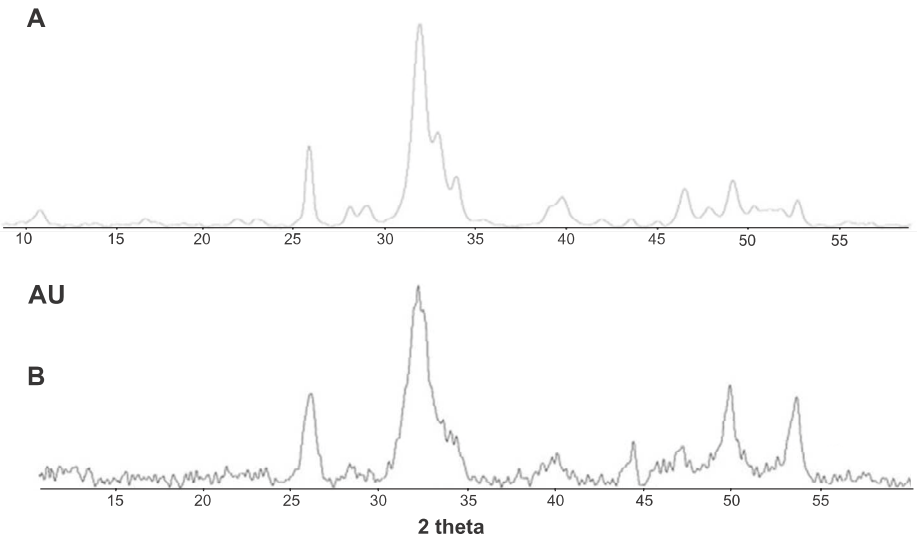

Figure 3 (**A**) Powder X-ray diffraction pattern of synthesized hydroxyapatite nanocrystals and (**B**) deproteinated bone hydroxyapatite.
Abbreviation: AU, arbitrary unit.

LF produces a strong surface interaction, with the negative HA nanocrystals having a zeta potential of – 20.5±1.5 mV and avoiding protein–protein interaction. This electrostatic interaction leads to formation of an LF monolayer coated onto the HA nanocrystals. The HA morphology and the nanodimension do not appreciably affect the conformation of the absorbed LF. At pH 7.4, the LF covering the HA nanocrystals appeared to be only slightly unfolded, with a small fraction of the alpha-helix structure being converted into turn while the beta-sheet content remained almost unchanged.[20] Nanohybrid composite made of biomimetic HA nanocrystals surface - covered of 0.8 mg/m^2 (LF-HA) were prepared in order to test their biological activity.

Antimicrobial and hemolytic activities

Synthetic biomimetic HA nanocrystals surface-functionalized with LF were tested for their antibacterial activity against *S. aureus A170*, *L. monocytogenes*, *S. enterica* serovar Paratyphi B, and *E. coli.* LF molecules delivered by the biomimetic HA nanocrystals were active against both Gram positive and Gram negative bacteria. LF molecules effectiveness depend on LF-HA concentration. The antimicrobial activity of LF-HA and LF is shown at different concentrations (300–500 µg/mL) in Table 1A and B. The antimicrobial activity of LF-HA at a concentration of 300 µg/mL is higher than that of unconiugated LF. The LF-HA nanohybrid composite at a concentration of 300 µg/mL had low hemolytic activity (10%) and the LC_{50} value was 526.7 µg/mL.

Cytotoxic activity and antioxidant capacity

LF-HA was slightly cytotoxic when tested in a THP-1 cell line at concentrations of 300–500 µg/mL. The THP-1 cells remained viable for up to 72 hours (Table 2). In addition,

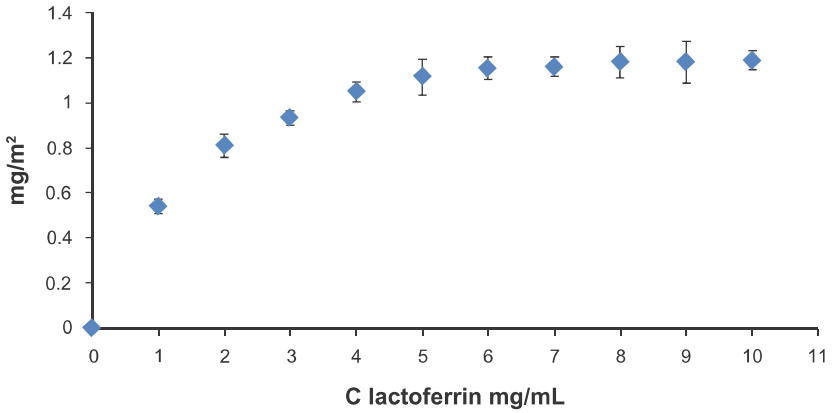

Figure 4 Adsorption isotherm of lactoferrin on biomimetic hydroxyapatite nanocrystals at pH 7.4. The adsorbed lactoferrin is plotted against the protein concentration after adsorption.

Table 1 Antimicrobial activity of LF-HA versus unconiugated LF

Strains	LF-HA 300 μg/mL	LF-HA 350 μg/mL	LF-HA 400 μg/mL	LF-HA 450 μg/mL	LF-HA 500 μg/mL
(A)					
Staphylococcus aureus	61%	65%	70%	77%	80%
Salmonella Paratyphi B	63%	66%	71%	78%	81%
Escherechia coli	65%	68%	72%	75%	78%
Listeria monocytogenes	60%	63%	70%	75%	80%
	LF 300 μg/mL	**LF 350 μg/mL**	**LF 400 μg/mL**	**LF 450 μg/mL**	**LF 500 μg/mL**
(B)					
Staphylococcus aureus	28%	30%	36%	40%	42%
Salmonella Paratyphi B	23%	28%	31%	35%	41%
Escherechia coli	25%	31%	36%	42%	48%
Listeria monocytogenes	22%	26%	30%	37%	40%

Note: (**A**) Antimicrobial activity at different concentrations (300–500 μg/mL) of LF-HA against Gram-positive (*Staphylococcus aureus* and *Listeria monocytogenes*) and Gram-negative (*Escherichia coli* and *Salmonella* Paratyphi B) bacteria (10^6 colony forming units per well; 60 μL). (**B**) Antimicrobial activity at different concentrations (300–500 μg/mL) of LF against Gram-positive (*S. aureus* and *L. monocytogenes*) and Gram-negative (*E. coli* and *Salmonella* Paratyphi B) bacteria (10^6 colony forming units per well; 60 μL).
Abbreviations: HA, hydroxyapatite; LF, lactoferrin.

LF-HA induced low production of NO_2 in THP-1 cells. Production of NO_2 was reduced in cells stimulated with lipopolysaccharide and then treated with LF-HA compared with control cells (stimulated only with lipopolysaccharide, Table 3). The LDH enzyme released by THP-1 cells was used as the endpoint for the study of cellular toxicity (Figure 1A).

LF-HA induced low production of LDH in THP-1 cells. Release of LDH into the medium is a sign of necrotic cell death,[34] and production of LDH was reduced in cells stimulated with lipopolysaccharide 10 μg/mL and then treated with LF-HA compared with the positive control provided by the kit (Figure 5A). The antioxidant properties of HA and LF alone or combined in the hybrid LF-HA composites was evaluated using the ABTS test (HA, 14,632 mmol/L; LF, 2,605 mmol/L; LF-HA, 15,294 mmol/L). A small increase in antioxidant activity was found in the LF-HA composite.

Immunomodulatory activity

We also investigated the immunomodulatory activity of LF-HA in THP-1 cells stimulated by lipopolysaccharide. For this purpose, the performance of selected cytokines, including TNF-α, IFN-γ, IL-17, IL-4, IL-12, IL-8, IL-6, and IL-10, was evaluated by enzyme-linked immunosorbent assay.

Cytokines can be considered as an important parameter for defining inflammation.[35] Treatment of THP-1 cells with acetylsalicylic acid or LF-HA did not induce any inflammatory response, and levels of TNF-α, IFN-γ, IL-17, IL-4, IL-6, IL-10, IL-12, and IL-8 appeared to be low. After stimulation of THP-1 cells by lipopolysaccharide, an increase in levels of proinflammatory cytokines, ie, TNF-α, IFN-γ, IL-6, and IL-17, was observed, with a peak after 4 hours (Figure 5B). After treatment of lipopolysaccharide-stimulated THP-1 cells with LF-HA, the levels of proinflammatory cytokines decreased, while the levels of others, such as IL-4, IL-10, IL-12, and IL-8, showed an increase, reaching a peak at 4 hours. On treating lipopolysaccharide-stimulated THP-1 cells with acetylsalicylic acid, there was a decrease in TNF-α, IFN-γ, IL-6, and IL-17 levels and an increase in IL-4, IL-10, IL-12, and IL-8 levels (Figure 5B). THP-1 cells were treated with lipopolysaccharide, the supernatant was collected at 2, 4, 6, 8, 12, and 24 hours, and TNF-α and IL-6 levels were quantified. These cytokines show a high level of expression for up to 8 hours (data not shown). In THP-1 cells stimulated with lipopolysaccharide and treated with LF-HA, TNF-α, and IL-6 levels started to decrease 4 hours after treatment.

Table 2 Analysis of cell viability

Time (h)	THP-1	THP-1 + LF-HA 300 μg/mL	THP-1 + LF-HA 350 μg/mL	THP-1 + LF-HA 400 μg/mL	THP-1 + LF-HA 450 μg/mL	THP-1 + LF-HA 500 μg/mL
24 h	99%	83%	76%	71%	70%	67%
48 h	96%	80%	74%	70%	67%	64%
72 h	90%	77%	72%	68%	65%	62%

Note: THP-1 cells were treated with LF-HA (300–500 μg/mL) and cell viability was determined at 24, 48, or 72 hours by the Trypan blue test.
Abbreviations: HA, hydroxyapatite; LF, lactoferrin; h, hours.

Table 3 Time couse of NO_2 production by THP-1 cells/macrophages.

	Time (h)		
	24 h	**48 h**	**72 h**
THP-1	0,596±0.02 μmol	0,76±0.08 μmol	0,996±0.04 μmol
THP-1 + LPS	3,910±0.01 μmol	4,415±0.2 μmol	5,312±0.03 μmol
LF-HA 300 μg/mL	1,120±0.04 μmol	1,520±0.25 μmol	1,720±0.04 μmol
LF-HA 350 μg/mL	1,140±0.03 μmol	1,449±0.12 μmol	1,740±0.046 μmol
LF-HA 400 μg/mL	1,175±0.1 μmol	1,775±0.16 μmol	1,875±0.038 μmol
LF-HA 450 μg/mL	1,25±0.04 μmol	1,655±0.07 μmol	1,958±0.04 μmol
LF-HA 500 μg/mL	1,278±0.04 μmol	1,878±0.09 μmol	1,968±0.16 μmol
LPS + LF-HA 300 μg/mL	1,814±0.12 μmol	1,940±0.01 μmol	1,991±0.25 μmol
LPS + LF-HA 350 μg/mL	1,775±0.04 μmol	1,970±0.04 μmol	2,075±0.10 μmol
LPS + LF-HA 400 μg/mL	1,950±0.013 μmol	1,980±0.03 μmol	2,19±0.02 μmol
LPS + LF-HA 450 μg/mL	2,159±0.11 μmol	2,359±0.07 μmol	2,431±0.2 μmol
LPS + LF-HA 500 μg/mL	2,250±0.17 μmol	2,395±0.14 μmol	2,249±0.18 μmol

Note: NO_2 production by untreated THP-1 cells, THP-1 cells stimulated with LPS (10 μg/mL), THP-1 cells treated with LF-HA (300–500 μg/mL) and THP-1 cells stimulated with LPS (10 μg/mL) and treated with LF-HA (300–500 μg/mL). The data are expressed as μmol of NO_2 for 10^6 input cells, and shown as the mean ± standard deviation of three different experiments, each performed in triplicate.

Abbreviations: HA, hydroxyapatite; LF, lactoferrin; LPS, lipopolysaccharide; h, hours.

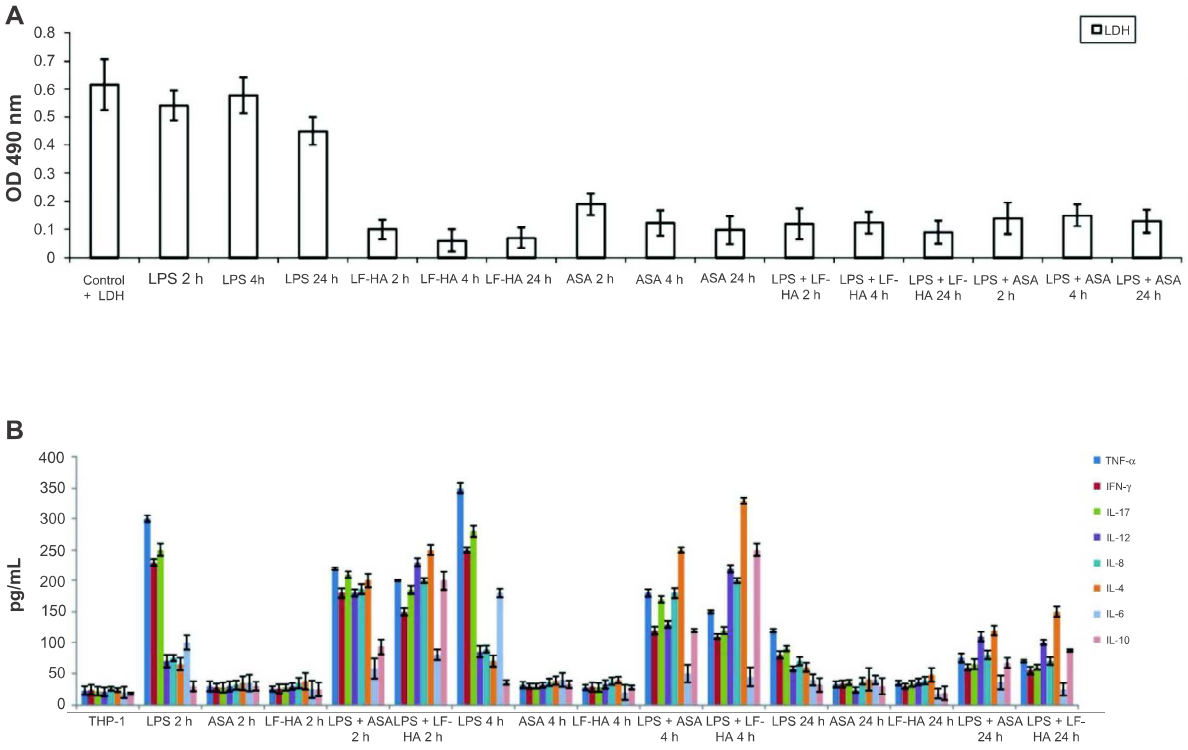

Figure 5 (**A**) LDH assay. The effect of LF-HA on LDH release in untreated THP-1 cells, THP-1 cells stimulated with LPS 10 μg/mL for 2, 4, or 24 hours, THP-1 cells treated with LF-HA 300 μg/mL or ASA 300 μg/mL for 2, 4, or 24 hours, and THP-1 cells stimulated with LPS 10 μg/mL and then treated with LF-HA 300 μg/mL or ASA 300 μg/mL for 2, 4, or 24 hours. Positive control: control plus LDH provided by the kit. (**B**) Anti-inflammatory activity. IFN-γ, TNF-α, IL-17, IL-4, IL-12, IL-8, IL-6, and IL-10 levels were determined by a sandwich enzyme-linked immunosorbent assay test in untreated THP-1 cells, THP-1 cells stimulated with LPS 10 μg/mL for 2, 4, or 24 hours, THP-1 cells treated with LF-HA 300 μg/mL or ASA 300 μg/mL for 2, 4, or 24 hours, and THP-1 cells stimulated with LPS 10 μg/mL and then treated with LF-HA 300 μg/mL or ASA 300 μg/mL for 2, 4, or 24 hours. Negative control: THP-1 cells in Roswell Park Memorial Institute medium. Results from the representative experiments are presented as the mean ± standard deviation.

Abbreviations: ASA, acetylsalicylic acid; HA, hydroxyapatite; LDH, lactate dehydrogenase; IFN-γ, interferon gamma; IL, interleukin; LF, lactoferrin; LPS, lipopolysaccharide; TNF-α, tumor necrosis factor alpha; h, hours.

In the presence of lipopolysaccharide, LF-HA specifically inhibits the release of proinflammatory cytokines and increases the secretion of anti-inflammatory cytokines, both in vivo and in vitro. LF-HA downregulates the synthesis of proinflammatory cytokines due to its ability to bind lipopolysaccharide through the LF domain. Therefore, LF-HA competes with lipopolysaccharide-binding protein for binding to lipopolysaccharide and blocks transport of endotoxins to mCD14, which is expressed on the surface of macrophages. By binding lipopolysaccharide, LF-HA prevents activation of NF-kB and consequently the production of proinflammatory cytokines.[36]

Based on the results obtained here, we can conclude that the performance of TNF-α and IL-6 in THP-1 cells stimulated with lipopolysaccharide and then treated with acetylsalicylic acid is comparable with that in cells stimulated with lipopolysaccharide and then treated with LF-HA. Further tests have shown that LF-HA downregulates the level of proinflammatory cytokines and that it also demonstrates immunomodulatory activity. These effects appeared to be comparable with those of acetylsalicylic acid, a well known anti-inflammatory drug (Figure 5B) that helps to regulate the immune response.

Conclusion

Careless prescribing has led to the ineffectiveness of some antibiotics that were once considered adequate.[35] In this situation, antimicrobial proteins, in their natural form alone or combined with other molecules, could represent a solution to this problem. Antimicrobial molecules are characterized by a broad spectrum of activity against Gram-positive and Gram-negative bacteria and have a low level of toxicity in eukaryotic cells.[6] In this work, we investigated the antimicrobial, anti-inflammatory, and antioxidant activity of an LF-HA nanohybrid composite composed of biomimetic HA nanocrystals surface-covered of 0.8 mg/m.

In conclusion, it can be stated that the known antibacterial, immunomodulatory, and antioxidant properties of LF are increased when molecules of this protein are surface-linked to biomimetic HA nanocrystals.[36,37,38] The present findings show that the LF-HA hybrid composite has potential with regard to preparation of antimicrobial and antioxidant material useful for the design of innovative technological biomedical applications.

Acknowledgments

The authors wish to thank Dr Giulia Graziani, Dr Salvatore Esposito, Filomena Di Ruocco, and Claudio Tracanna for their assistance for this research. In addition, they thank the RBAP114AMK, RINAME Project (funds for selected research topics) and the Interuniversity Consortium for Research on Chemistry of Metals in Biological Systems and Chemical Center Srl for financial support.

Disclosure

The authors report no conflicts of interest and that they received no payment for preparation of this paper.

References

1. Livermore DM. The need for new antibiotics. *Clin Microbiol Infec*. 2004;4:1–9.
2. Capparelli R, Amoroso MG, Palumbo D, Iannaccone M, Faleri C, Cresti M. Two plant puroindolines colocalize in wheat seed and in vitro synergistically fight against pathogens. *Plant Mol Biol*. 2005;58:857–867.
3. Palumbo D, Iannaccone M, Porta A, Capparelli R. Experimental antibacterial therapy with puroindolines, lactoferrin and lysozyme in *Listeria monocytogenes*-infected mice. *Microbes Infect*. 2010;12:538–545.
4. Capparelli R, Ventimiglia I, Palumbo D, et al. Expression of recombinant puroindolines for the treatment of staphylococcal skin infections (*Acne vulgaris*). *J Biotechnol*. 2007;128:606–614.
5. Capparelli R, Romanelli A, Iannaccone M, et al. Synergistic antibacterial and anti-inflammatory activity of temporin A and modified temporin B in vivo. *PLoS One*. 2009;4:e7191.
6. Capparelli R, De Chiara F, Nocerino N, et al. New perspectives for natural antimicrobial peptides: application as antinflammatory drugs in a murine model. *BMC Immunol*. 2012;13:61.
7. González-Chávez SA, Arévalo-Gallegos S, Rascón-Cruz Q. Lactoferrin: structure, function and applications. *Int J Antimicrob Agents*. 2009;33:301 .e1–301 .e8.
8. Valenti P, Antonini G. Lactoferrin: an important host defence against microbial and viral attack. *Cell Mol Life Sci*. 2005;62:2576–2587.
9. Metz-Boutique MH, Jolles J, Mazurier J, et al. Human lactotransferrin: amino acid sequence and structural comparisons with other transferrins. *Eur J Biochem*. 1984;145:659–676.
10. Steijns JM, Van Hooijdonk AC. Occurrence structure biochemical properties and technological characteristics of lactoferrin. *Br J Nutr*. 2000;84:7–11.
11. Conesa C, Sánchez L, Rota C, et al. Isolation of lactoferrin from milk of different species: calorimetric and antimicrobial studies. *Comp Biochem Physiol Part B*. 2008;150:131–139.
12. Legrand D, Mazurier J. A critical review of the roles of host lactoferrin in immunity. *Biometals*. 2010;23:365–376.
13. Sánchez L, Peiró JM, Oria R, Castillo H, Brock JH, Calvo M. Kinetic parameters for denaturation of bovine milk lactoferrin. *J Food Sci*. 1992;57:873–879.
14. Iafisco M, Foltran I, Di Foggia M, Bonora S, Roveri N. Calorimetric and Raman investigation of cow's milk lactoferrin. *J Therm Anal Calorim*. 2011;103:41–47.
15. Latour RA. In the biomaterials field, its study is fundamental: to learn more about the biomineralization process in vivo, but also to test the material performance in the biological environment. *Biointerphases*. 2008;3:FC2–FC12.
16. Dee KC, Puleo DA, Bizios R. *An Introduction to Tissue Biomaterial Interactions*. Hoboken, NJ, USA: Wiley-Liss; 2003.
17. Roveri N, Palazzo B, Iafisco M. The role of biomimetism in developing nanostructured inorganic matrices for drug delivery. *Expert Opin Drug Deliv*. 2008;5:861–877.
18. Kandori K, Fudo A, Ishikawa T. Adsorption of myoglobin onto various synthetic hydroxyapatite particles. *Phys Chem Chem Phys*. 2000;2:2015–2020.

19. Akazawa T, Kobayashi M, Yoshida M, et al. Improved liquid chromatographic separation of different proteins by designing functional surfaces of cattle bone-originated apatite. *J Chromatogr A*. 1999;862: 217–220.
20. Iafisco M, Di Foggia M, Bonora S, Prat M, Roveri N. Adsorption and spectroscopic characterization of lactoferrin on hydroxyapatite nanocrystals. *Dalton Trans*. 2011;40:820–827.
21. Iafisco M, Palazzo B, Marchetti M, et al. Smart delivery of antitumoral platinum complexes from biomimetic hydroxyapatite nanocrystals. *J Mater Chem*. 2009;19:8385–8392.
22. Iafisco M, Palazzo B, Martra G, et al. Nanocrystalline carbonate-apatites: role of Ca/P ratio on the upload and release of anticancer platinum bisphosphonates. *Nanoscale*. 2012;4:206–217.
23. Palazzo B, Walsh D, Iafisco M, et al. Amino acid synergetic effect on structure, morphology and surface properties of biomimetic apatite nanocrystals. *Acta Biomater*. 2009;5:1241–1252.
24. Blaiotta G, Ercolini D, Pennacchia C, et al. PCR detection of staphylococcal enterotoxin genes in *Staphylococcus* spp. strains isolated from meat and dairy products. Evidence for new variants of seG and seI in *S. aureus* AB-8802. *J Appl Microbiol*. 2004;97:719–730.
25. Bubert A, Hein I, Rauch M, et al. Detection and differentiation of *Listeria* spp. by a single reaction based on multiplex PCR. *Appl Environ Microbiol*. 1999;65:4688–4692.
26. Chiu CH, Ou JT. Rapid identification of *Salmonella* serovars in feces by specific detection of virulence genes, invA and spvC, by an enrichment broth culture-multiplex PCR combination assay. *J Clin Microbiol*. 1996;34:2619–2622.
27. Janezic KJ, Ferry B, Hendricks EW, et al. Phenotypic and genotypic characterization of *Escherichia coli* isolated from untreated surface waters. *Open Microbiol J*. 2013;7:9–19.
28. Re R, Pellegrini N, Proteggente A, Pannala A, Yang M, Rice-Evans C. Antioxidant activity applying an improved ABTS radical cation decolorization assay. *Free Radic Biol Med*. 1999;26: 1231–1237.
29. Rozalska B, Wadstrom T. Interferon-γ, interleukin-1 and tumor necrosis factor-α synthesis during experimental murine staphylococcal infection. *FEMS Immunol Med Microbiol*. 1993;7:145–152.
30. Sherman BC. 2004. Magnesium Omeprazole. US Patent 6,713,495.2004.
31. Brunauer S, Emmett PH, Teller E. Adsorption of gases in multimolecular layers. *J Am Chem Soc*. 1938;60:309–319.
32. Sønju Clasen AB, Ruyter IE. Quantitative determination of type A and type B carbonate in human deciduous and permanent enamel by means of Fourier transform infrared spectrometry. *Adv Dent Res*. 1997;11: 523–527.
33. Pan F, Zhao X, Waigh TA, Lu JR, Miano F. Interfacial adsorption and denaturization of human milk and recombinant rice lactoferrin. *Biointerphases*. 2008;3:FB36–FB47.
34. Awad WA, Aschenbach JR, Zentek J. Cytotoxicity and metabolic stress induced by deoxynivalenol in the porcine intestinal IPEC-J2 cell line. *J Anim Physiol Anim Nutr*. 2012;96:709–716.
35. Gould IM, Bal AM. New antibiotic agents in the pipeline and how they can help overcome microbial resistance. *Virulence*. 2013;4:185–191.
36. Håversen L, Ohlsson BG, Hahn-Zoric M, Hanson LA, Mattsby-Baltzer I. Lactoferrin down-regulates the LPS-induced cytokine production in monocytic cells via NF-kB. *Cell Immunol*. 2002;220:83–95.
37. Legrand D, Elass E, Carpentier M, Mazurier J. Lactoferrin: a modulator of immune and inflammatory responses. *Cell Mol Life Sci*. 2005;62: 2549–2559.
38. Actor JK, Hwang SA, Kruzel ML. Lactoferrin as a natural immune modulator. *Curr Pharm Des*. 2009;15:1956–1973.

Special Issue Article

Journal of PeptideScience

Received: 30 October 2012 Revised: 6 December 2012 Accepted: 6 December 2012 Published online in Wiley Online Library: 19 February 2013

(wileyonlinelibrary.com) DOI 10.1002/psc.2479

Antimicrobial peptides from plants: stabilization of the γ core of a tomato defensin by intramolecular disulfide bond‡

C. Avitabile,[a] R. Capparelli,[b] M. M. Rigano,[b] A. Fulgione,[b] A. Barone,[b] C. Pedone[a] and A. Romanelli[a]*

Cysteine-containing antimicrobial peptides of diverse phylogeny share a common structural signature, the γ core, characterized by a strong polarization of charges in two antiparallel β sheets. In this work, we analyzed peptides derived from the tomato defensin SolyC07g007760 corresponding to the protein γ core and demonstrated that cyclization of the peptides, which results in segregation of positive charges to the turn region, produces peptides very active against Gram negative bacteria, such as *Salmonella enterica* and *Helicobacter pylori*. Interestingly, these peptides show very low hemolytic activity and thus represent a scaffold for the design of new antimicrobial peptides. Copyright © 2013 European Peptide Society and John Wiley & Sons, Ltd.

Keywords: tomato defensin; cyclization; antimicrobial

Introduction

A tremendous effort has been recently devoted to the discovery of biologically active peptides from natural sources [1–3]. Plants produce a wide variety of antimicrobial peptides and proteins showing activity against either plant or human pathogens [4]. Many of these, such as thionins and knottins, are rich in cysteines and are stabilized by a number of disulfide bonds [5,6]. Interestingly, some of the structural features displayed by peptides produced in plants are well conserved also within proteins produced by evolutionarily diverse organisms, and in fact, the existence of multidimensional signatures for antimicrobial peptides has been hypothesized [7–9]. The γ core motif has recently been indicated as a three dimensional signature for antimicrobial peptides or proteins and, generally, as a feature shown by membrane-active proteins. In particular, the γ core motif, characterized by a conserved CXG sequence and two antiparallel β sheets, is common to host defence polypeptides showing multiple disulfide bonds such as toxins, kinocidins, and thionins [10,11]. This structural motif can be generated by different amino acid sequences and can exist in the dextromeric or levomeric form, depending on whether it is derived by the amino acid forward or reverse sequence (Figure 1). In all cases, γ core motifs show polarization of positive charge and segregation of hydrophobic amino acids. There are some cases in which the only γ core is sufficient for the peptide antimicrobial activity, as observed for protegrins, θ defensin RTD-1, and other cases in which the γ core represents the scaffold around which helices and sheets packs, as for kinocidins [12,13].

In a recent paper, we identified, after a bioinformatics analysis of the tomato genome, the tomato defensin SolyC07g007760 (iTAG v.2.3) and demonstrated that a synthetic peptide (SolyC) corresponding to its γ core exerts antimicrobial activity against both Gram positive and Gram negative bacteria, being particularly active against different strains of the Gram negative bacterium *Helicobacter pylori* [14,15]. Interestingly, the peptide SolyC was able to discriminate between pathogens and probiotic bacteria, killing only the minority of the probiotic tested. In addition, SolyC downregulated the proinflammatory cytokines to an extent comparable with the known anti-inflammatory drug acetyl salicylic acid and did not cause red blood cell hemolysis and was not toxic toward eukaryotic cells.

SolyC is a peptide composed by 17 amino acids and contains three cysteines in positions 6, 13, and 15. The results described so far were obtained employing the peptide in its linear form. The presence of three cysteines that might be subjected to spontaneous oxidation and the observation that in typical γ cores those cysteines are involved in disulfide bonds urged us to investigate how formation of disulfide bonds in a controlled fashion could affect the secondary structure and the antimicrobial activity of the peptide. Two peptides in which Cys13 or Cys15 was mutated into a serine were obtained in the linear and oxidized form. Disulfide bonds were formed between C6 and C13 (SolyC1) or C6 and C15 (SolyC2); in both cases, one cysteine was missing. Truncated peptides, starting from the conserved GXC motif, were also obtained in the linear and oxidized form. The secondary structure of all peptides was analyzed by circular dichroism (CD); the antimicrobial activity of the peptides was tested against Gram positive and Gram negative bacteria. All the oxidized peptides

* *Correspondence to: Alessandra Romanelli, University of Naples 'Federico II', School of Biotechnological Sciences, Department of Biological Sciences, Via Mezzocannone 16, 80134, Naples, Italy. E-mail: alessandra.romanelli@unina.it*

‡ *Special issue devoted to contributions presented at the 13th Naples Workshop on Bioactive Peptides, June 7–10, 2012, Naples.*

a *University of Naples 'Federico II', School of Biotechnological Sciences, Department of Biological Sciences, Via Mezzocannone 16, 80134, Naples Italy*

b *University of Naples 'Federico II', School of Biotechnological Sciences, Department of Soil, Plant, Environmental and Animal Production Sciences, Via Università 100, 80055, Portici Italy*

Journal of PeptideScience

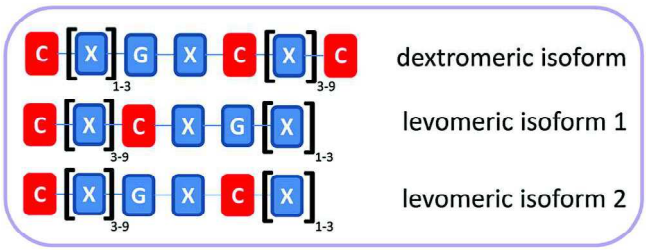

Figure 1. Schematic representation of the gamma core isoforms.

are highly active against Gram negative bacteria; the linear peptide SolyC2 shows antimicrobial activity against Gram negative bacteria comparable with that of the reference peptide SolyC, whereas linear SolyC1 exhibits an antimicrobial activity against Gram negative bacteria at higher concentrations. The activity of modified peptides against Gram positive bacteria was found in all cases lower as compared with that of the reference peptide. These results suggest that the interaction of the peptides with the membranes of Gram negative bacteria is stronger when the positive charges are exposed, and this likely occurs when the peptides are in the oxidized form, in which the antiparallel β sheets are constrained by the disulfide bond.

Materials and Methods

Reagents

The amino acids used for the peptide synthesis, Fmoc-Arg(Pbf)-OH, Fmoc-Asn(Trt)-OH, Fmoc-Cys(Trt)-OH, Fmoc-Gly-OH, Fmoc-Lys (Boc)-OH, Fmoc-Phe-OH, Fmoc-Ser(OtBu)-OH, Fmoc-Thr(tBu)-OH, the Rink amide MBHA resin and the activators *N*-hydroxybenzotriazole (HOBT), and *O*-benzotriazole-*N*,*N*,*N*′,*N*′-tetramethyl-uronium-hexafluoro-phosphate (HBTU), were purchased from Novabiochem (Gibbstown, NJ, USA). Acetonitrile was from Reidel-deHaën (Seelze, Germany) and dry *N*,*N*-dimethylformamide (DMF) from LabScan (Dublin, Ireland). All other reagents were from Sigma Aldrich (Milan, Italy). LC-MS analyses were performed on a LC-MS Thermo Finnigan with an electrospray source (MSQ) on a Phenomenex Jupiter 4μ Proteo (50 × 4.6 mm) column for all peptides except for SolyC-t that was analyzed on a Jupiter 4μ Proteo (150 × 4.6 mm) column. Purification was carried out on an Onyx monolithic semi-prep C18 (100 × 10 mm) column.

Synthesis

Peptides were synthesized on solid phase by Fmoc chemistry on the MBHA (0.54 mmol/g) resin by consecutive deprotection, coupling, and capping cycles [16]. Deprotection: 30% piperidine in DMF, 5 min (2×). Coupling: 2.5 equivalents of amino acid + 2.49 equivalent of HOBT/HBTU (0.45 M in DMF/DMSO 75/25 v/v) + 3.5 equivalents NMM, 40 min. Capping: acetic anhydride/DIPEA/DMF 15/15/70 v/v/v, 5 min.

Peptides were cleaved off from the resin and deprotected by treatment of the resin with a solution of TFA/TIS/EDT/H_2O 94/1/2.5/2.5 v/v/v/v, 3 h, rt. TFA was concentrated, and peptides were precipitated in cold ethylic ether. Analysis of the crudes was performed by LC-MS using a gradient of acetonitrile (0.1% TFA) in water (0.1% TFA) from 5% to 70% in 15 min. Purification was performed by semipreparative RP-HPLC using a gradient of acetonitrile (0.1% TFA) in water (0.1% TFA) from 5% to 70% in 15 min.

SolyC (Da): calculated 1994.30; $[M+2H]^{2+}$: 998.16; $[M+3H]^{3+}$: 665.77; found: $[M+2H]^{2+}$: 997.55; $[M+3H]^{3+}$: 665.64; retention time: 5.40 min.
SolyC-t (Da): calculated 1703.01; $[M+2H]^{2+}$: 853.50; $[M+3H]^{3+}$: 568.67; found: $[M+1H]^{1+}$: 1702.58; $[M+2H]^{2+}$: 852.29; $[M+3H]^{3+}$: 568.52; retention time: 12.0 min.
SolyC1 (Da): calculated 1978.26; $[M+2H]^{2+}$: 990.13; $[M+3H]^{3+}$: 660.42; found: $[M+2H]^{2+}$: 990,13; $[M+3H]^{3+}$: 660.41; retention time: 5.12 min.
SolyC1-t (Da): calculated 1686.95; $[M+2H]^{2+}$: 844.47; $[M+3H]^{3+}$: 563.31; found: $[M+2H]^{2+}$: 844.40; $[M+3H]^{3+}$: 563.21; retention time: 5.12 min.
SolyC2 (Da): calculated 1978.26; $[M+2H]^{2+}$: 990.13; $[M+3H]^{3+}$: 660.42; found: $[M+2H]^{2+}$: 989.90; $[M+3H]^{3+}$: 660.21; retention time: 5.33 min.
SolyC2-t (Da): calculated 1686.95; $[M+2H]^{2+}$: 844.47; $[M+3H]^{3+}$: 563.31; found: $[M+2H]^{2+}$: 844.03; $[M+3H]^{3+}$: 563.23; retention time: 4.93 min.

Oxidation Reaction

Disulfide-bridged analogs were obtained from the purified linear peptides after an oxidation reaction. Linear peptides were dissolved in a mixture of H_2O/acetic acid (95/5, v/v) at a final concentration of 2.5 mM (9 mL total volume); pH was adjusted to 6 with ammonium hydrogen carbonate and then DMSO (1 mL) was added. The reaction was complete after 24 h. Analysis of the crudes was performed by LC-MS using a gradient of acetonitrile (0.1% TFA) in water (0.1% TFA) from 5% to 70% in 15 min. Purification was performed by semipreparative RP-HPLC using a gradient of acetonitrile (0.1% TFA) in water (0.1% TFA) from 5% to 70% in 15 min. Peptides were characterized by ES mass spectrometry.
SolyC1-ox (Da): calculated 1976.26; $[M+2H]^{2+}$: 989.13; $[M+3H]^{3+}$: 659.75; found: $[M+2H]^{2+}$: 988.70; $[M+3H]^{3+}$: 659.60; retention time: 5.35 min.
SolyC1-t-ox (Da): calculated 1684.94; $[M+2H]^{2+}$: 843.47; $[M+3H]^{3+}$: 562.64; found: $[M+2H]^{2+}$: 843.23; $[M+3H]^{3+}$: 562.53; retention time: 4.96 min.
Solyc2-ox (Da): calculated 1976.26; $[M+2H]^{2+}$: 989.13; $[M+3H]^{3+}$: 659.75; found: $[M+2H]^{2+}$: 988.60; $[M+3H]^{3+}$: 659.60; retention time: 5.10 min.
SolyC2-t-ox (Da): calculated 1684.94; $[M+2H]^{2+}$: 843.47; $[M+3H]^{3+}$: 562.64; found: $[M+2H]^{2+}$: 843.26; $[M+3H]^{3+}$: 562.50; retention time: 5.15 min.

Bacteria

Bacterial isolates were from patients hospitalized at the Medical School of the University of Naples 'Federico II' and at the 'Villa Betania' hospital (Naples, Italy). Species identification was carried out by PCR [17–21]. Bacteria were grown at 37 °C in Tryptic Soy Broth (TSB) or Luria Broth (LB) medium, harvested in the exponential phase (OD 600 nm 0.6–0.8), centrifuged (10 min at 8×10^3 *g*), and resuspended in Muller Hinton broth at the concentration of ~10^5 CFU/ml. The resistance/susceptibility of the different strains used in this study to conventional antibiotics was also determined using the disk diffusion method on Mueller–Hinton agar according to the NCCLS guidelines 2002 (data not shown).

Antibacterial and Hemolytic Activity

Bacteria were distributed in triplicate into plates (60 μl/well), mixed with dilutions of the peptides (5–100 μg/ml; 40 μl/well),

and incubated at 37 °C for 20 h. The minimal concentration of peptides causing 100% growth inhibition (MIC100) was determined by measuring the absorbance at 600 nm (Biorad microplate reader model 680, CA) [22]. The test was performed in triplicate. The hemolytic activity of the peptides was tested using mouse red blood cells. The hemolytic activity was measured according to the formula OD peptide − OD negative control/OD positive control − OD negative control × 100, where the negative control (0% hemolysis) was represented by erythrocytes suspended in saline and the positive control (100% hemolysis) was represented by the erythrocytes lysed with 1% triton X100 [22].

The LC50 value relative to the SolyC was calculated as described [23].

Circular dichroism

Circular dichroism spectra were recorded at 25 °C using a 1 cm quartz cell with the Jasco-810 spectropolarimeter using a 260–200 nm measurement range, 100 nm/min scanning speed, 1 nm bandwidth, 4 s response time, 0.5 nm data pitch.

Peptides concentration for CD measurement was 25 μM. CD spectra were registered in 10 mM sodium phosphate buffer, pH 7 and in 10 mM sodium phosphate, 20 mM SDS buffer, pH 7.

Results

Peptide Design and Synthesis

The SolyC peptide (Table 1) contains the γ core sequence of the tomato defensin Solyc07g007760 and shows strong similarity in the primary sequence with the levomeric form of porcine protegrin PG-1. In PG-1, four cysteines form two disulfide bonds, one involving C6 and C15 and the other C8 and C13, which force the peptide to fold into two antiparallel beta sheets; the oxidation of cysteines induces the formation of a turn characterized by a strong concentration of positive charges [24,25].

SolyC contains only three cysteines; therefore, to induce the peptide to assume a PG-1-like structure, only one disulfide bond can be formed. We designed two peptides with a different disulfide pattern, with the aim to explore the effect of cyclization on the antimicrobial activity of the peptide, to understand whether there is a preference for the formation of one of the two disulfides and also whether there is a difference in the activity of the peptides with cycles of different size (Table 1). Because in γ cores cysteines contained in sequences CXC are rarely connected by disulfide bonds [26], we explored only two of the possible combinations of disulfides, namely C6–C13 (SolyC1) and C6–C15 (SolyC2) and mutated the cysteine not involved in the disulfide into a serine. To investigate the effect of reducing the hydrophobicity of the peptide, we also obtained truncated peptides, lacking three amino acids at the N-terminus. In the truncated peptides, the residues that characterize the γ core motif GXC were conserved (Table 1). HPLC retention times for truncated peptides are similar or lower as compared with those of the full length peptides, as expected comparing the mean hydrophobicity calculated for each peptide (Table 1) [27].

All peptides were obtained in the linear and oxidized form. Oxidation was carried out incubating linear peptides with DMSO (10%) at pH 6.0. LC-MS analysis of the peptides, showing for the majority of the peptides a decrease of the retention time and a reduction of 2 units in the mass, confirmed that the reaction occurred (Figure 2).

Table 1. Peptide sequences, names, reference number, and mean hydrophobicity

Peptide sequence	Name	Number	Mean hydrophobicity
FSGGNCRGFRRRCFCTK	SolyC	1	−0.71
GNCRGFRRRCFCTK	SolyC-t	2	−0.98
FSGGNCRGFRRRCFSTK	SolyC1	3	−0.91
GNCRGFRRRCFSTK	SolyC1-t	4	−1.22
FSGGNCRGFRRRSFCTK	SolyC2	5	−0.91
GNCRGFRRRSFCTK	SolyC2-t	6	−1.22
FSGGNCRGFRRRCFSTK	SolyC1-ox	7	−0.91
GNCRGFRRRCFSTK	SolyC1-t-ox	8	−1.22
FSGGNCRGFRRRSFCTK	SolyC2-ox	9	−0.91
GNCRGFRRRSFCTK	SolyC2-t-ox	10	−1.22

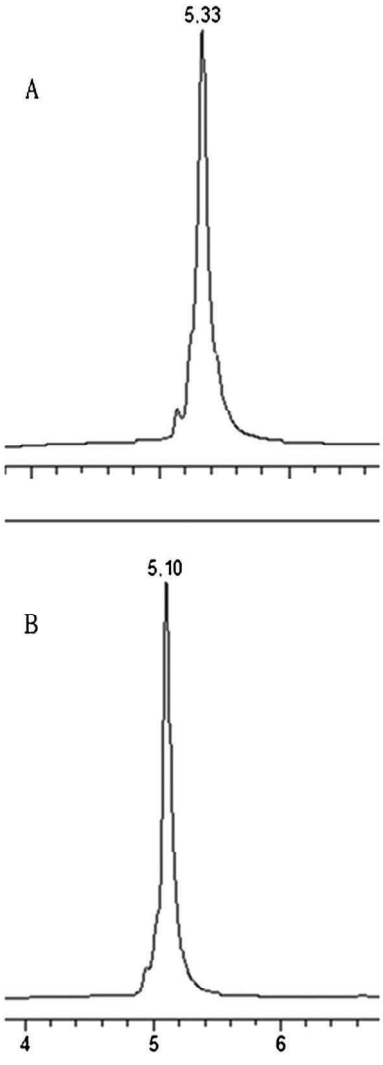

Figure 2. Comparison of the LC profiles for SolyC2 in the linear (A) and oxidized form (B). Zoom between 4 and 6 min of the LC run.

Journal of PeptideScience

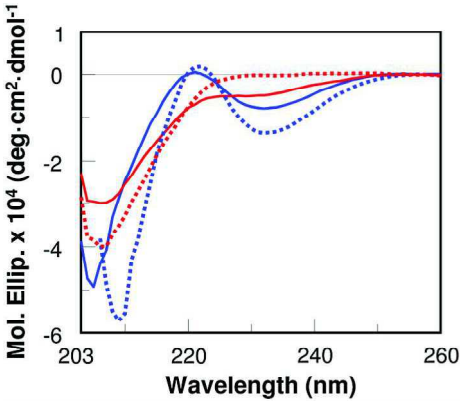

Figure 3. CD spectra of SolyC2 (blue) and SolyC2-ox (red) (50 μM) recorded in 10 mM phosphate buffer pH 7 (continuous line) and in 10 mM phosphate buffer, 30 mM SDS pH 7 (dotted lines).

Secondary Structure Studies

Linear and oxidized peptides were analyzed by CD at a 50 μM concentration in phosphate buffer, pH7. Peptides are mostly in an unordered form; spectra for the linear peptides, in fact, show one minimum around 204 nm and a very shallow minimum around 230 nm; upon oxidation, the minimum shifts toward 207 nm. Spectra recorded in the presence of SDS 30 mM are in most cases very similar to those recorded in buffer but more intense (Figure 3).

Antimicrobial Activity Test

The antimicrobial activity of the peptides was tested against the Gram positive bacteria *Staphylococcus aureus*, *Staphylococcus epidermidis*, *Listeria monocytogenes* and against the Gram negative bacteria *H. pylori* and *Salmonella enterica* (Table 2). For the standard peptide SolyC, truncation results in loss of activity against the Gram positive *Staphilococci*, whereas no difference was found when the peptides SolyC and SolyC-t were tested against Gram negative bacteria. When tested against Gram positive bacteria, the analogs containing two cysteines (SolyC1 and SolyC2) show a reduced antimicrobial ability as compared with the reference peptide SolyC; MIC values are in all cases higher than that of SolyC, and there is no large difference between the activity of linear and oxidized peptides. Peptides are in general more active against Gram negative bacteria; linear peptides show lower MIC in the full length version as compared with the truncated form. Noteworthy, SolyC2, the peptide having the disulfide between C6 and C15, shows activity identical to that of the reference peptide. Oxidation results in an increase of the antimicrobial activity of the modified peptides against Gram negative bacteria, either in the extended or in the truncated form: all oxidized peptides exhibit activity identical or comparable with that of the reference peptide.

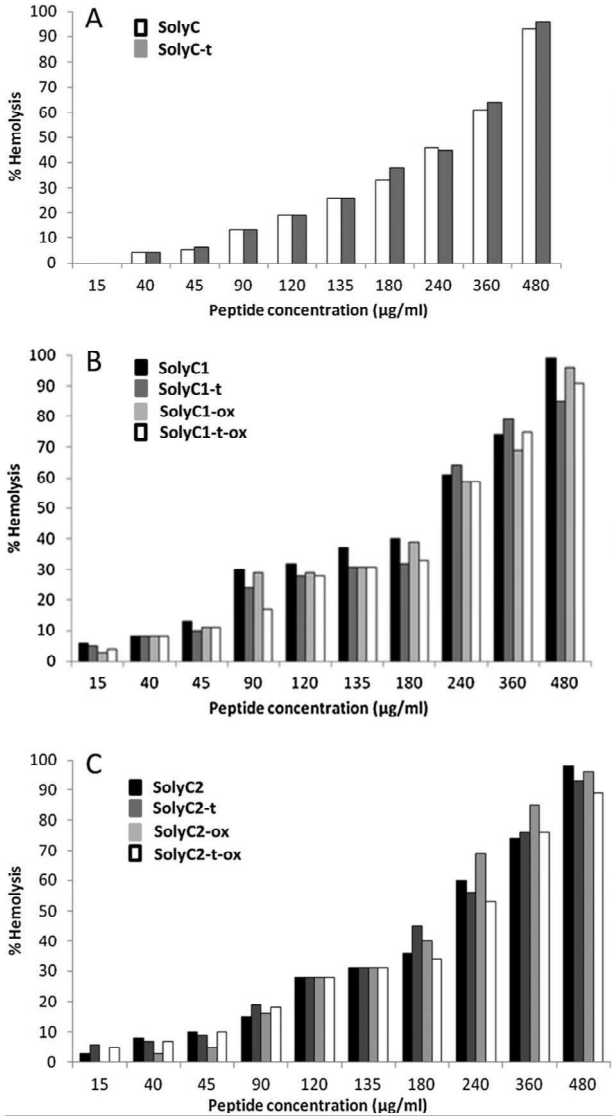

Figure 4. Hemolytic activity of the peptides measured at different concentrations.

The hemolytic activity of the peptides was tested for all peptides at several concentrations (Figure 4). Up to 90 μg/ml, all peptides have hemolytic activity below 30%. At low

Table 2. Antimicrobial activity of the peptides against Gram positive and Gram negative bacteria

Strains	MIC_{100} (μg/ml)									
	Peptide number									
	1	2	3	4	5	6	7	8	9	10
Staphylococcus aureus	40	50	50	50	80	80	80	50	100	80
Staphylococcus epidermidis	40	80	100	100	100	100	100	100	100	100
Listeria monocytogenes	80	80	80	80	80	80	80	80	80	80
Salmonella serovar paratyphi B	15	15	40	80	15	40	15	15	15	20
Helicobacter pylori	15	15	15	15	15	20	15	15	20	20

Table 3. LC50 for the SolyC and SolyC analogs

	Peptide number									
	1	2	3	4	5	6	7	8	9	10
LC50 (μg/ml)	275.2	266.7	212.3	228.5	226.5	213.0	229.6	231.0	197.4	235.1

concentrations, all long linear peptides and the oxidized form of SolyC1 show hemolytic activity comparable with that of truncated peptides. Interestingly, SolyC2 has in the long oxidized form (SolyC2-ox) very low hemolytic activity, comparable with that of the standard peptide.

LC50 measured for all peptides was found lower for the peptides containing only two cysteines as compared with SolyC (Table 3). The lowest LC50 value was observed for SolyC2 in the oxidized form (SolyC2-ox).

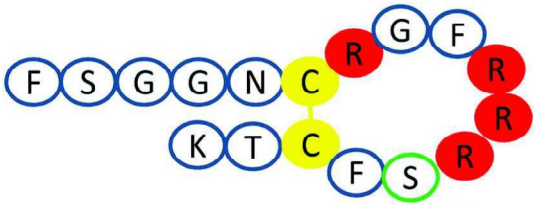

Figure 5. Schematic representation of the peptide SolyC2-ox; in red is the positively charged amino acids in the turn, in yellow is the cysteines involved in the disulfide bond, and in green is the cysteine residue mutated into serine.

Discussion

Peptides containing a γ core motif and, in particular, analogs of protegrins have widely been studied as they are capable to exert antimicrobial activity even at high salt concentrations, unlike other antimicrobial peptides that form sheets such as β defensins [28,29]. Interestingly, the PG-1 analog IB-367 has been tested in phase II clinical trials for the treatment of oral mucositis, and PG-1-based peptidomimetics were found to be active at nanomolar concentrations against *Pseudomonas aeruginosa* [30,31]. It has been reported that the stabilization of the hairpin is necessary for the activity: PG-1 analogs lacking cysteines, in which the hairpin is stabilized by a tryptophan zipper motif, possess antimicrobial activity comparable with PG-1 [32]. In PG-1, the number of disulfide bonds and their position affect the activity; analogs of PG-1 with a single disulfide bond possess antimicrobial activity comparable with PG-1 in the linear form.

The γ core of the tomato defensin family, to which SolyC peptides belong, has a strong similarity in the amino acid sequence with the γ core of other plant defensins as the Medicago sativa defensin 4 (MtDef4), and also with the levomeric form of PG-1 [9,33]. The three-dimensional structures of plant defensins, which are composed of about 50–60 amino acids, are very complex, and cysteines belonging to the γ core form disulfide bonds with cysteines located outside of the γ core [34–36]. In self-consistent γ cores as PG-1 and RTD-1, instead, the beta-hairpin structure is stabilized by two disulfide bonds between cysteines inside the γ core. SolyC is a fragment of a tomato defensin and, as most of the plant defensins, has a very conserved GXCRG motif within the γ core with three cysteines. It is reasonable to think that SolyC has a structural organization similar to that of plant defensin in which cysteines in the γ core are not connected between them. As we have demonstrated in a previous paper that the linear fragment SolyC possess high antimicrobial activity, we now explored the possibility of stabilizing the peptide structure introducing in a controlled fashion one disulfide bond and evaluated the effects of cyclization on the peptide antimicrobial activity and secondary structure. Furthermore, similar studies were carried out on truncated peptides.

In SolyC, cysteines are located in position i, i + 7, and i + 9; peptides with disulfide bonds between Cys i – i + 7 (SolyC1) and i – i + 9 (SolyC2) were obtained. The secondary structure of all peptides was analyzed by CD in phosphate buffer and in phosphate buffer containing SDS: both linear and oxidized peptides seem to be in an unordered form (Figure 3). All the analogs are more active against Gram negative than against Gram positive bacteria; these results are in line to what has been reported for PG-1 and PG-1 analogs with a single disulfide bond [28]. Interestingly, cyclic peptides are generally more active than linear ones against Gram negative bacteria. Cyclization induces a strong polarization of the peptides, confining the positive charges in the turn and the hydrophobic residues on the 'tails' and reasonably allows the peptide to interact with the bacterial LPS, neutralizing and permeating it (Figure 5). Recent studies aimed to characterize the interaction of rationally designed peptides with the LPS demonstrate that amphipatic peptides are active antimicrobials as they assume the structure of a β boomerang upon interaction with LPS, exerting their activity by disaggregating it [37]. These peptides are mimics of the outer membrane, as they possess a polar head and hydrophobic tails and easily intercalate into LPS. The SolyC cyclic analogs are already in the active conformation with the segregation of charges, and therefore, it is likely that they exert their activity as the β boomerang peptides do.

SolyC2 in the full length and truncated version shows antimicrobial activity identical to that of the reference peptide SolyC. These result may be interpreted hypothesizing that, in the experimental conditions employed for the activity test, SolyC spontaneously oxidizes, and the formation of the disulfide bond between Cys in position i and i + 9 is favored. As in SolyC2, only the disulfide bridge between Cys i and i + 9 can be formed, it is reasonable to think that the linear peptide spontaneously converts into the oxidized form that corresponds also to the active form. This hypothesis is consistent with the observation that full length SolyC2 in the linear and oxidized form has the same antimicrobial activity as the reference SolyC. Interestingly, in SolyC2, the cysteines involved in the disulfide bond are located in positions identical to external cysteines of PG-1, reproducing the cyclization pattern of the highly active 'bullet' peptide proposed by Harwig [28].

The observation that there is no difference in the activity against Gram negative bacteria of cyclic SolyC1 and SolyC2 derivatives, which differ in the number of amino acids included in the cycle, suggests that the charge segregation and not the dimension of the cycle is crucial for activity.

Journal of PeptideScience

All peptides at concentrations up to threefold that of MIC show very low hemolytic activity, indicating that these peptides are selective for bacterial outer membrane. The lowest percentage of hemolytic activity was found for the oxidized SolyC2. LC50 calculated for all peptides on murine red blood cells is lower for SolyC2, confirming the selectivity for negatively charged membrane (as the bacterial LPS) versus zwitterionic membranes (as the erythrocytes).

In conclusion, we have demonstrated that isolated γ cores of plant defensins possess strong antimicrobial activity against Gram negative bacteria; formation of an intramolecular disulfide bond stabilizes the peptides in the 'active' conformation. We found that the peptide SolyC2, which reproduces the disulfide bond pattern observed in PG-1, shows a high selectivity towards bacterial outer membrane and possess very low hemolytic activity at concentrations that are threefold the MIC. These results encourage future studies on the antimicrobial activity of isolated γ core peptides from plants due to their strength and specificity of action.

References

1 Ganz T. Defensins: antimicrobial peptides of innate immunity. *Nat. Rev. Immunol.* 2003; **3**: 710–720.
2 Zanetti M, Gennaro R, Romeo D. Cathelicidins: a novel protein family with a common proregion and a variable C-terminal antimicrobial domain. *FEBS Lett.* 1995; **374**: 1–5.
3 Schittek B, Hipfel R, Sauer B, Bauer J, Kalbacher H, Stevanovic S, Schirle M, Schroeder K, Blin N, Meier F, Rassner G, Garbe C. Dermcidin: a novel human antibiotic peptide secreted by sweat glands. *Nat. Immunol.* 2001; **2**: 1133–1137.
4 Castro MS, Fontes W. Plant defense and antimicrobial peptides. *Protein Pept. Lett.* 2005; **12**: 13–18.
5 Stec B. Plant thionins--the structural perspective. *Cell. Mol. Life Sci.* 2006; **63**: 1370–1385.
6 Chiche L, Heitz A, Gelly JC, Gracy J, Chau PT, Ha PT, Hernandez JF, Le-Nguyen D. Squash inhibitors: from structural motifs to macrocyclic knottins. *Curr. Protein Pept. Sci.* 2004; **5**: 341–349.
7 Yeaman MR, Yount NY. Unifying themes in host defence effector polypeptides. *Nat. Rev. Microbiol.* 2007; **5**: 727–740.
8 Yount NY, Andres MT, Fierro JF, Yeaman MR. The gamma-core motif correlates with antimicrobial activity in cysteine-containing kaliocin-1 originating from transferrins. *Biochim. Biophys. Acta* 2007; **1768**: 2862–2872.
9 Yount NY, Yeaman MR. Multidimensional signatures in antimicrobial peptides. *Proc. Natl. Acad. Sci. U.S.A.* 2004; **101**: 7363–7368.
10 Yeaman MR, Yount NY, Waring AJ, Gank KD, Kupferwasser D, Wiese R, Bayer AS, Welch WH. Modular determinants of antimicrobial activity in platelet factor-4 family kinocidins. *Biochim. Biophys. Acta* 2007; **1768**: 609–619.
11 Pelegrini PB, Franco OL. Plant gamma-thionins: novel insights on the mechanism of action of a multi-functional class of defense proteins. *Int. J. Biochem. Cell Biol.* 2005; **37**: 2239–2253.
12 Steinberg DA, Hurst MA, Fujii CA, Kung AH, Ho JF, Cheng FC, Loury DJ, Fiddes JC. Protegrin-1: a broad-spectrum, rapidly microbicidal peptide with in vivo activity. *Antimicrob. Agents Chemother.* 1997; **41**: 1738–1742.
13 Tran D, Tran PA, Tang YQ, Yuan J, Cole T, Selsted ME. Homodimeric theta-defensins from rhesus macaque leukocytes: isolation, synthesis, antimicrobial activities, and bacterial binding properties of the cyclic peptides. *J. Biol. Chem.* 2002; **277**: 3079–3084.
14 The tomato genome sequence provides insights into fleshy fruit evolution. *Nature* 2012; **485**: 635–641.
15 Rigano MM, Romanelli A, Fulgione A, Nocerino N, D'Agostino N, Avitabile C, Frusciante L, Barone A, Capuano F, Capparelli R. A novel synthetic peptide from a tomato defensin exhibits antibacterial activities against Helicobacter pylori. *J. Pept. Sci.* 2012; **12**: 755–762.
16 Romanelli A, Moggio L, Montella RC, Campiglia P, Iannaccone M, Capuano F, Pedone C, Capparelli R. Peptides from Royal Jelly: studies on the antimicrobial activity of jelleins, jelleins analogs and synergy with temporins. *J. Pept. Sci.* 2011; **17**: 348–352.
17 Becker K, Roth R, Peters G. Rapid and specific detection of toxigenic Staphylococcus aureus: use of two multiplex PCR enzyme immunoassays for amplification and hybridization of staphylococcal enterotoxin genes, exfoliative toxin genes, and toxic shock syndrome toxin 1 gene. *J. Clin. Microbiol.* 1998; **36**: 2548–2553.
18 Hong Y, Liu T, Lee MD, Hofacre CL, Maier M, White DG, Ayers S, Wang L, Berghaus R, Maurer JJ. Rapid screening of Salmonella enterica serovars Enteritidis, Hadar, Heidelberg and Typhimurium using a serologically-correlative allelotyping PCR targeting the O and H antigen alleles. *BMC Microbiol.* 2008; **8**: 178.
19 Tomasini ML, Zanussi S, Sozzi M, Tedeschi R, Basaglia G, De Paoli P. Heterogeneity of cag genotypes in Helicobacter pylori isolates from human biopsy specimens. *J. Clin. Microbiol.* 2003; **41**: 976–980.
20 Bubert A, Hein I, Rauch M, Lehner A, Yoon B, Goebel W, Wagner M. Detection and differentiation of Listeria spp. by a single reaction based on multiplex PCR. *Appl. Environ. Microbiol.* 1999; **65**: 4688–4692.
21 Martineau F, Picard FJ, Roy PH, Ouellette M, Bergeron MG. Species-specific and ubiquitous DNA-based assays for rapid identification of Staphylococcus epidermidis. *J. Clin. Microbiol.* 1996; **34**: 2888–2893.
22 Capparelli R, Romanelli A, Iannaccone M, Nocerino N, Ripa R, Pensato S, Pedone C, Iannelli D. Synergistic antibacterial and anti-inflammatory activity of temporin A and modified temporin B in vivo. *PLoS One* 2009; **4**: e7191.
23 Vinhal Costa Orsine J, Vinhal da Costa R, Carvalho da Silva R, de Fatima Menezes Almeida Santos M, Carvalho Garbi Novaes MR. The acute cytotoxicity and lethal concentration (LC50) of Agaricus sylvaticus through hemolytic activity on human erythrocyte. *Intl. J. Nutr. Metabol.* 2012; **4**: 19–23.
24 Fahrner RL, Dieckmann T, Harwig SS, Lehrer RI, Eisenberg D, Feigon J. Solution structure of protegrin-1, a broad-spectrum antimicrobial peptide from porcine leukocytes. *Chem. Biol.* 1996; **3**: 543–550.
25 Mani R, Cady SD, Tang M, Waring AJ, Lehrer RI, Hong M. Membrane-dependent oligomeric structure and pore formation of a beta-hairpin antimicrobial peptide in lipid bilayers from solid-state NMR. *Proc. Natl. Acad. Sci. U.S.A.* 2006; **103**: 16242–16247.
26 Yount NY, Yeaman MR. Emerging themes and therapeutic prospects for anti-infective peptides. *Annu. Rev. Pharmacol. Toxicol.* 2012; **52**: 337–360.
27 Kyte J, Doolittle RF. A simple method for displaying the hydropathic character of a protein. *J. Mol. Biol.* 1982; **157**: 105–132.
28 Harwig SS, Waring A, Yang HJ, Cho Y, Tan L, Lehrer RI. Intramolecular disulfide bonds enhance the antimicrobial and lytic activities of protegrins at physiological sodium chloride concentrations. *Eur. J. Biochem.* 1996; **240**: 352–357.
29 Goldman MJ, Anderson GM, Stolzenberg ED, Kari UP, Zasloff M, Wilson JM. Human beta-defensin-1 is a salt-sensitive antibiotic in lung that is inactivated in cystic fibrosis. *Cell* 1997; **88**: 553–560.
30 Mosca DA, Hurst MA, So W, Viajar BS, Fujii CA, Falla TJ. IB-367, a protegrin peptide with in vitro and in vivo activities against the microflora associated with oral mucositis. *Antimicrob. Agents Chemother.* 2000; **44**: 1803–1808.
31 Srinivas N, Jetter P, Ueberbacher BJ, Werneburg M, Zerbe K, Steinmann J, Van der Meijden B, Bernardini F, Lederer A, Dias RL, Misson PE, Henze H, Zumbrunn J, Gombert FO, Obrecht D, Hunziker P, Schauer S, Ziegler U, Kach A, Eberl L, Riedel K, DeMarco SJ, Robinson JA. Peptidomimetic antibiotics target outer-membrane biogenesis in Pseudomonas aeruginosa. *Science* 2010; **327**: 1010–1013.
32 Lai JR, Huck BR, Weisblum B, Gellman SH. Design of non-cysteine-containing antimicrobial beta-hairpins: structure-activity relationship studies with linear protegrin-1 analogues. *Biochemistry* 2002; **41**: 12835–12842.
33 Sagaram US, Pandurangi R, Kaur J, Smith TJ, Shah DM. Structure-activity determinants in antifungal plant defensins MsDef1 and MtDef4 with different modes of action against Fusarium graminearum. *PLoS One* 2011; **6**: e18550.
34 Janssen BJ, Schirra HJ, Lay FT, Anderson MA, Craik DJ. Structure of Petunia hybrida defensin 1, a novel plant defensin with five disulfide bonds. *Biochemistry* 2003; **42**: 8214–8222.
35 Fant F, Vranken W, Broekaert W, Borremans F. Determination of the three-dimensional solution structure of Raphanus sativus antifungal protein 1 by 1H NMR. *J. Mol. Biol.* 1998; **279**: 257–270.
36 Fant F, Vranken WF, Borremans FA. The three-dimensional solution structure of Aesculus hippocastanum antimicrobial protein 1 determined by 1H nuclear magnetic resonance. *Proteins* 1999; **37**: 388–403.
37 Bhunia A, Mohanram H, Domadia PN, Torres J, Bhattacharjya S. Designed beta-boomerang antiendotoxic and antimicrobial peptides: structures and activities in lipopolysaccharide. *J. Biol. Chem.* 2009; **284**: 21991–22004.

Research Article

Journal of PeptideScience

Received: 25 July 2012 Revised: 3 October 2012 Accepted: 5 October 2012 Published online in Wiley Online Library

(wileyonlinelibrary.com) DOI 10.1002/psc.2462

A novel synthetic peptide from a tomato defensin exhibits antibacterial activities against *Helicobacter pylori*

M. M. Rigano,[a] A. Romanelli,[b] A. Fulgione,[a] N. Nocerino,[a] N. D'Agostino,[c] C. Avitabile,[b] L. Frusciante,[d] A. Barone,[a] F. Capuano[e] and R. Capparelli[a]*

Defensins are a class of cysteine-rich proteins, which exert broad spectrum antimicrobial activity. In this work, we used a bioinformatic approach to identify putative defensins in the tomato genome. Fifteen proteins had a mature peptide that includes the well-conserved tetradisulfide array. We selected a representative member of the tomato defensin family; we chemically synthesized its γ-motif and tested its antimicrobial activity. Here, we demonstrate that the synthetic peptide exhibits potent antibacterial activity against Gram-positive bacteria, such as *Staphylococcus aureus* A170, *Staphylococcus epidermidis*, and *Listeria monocytogenes*, and Gram-negative bacteria, including *Salmonella enterica* serovar Paratyphi, *Escherichia coli*, and *Helicobacter pylori*. In addition, the synthetic peptide shows minimal (<5%) hemolytic activity and absence of cytotoxic effects against THP-1 cells. Finally, SolyC exerts an anti-inflammatory activity *in vitro*, as it downregulates the level of the proinflammatory cytokines TNF-α and IFN-γ. Copyright © 2012 European Peptide Society and John Wiley & Sons, Ltd.

Supporting information may be found in the online version of this article.

Keywords: antimicrobial peptide; defensin; tomato; *Helicobacter pylori*

Introduction

Attention towards new antimicrobial agents is growing because of the rising of antibiotic and multidrug bacterial resistance [1,2]. Particular interest is devoted to the development of novel antibiotics against *Helicobacter pylori*, a Gram-negative bacterium that chronically infects the gastric mucosa of more than half of the human population and sometimes causes severe diseases, such as gastric cancer [3]. *H. pylori* LPS shows extremely low endotoxic activity, compared with typical Gram-negative LPSs, allowing it to establish chronic colonization without causing a systemic inflammatory response [4]. Currently, the prevalent approach for *H. pylori* eradication is based on antibiotic treatment. However, antibiotics cause serious effects on the intestinal microflora and induce antibiotic-resistant strains [5].

Antimicrobial peptides are cationic molecules of the innate immune system and represent a valid defense mechanism against infections because of their broad spectrum antibiotic activity and low eukaryotic cell toxicity. In addition, they rarely induce bacterial resistance [1,6]. Defensins are the only class of peptides in the innate immune response that is conserved among plants, invertebrates, and vertebrates [7]. They are cysteine-rich proteins with a common three-dimensional structure rich in β-sheets [1]. Plant defensins (originally classified as γ-thionins, [8]) are small, basic, highly stable proteins with antifungal and antibacterial properties [8,9]. Their structure resembles that of insect and mammalian defensins, corroborating the idea that all defensins evolved from a single precursor [8]. Indeed, Yount and Yeamen [10] identified a conserved γ-core motif ($GXCX_{3-9}C$) – composed of two antiparallel β-sheets and an interposed loop [10] – in disulphide-containing AMPs from several phylogenetically diverse organisms. This motif has a net cationic charge and can be found in other host-defense polypeptides with antimicrobial activity, such as venoms, toxins, or microbicidal chemokines [11].

The recent release of the tomato genome sequence [12] facilitates the identification of genes encoding proteins with potential antimicrobial activity. In this work, we used bioinformatics methods to identify and characterize tomato defensins. Then, on the basis of sequence information, we selected a representative member of the family; we chemically synthesized a peptide (SolyC) corresponding

* *Correspondence to: Rosanna Capparelli, University of Naples 'Federico II', School of Biotechnological Sciences, Department of Soil, Plant, Environmental and Animal Production Sciences, Via Università 100, 80055 Portici, Naples, Italy. E-mail: capparel@unina.it*

a *University of Naples 'Federico II', School of Biotechnological Sciences, Department of Soil, Plant, Environmental and Animal Production Sciences, Via Università 100, 80055, Portici, Italy*

b *University of Naples 'Federico II', School of Biotechnological Sciences, Department of Biological Sciences, Via Mezzocannone 16, 80134, Naples, Italy*

c *CRA-ORT, Agricultural Research Council, Research Centre for Vegetable Crops, Via Cavalleggeri 25, 84098, Pontecagnano, SA, Italy*

d *University of Naples 'Federico II', Department of Soil, Plant, Environmental and Animal Production Sciences, Via Università 100, 80055, Portici, Italy*

e *Department of Food Inspection IZS ME, via Salute 2, 80055, Portici, Italy*

Abbreviations used: *LPS, lipopolysaccharide; AMP, antimicrobial peptides; ASA, acetylsalicylic acid; MIC, minimum inhibitory concentration.*

to its γ-motif and finally tested its antimicrobial activity. We demonstrate that SolyC has antibacterial activity against a panel of human pathogens, including *H. pylori*, and displays anti-inflammatory activity *in vitro*.

Material and Methods

Bioinformatics Analysis

HMM profile PF00304 was retrieved from Pfam [13]. The *hmmsearch* program (e-value $1e^{-5}$; http://hmmer.org) was used to search against tomato proteins (iTAG v.2.3). Further, 57 plant defensins were retrieved from PhytAMP [14].

Multiple protein sequence alignments were generated using ClustalW [15]. Sequence distances were calculated with PROTDIST using the Dayhoff PAM matrix, and neighbor-joining trees were built using NEIGHBOR (from Phylip v3.67; http://evolution.genetics.washington.edu/phylip.html). Unrooted trees were displayed with FigTree (v.1.3.1; http://tree.bio.ed.ac.uk/software/ figtree/).

The overall charge of the γ-core motifs and of the synthetic peptide was estimated at pH 7 using Biochemistry online (http://vitalonic.narod.ru/biochem).

Peptide Synthesis

The amino acids used for the peptide synthesis Fmoc-Phe-OH, Fmoc-Ser(OtBu)-OH, Fmoc-Gly-OH, Fmoc-Asn(Trt)-OH, Fmoc-Cys (Trt)-OH, Fmoc-Arg(Pbf)-OH, Fmoc-Thr(OtBu), Fmoc-Lys(Boc)-OH, the Rink amide MBHA, and the activators *N*-hydroxybenzotriazole (HOBT) and *O*-benzotriazole-*N*,*N*,*N*′,*N*′-tetramethyl-uronium-hexafluoro-phosphate (HBTU) were purchased from Novabiochem. Acetonitrile (ACN) was from Reidel-deHaën and dry *N*,*N*-dimethyl-formamide (DMF) from LabScan. All other reagents were from Sigma Aldrich. LC-MS analyses were performed on an LC-MS Thermo Finnigan with an electrospray source (MSQ) on a Phenomenex Jupiter 5 μ C18 300 Å, (150 × 4.6 mm) column. Purification was carried out on a Phenomenex Jupiter 10 μ Proteo 90 Å (250 × 10 mm) column. The Peptide SolyC (FSGGNCRGFRRRCFCTK-NH_2) was synthesized on solid phase by Fmoc chemistry on the MBHA (0.54 mmol/g) resin by consecutive deprotection, coupling, and capping cycles [16]. Deprotection: 30% piperidine in DMF, 5 min (2×). Coupling: 2.5 equivalents of amino acid + 2.49 equivalents of HOBT/HBTU (0.45 M in DMF) + 3.5 equivalents NMM, 40 min. Capping: acetic anhydride/DIPEA/DMF 15/15/70 v/v/v, 5 min. The peptide was cleaved off the resin and deprotected by treatment of the resin with a solution of TFA/TIS/H_2O 95/2.5/2.5 v/v/v, 90 min. TFA was concentrated, and peptides were precipitated in cold ethylic ether. Analysis of the crudes was performed by LC-MS using a gradient of ACN (0.1% TFA) in water (0.1% TFA) from 5% to 70% in 30 min. Purification was performed by semipreparative RP-HPLC using a gradient of ACN (0.1% TFA) in water (0.1% TFA) from 5% to 70% in 30 min.

The identity of the peptide SolyC (FSGGNCRGFRRRCFCTK-NH_2) was verified by mass spectrometry.

Calculated mass (Da): 1994.33, $[M+2H]2^+$: 998.16; $[M+3H\,3^+]$: 665.77; found (Da): $[M+H]^+$ 1995.49; $[M+2H]2^+$: 997.75; $[M+3H\,3^+]$: 665.77.

Bacteria

List and origin of the different strains used in this study, as well as their resistance/susceptibility to conventional antibiotics are reported in Tables S1 and S2. Bacterial isolates were from patients hospitalized at the Medical School of the University of Naples 'Federico II' and at the 'Villa Betania' hospital (Naples, Italy). Species identification was carried out by PCR [17–21]. Bacteria were grown at 37 °C in TSB or LB medium, harvested in the exponential phase (OD 600 nm 0.6–0.8), centrifuged (10 min at 8×10^3 g) and resuspended in Muller Hinton broth at the concentration of ~10^5 CFU/ml. The antibiotic-susceptibility profile of strains was determined using the disk diffusion method on Mueller-Hinton agar, according to the NCCLS guidelines (2002). The antibiotics used and their concentrations were as follows: trimethropim + sulfamethoxazole (25 μg; SXT), sulphonamide (300 μg; S3, SUL), nalidixic acid (30 μg; NA), enrofloxacin (10 μg; ENX), ciprofloxacin (5 μg; CIP), ampicillin (10 μg; AMP), cefalotin (30 μg; KF, CF), tetracycline (30 μg; TE, TET), gentamicin (10 μg; CN, GEN), kanamycin (30 μg; K,KAN), ceftazidime (30 μg; CAZ), streptomycin (10 μg; S, STR), chloramphenicol (30 μg; C, CLO), amoxicillin + clavulamic acid (30 μg; AMC), cefoxitin (30 μg; FOX). All antibiotics were provided by OXOID and Becton Dickinson.

Antibacterial and Hemolytic Activity

Bacteria were distributed in triplicate into plates (60 μl/well), mixed with SolyC dilutions (5–100 μg/ml; 40 μl/well) and incubated at 37 °C for 20 h. The minimal concentration of SolyC causing 100% growth inhibition (MIC_{100}) was determined by measuring the absorbance at 600 nm (Biorad microplate reader model 680, CA). The antibacterial activity was measured by spotting 10 μl from each well on TSA or LB agar and counting the CFUs [22]. The antibacterial test was extended to the probiotic bacteria *Lactobacillus plantarum* and *Lactobacillus paracasei*. The test was performed in triplicate. SolyC was tested for its hemolytic activity using mouse red blood cells. The hemolytic activity was measured according to the formula $OD_{peptide} - OD_{negative\ control}/OD_{positive\ control} - OD_{negative\ control} \times 100$ where the negative control (0% hemolysis) was represented by erythrocytes suspended in saline and the positive control (100% hemolysis) was represented by the erythrocytes lysed with 1% triton X100 [22].

The LC50 value relative to the SolyC was calculated as described [23].

Cell Culture

The THP-1 human acute monocytic leukemia cells (American Tissue Culture Collection, MD, USA) were cultured in complete medium (CM) consisting of RPMI medium (Gibco, Scotland), 10% fetal bovine serum, 100 IU/ml penicillin, and 100 μg/ml streptomycin (all from Gibco). Cell adhesion was induced with phorbol myristate acetate (2 μg/ml/well).

Cell Viability

Trypan blue test

THP-1 cells (10^6 cells/well) were let adhere (37 °C, 5% CO_2) in CM. Then, they were incubated first with SolyC (60–120 μg/ml for 24, 48, or 72 h), and then with 1% trypsin (1.5 ml/well at 37 °C for 3 min) and finally with CM (3 ml/well). The whole mixture was transferred into a test tube and centrifuged (3 min at 1000 g). The pellet was resuspended in 1 ml CM. A 10 μl of cell suspension was mixed with 10 μl of Trypan blue, and the percentage of viability was determined using the formula: N° viable cells/(N° non viable cells + viable cells) × 100.

Journal of PeptideScience

MTT

Cell viability was determined by the CellTiter 96® AQueous One Solution Cell Proliferation Assay (MTS) (Promega, WI, USA). THP-1 cells (2500/well) were incubated at 37 °C in 5% CO_2. SolyC (60 μg/ml and 120 μg/ml) or PBS was added to the medium after cell adhesion. At each time point, MTS solution (20 μl/well) was added. Absorbance was recorded at 490 nm after 2 h using an EnVision 2102 multilabel reader (PerkinElmer, USA).

Nitrite Formation in THP-1 Cells

THP-1 cells adhesion (10^6/well) was induced with phorbol myristate acetate (2 μg/ml/well; 12 h) and then stimulated for 24, 48, or 72 h with LPS (10 μg/ml), SolyC (50 μg/ml), or with a combination of both. Nitrite accumulation (NO_2^-, μmol/10^6 cells) in the medium was determined by the Griess reaction [24].

ELISA Test of Proinflammatory Cytokines

TNF-α and IFN-γ levels were estimated by the sandwich ELISA assay. Briefly, THP-1 cells (10^6 cells/well) were stimulated with LPS (10 μg/ml; 1 h), treated with 50 μg/ml ASA or SolyC (50, 100, or 120 μg/ml; 1 h) in the presence or absence of LPS (10 μg/ml). The supernatants from these cells (100 μl/well) were transferred into the wells of a plate previously coated with mouse anti-human TNF-α (BD Pharmingen; 50 μl diluted 2×10^{-3}/well) or mouse anti-human IFN-γ (Biosciences, 50 μl diluted 2×10^{-3}/well) along with a second dose of anti-IFN-γ or TNF-α, HRP-labeled rabbit anti mouse IgG diluted 10^{-3} (100 μl/well) and TMB peroxidase substrate (BIORAD; 100 μl/well), in the order. The optical density of each well was read at 405 nm using a microplate reader (Bio-Rad, Japan). Triplicate positive and negative controls were included in each plate [25].

Ethical Treatment

The study investigated *in vitro* the antibacterial activity of a synthetic peptide on *H. pylori* isolates provided by 'Villa Betania' hospital (Naples, Italy). The study neither investigate clinical aspects of the disease nor it uses human specimen. The study therefore does not require the Ethic Committee approval.

Results

Bioinformatics Analysis

A total of 16 defensin proteins were identified by using the Pfam HMM profile PF00304 (Table 1). An additional protein (tagged with * in Table 1) was initially included in this dataset based on the iTAG functional annotation [12].

All proteins but two have a mature peptide that includes the eight conserved cysteines involved in disulfide bonds essential for structural folding [8]. The most represented consensus sequence is C–X_{10}–C–X_5–C–X_3–C–X_9–C–X_6–C–X–C–X_3–C, present in 11 out of 15 proteins. The spacing of cysteines is different in some instances. By contrast, the Solyc07g016120 and Solyc11g028060 proteins lack the tetradisulfide array (Table 1) and were excluded from the subsequent phylogenetic analyses. We assigned 12 proteins to the class I of plant defensins, characterized by an endoplasmic reticulum signal sequence and a mature defensin domain. The remaining three proteins were assigned to the class II of plant defensins, characterized by the presence of an additional C-terminal prodomain (Table 1; [26]). With the exception of Solyc11g028060 and Solyc07g007760, which consist of one and three exons, respectively, nearly all the identified γ-thionins are composed of two exons. Finally, we investigated the chromosomal localization of these genes: three are on chromosomes 4, eight on chromosome 7, five on chromosome 11, and one on chromosome 9. Also, we identified a cluster of five members on chromosome 7 and a cluster of three members on chromosome 11.

The 15 mature defensin peptides were used to generate the multiple sequence alignment shown in Figure 1A. Tomato defensins exhibit clear sequence conservation, just like plant γ-thionins. Importantly, the γ-core motifs differ among tomato defensins in their primary amino acid sequences, even if distinct groups of γ-core motifs can be clearly distinguished based on sequence similarity (Figure 1A).

To show the phylogenetic relationships within the tomato defensin family, an unrooted neighbor-joining tree was built (Figure 1B). Two distinct clades were clearly visible. The first one includes class II defensins, whereas the second one includes class I γ-thionins. This clade can be further divided into four subclades. The largest subclade includes five members, four of which belong to the gene cluster identified on chromosome 7. An additional neighbor-joining tree included all the plant defensins collected from the PhytAMP database ([14]; supplementary figure 1). The clustering of class I and class II defensins was still clearly observable. Indeed, class II tomato defensins are grouped with further proteins from *Petunia hybrida* and *Nicotiana* confirming that these defensins are typical of the Solanaceae family [26]. Solyc07g007760 was selected as representative of the tomato defensin family because the primary sequence of its γ-core motif is almost identical to that of five more tomato defensins, and it displays features compatible with antimicrobial activity, such as its total net charge, which is +5 (Figure 1A). A 17 amino acid long peptide (highlighted in Figure 1A) containing the γ-core motif sequence of the defensin Solyc07g007760 was chemically synthesized and tested for antibacterial activity.

Characterization of Bacterial Strains

The different bacteria strains used in this study were characterized by phenotypical (antibiotic resistance/susceptibility patter) analysis. Results of antibiotic resistance are reported in Table S2. All *H. pylori* strains were resistant to ampicillin (10 μg; AMP), gentamicin (10 μg; CN, GEN), kanamycin (30 μg; K,KAN), streptomycin (10 μg; S, STR), and amoxicillin + clavulamic acid (30 μg; AMC) and sensitive to the remaining antibiotics tested. *Staphylococcus aureus* A170 and *Staphylococcus epidermidis* were sensitive to all antibiotics except to nalidixic acid (30 μg; NA). *Salmonella enterica* serovar Paratyphi was resistant to tetracycline (30 μg; TE, TET) and sensitive to the other antibiotics, whereas the remaining strains were sensitive to all antibiotics.

Antibacterial and Anti-inflammatory Activity

The synthetic peptide SolyC showed antimicrobial activity against Gram-negative bacteria, including *Helicobacter pylori*, at low concentration (MIC: 15 μg/ml) and, at higher concentration (MIC: 40 μg/ml), also against Gram-positive bacteria (Table 2). In addition, SolyC displayed very low antibacterial activity (much lower than that of gentamicin) against probiotic bacteria (*L. plantarum* and *L. paracasei*) (Table 3). The synthetic peptide, at 50 μg/ml, displayed

Table 1. List of tomato defensins[a]

gene id	Chromosome	gene coordinates	Num. exons	protein length	class	spacing of cysteine residues
Solyc04g008470	4	2087094-2089108	2	73	I	C-X_{10}-C-X_5-C-X_3-C-X_9-C-X_6-C-X-C-X_3-C
Solyc04g009590	4	2983229-2984644	2	76	I	C-X_{10}-C-X_5-C-X_3-C-X_9-C-X_8-C-X-C-X_3-C
Solyc04g072470	4	57080225-570813	2	80	I	C-X_{10}-C-X_5-C-X_3-C-X_9-C-X_7-C-X-C-X_3-C
Solyc07g006380	7	1207489-1208297	2	105	II	C-X_{10}-C-X_5-C-X_3-C-X_9-C-X_6-C-X-C-X_3-C
Solyc07g007710	7	2362299-2363266	2	76	I	C-X_{10}-C-X_5-C-X_3-C-X_9-C-X_6-C-X-C-X_3-C
Solyc07g007730	7	2374606-2376176	2	79	I	C-X_{10}-C-X_5-C-X_3-C-X_9-C-X_6-C-X-C-X_3-C
Solyc07g007740	7	2383190-2383538	2	76	I	C-X_{10}-C-X_4-C-X_3-C-X_9-C-X_8-C-X-C-X_3-C
Solyc07g007750	7	2390188-2391454	2	75	I	C-X_{10}-C-X_5-C-X_3-C-X_9-C-X_6-C-X-C-X_3-C
Solyc07g007760	7	2394467-2396320	3	78	I	C-X_{10}-C-X_5-C-X_3-C-X_9-C-X_6-C-X-C-X_3-C
Solyc07g009260	7	4313698-4315233	2	76	I	C-X_{10}-C-X_4-C-X_3-C-X_9-C-X_8-C-X-C-X_3-C
Solyc07g016120	7	6304496-6305153	2	88	n.d.	C-X_{10}-C-X_5-C-X_3-C
Solyc09g074440	9	61747475-617482	2	74	I	C-X_{10}-C-X_5-C-X_3-C-X_9-C-X_6-C-X-C-X_3-C
Solyc11g006260	11	1008356-1008972	2	76	I	C-X_{10}-C-X_5-C-X_3-C-X_9-C-X_6-C-X-C-X_3-C
Solyc11g006950	11	1452336-1452920	2	73	I	C-X_{10}-C-X_5-C-X_3-C-X_9-C-X_6-C-X-C-X_3-C
Solyc11g028040	11	16598859-16599530	2	105	II	C-X_{10}-C-X_5-C-X_3-C-X_9-C-X_6-C-X-C-X_3-C
Solyc11g028060*	11	16615578-16615835	1	85	n.d.	C-X_6-C-X-C-X_3-C
Solyc11g028070	11	16643406-16644076	2	105	II	C-X_{10}-C-X_5-C-X_3-C-X_9-C-X_6-C-X-C-X_3-C

[a]This table shows, for each sequence, chromosomal localization, gene coordinates, number of exons, protein length, class, and the consensus sequence describing the spacing of cysteines. Gray rows indicate proteins that lack the tetradisulfide array. '*' identified based only on the iTAG functional annotation. n.d., not determined.

<5% hemolytic activity, and the LC50 value was 0.27 mg/ml. In addition, at 60–120 μg/mL, displayed no cytotoxic effects, SolyC-treated THP-1 cells remained viable for up to 72 h (Figure 2A and B). Furthermore, SolyC reduced ($p < 0.01$) the production of NO_2^- by cells stimulated with LPS, compared with control cells (stimulated with LPS, but not treated with SolyC) (Table 4).

Journal of PeptideScience

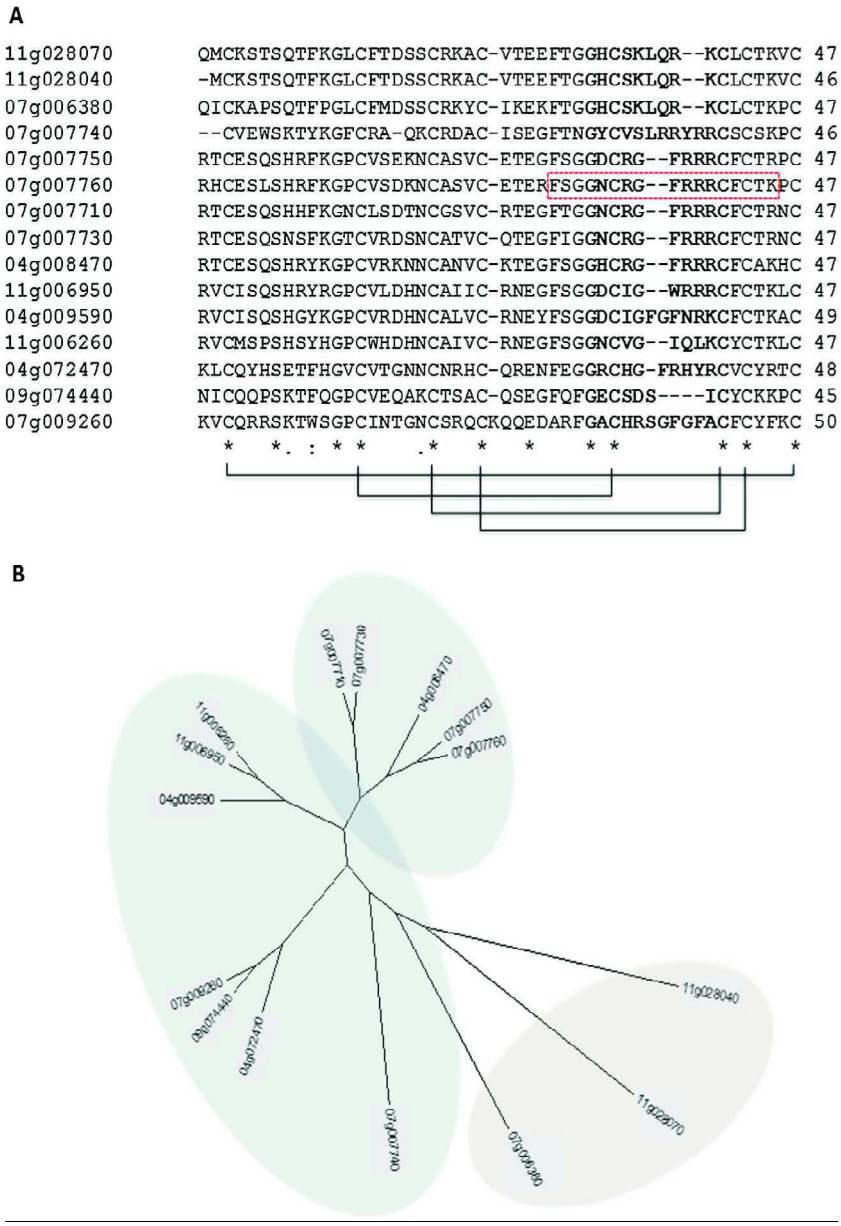

Figure 1. (A) Multiple alignment of the 15 tomato mature defensin proteins. Disulfide bonds between the eight conserved cysteines are shown by connecting lines. Gamma-core motifs are shown in bold. The sequence of the synthetic peptide SolyC is highlighted in the box. (B) The alignment in (A) was used to generate the phylogenetic tree for the tomato defensin family.

THP-1 cells, stimulated with LPS and then challenged with ASA or SolyC, showed significantly lower levels of TNF-α and IFN-γ, compared with cells treated with LPS. The results show that both SolyC and ASA curb the synthesis of the proinflammatory cytokines TNF-α and IFN-γ (Figure 3A and B). In the absence of the agent causing inflammation (LPS), SolyC or ASA does not induce inflammation (Figure 3A and B). These experiments demonstrate that SolyC exerts anti-inflammatory activity.

Discussion

In this paper, we investigated the antimicrobial and anti-inflammatory activity of a synthetic peptide derived from the tomato defensin family. Plant defensins are appropriate candidates for therapeutic applications because of their broad range of antimicrobial activity, their stability, and low cytotoxicity in humans [9].

We are aware that via Hidden Markov Model searches, a genome wide search of defensin-like genes is possible [27]. However, our aim was to identify a reliable defensin core gene set rather than detecting all the possible defensin-like genes present in the tomato genome. We identified 17 tomato defensins, which are composed of two exons and one intron of variable size. As in the case of plant defensins, the first exon almost entirely encodes the signal peptide, whereas the second encodes the central defensin domain [6]. Then, we grouped the tomato defensins according to their class membership. It is well documented that plant defensins can be divided into two classes and that defensins of class II are limited to solanaceous plants [26]. As a member of the Solanaceae, tomato has defensins

Table 2. List of the bacteria strains used in this study and SolyC MIC for each strain

Bacterial species/strains	SolyC MIC (μg/ml)
Gram +	
Staphylococcus aureus A170	40
Staphylococcus epidermidis	40
Listeria monocytogenes	40
Gram −	
Salmonella enterica serovar Paratyphi	15
Escherichia coli	15
Helicobacter pylori VB*1	15
Helicobacter pylori VB*2	10
Helicobacter pylori VB*3	15
Helicobacter pylori VB*4	12
Helicobacter pylori VB*5	15
Helicobacter pylori VB*6	10
Helicobacter pylori VB*7	15
Helicobacter pylori VB*8	10
Helicobacter pylori VB*9	10
Helicobacter pylori VB*10	15

* Villa Betania hospital.

Table 3. Antimicrobial activity of SolyC and Gentamicin on probiotic bacteria

	SolyC[a] 50 μg/ml	Gentamicin[a] 5 μg/ml
Lactobacillum plantarum	15% ± 2	97% ± 4
Lactobacillum paracasei	13% ± 2	96% ± 3

[a]Data are reported as percentage of bacterial growth inhibition ± standard deviation.

belonging to both classes (Table 1). Finally, a genome overview allowed two defensin gene clusters to be identified. Defensin gene clusters have been already observed in Arabidopsis, and it has been assumed that individual clusters have evolved through local duplications [27]. The same mechanism very likely caused the expansion of tomato defensin gene family.

In this work, we were interested in the identification and synthesis of novel peptides active against human pathogens. By sequence alignment with known γ-motifs, which are recognized to be the major determinants of the antimicrobial activity of several peptides produced by organism belonging to all kingdoms of life, we identified in the defensin Solyc07g007760 its putative γ-motif [28].

It is known that plant defensins are mainly active against fungal pathogens and, less frequently, against Gram-positive bacteria [6]. In this study, we showed that SolyC controls the bacterial load and, surprisingly, especially the growth of the Gram-negative

Table 4. NO_2^- production of THP-1 cells subjected to four treatment protocols

Treatment	NO_2^- production[a]		
	24 h[b]	48 h[b]	72 h[b]
No treatment	0.118 ± 0.05**	0.254 ± 0.03**	0.557 ± 0.01**
SolyC	0.118 ± 0.02**	0.277 ± 0.03**	0.55 ± 0.03**
LPS	1.938 ± 0.2	2.75 ± 0.4	4.09 ± 0.3
LPS + SolyC	0.59 ± 0.05**	0.925 ± 0.03**	1.332 ± 0.1**

[a]Data are expressed as micromoles of NO_2^- for 10^6 input cells and are means ± standard deviation of three different experiments each performed in triplicate.

[b]Time of incubation.

** $p < 0.01$ *versus* LPS according to Student's *t* test.

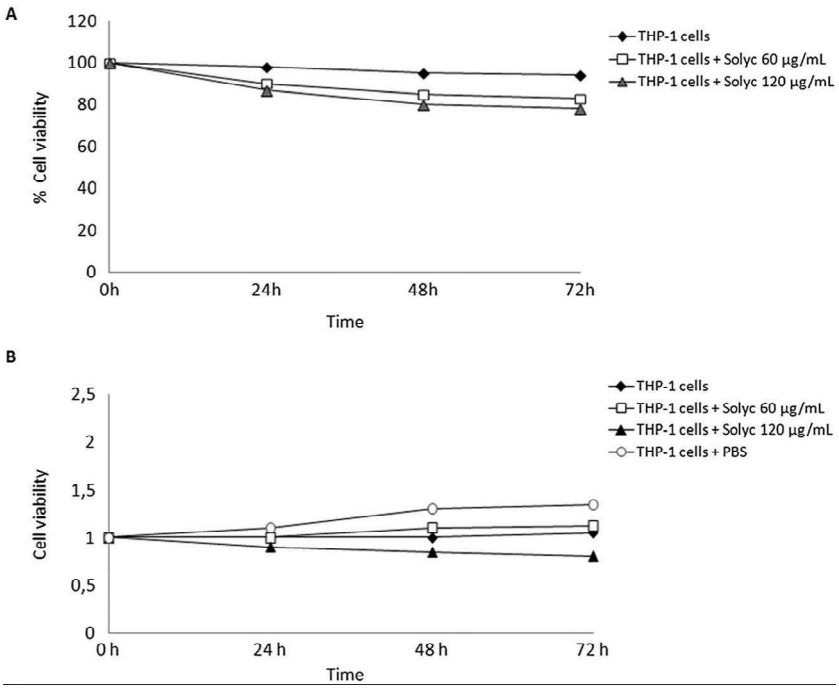

Figure 2. Analysis of cell viability. (A) THP-1 cells were treated with SolyC, and cell viability was determined by Trypan blue test. (B) THP-1 cells were treated with SolyC or PBS, and cell viability was determined by MTT assay.

Journal of PeptideScience

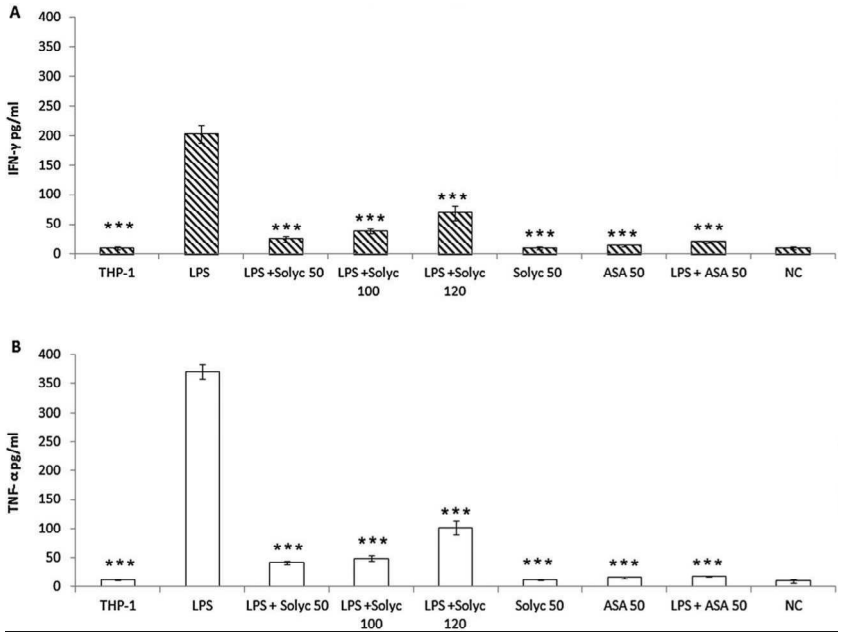

Figure 3. Anti-inflammatory activity. The levels of IFN-γ (A) and TNF-α (B) were determined by a sandwich ELISA test in THP-1 cells untreated; THP-1 cells stimulated with LPS for 1 h and then treated with SolyC (50, 100, or 120 μg/ml); THP-1 cells treated with Solyc (50 μg/ml) or ASA (50 μg/ml) for1 h; THP-1 cell stimulated with LPS for 1 h and then treated with ASA (50 μg/ml). Negative Control (NC): culture medium RPMI. Results from two representative experiments are presented as mean value $\pm$ SD. Statistical analysis was performed by Student's *t* test, ***$p < 0.001$.

bacterium *H. pylori*. This could be probably due to a strong electrostatic interaction between the cationic peptide SolyC and the anionic bacterial membranes. Work is under way to elucidate the interaction of the tomato peptide with the bacterial membrane and to determine the relative contribution of other residues on the antibacterial potency of this peptide.

In addition, we demonstrated that SolyC downregulates the level of proinflammatory cytokines and that this effect is comparable with that of ASA, a well-known anti-inflammatory drug. It is reported that human defensins in mixture with microbial antigens attenuate proinflammatory cytokine responses by dendritic cells in culture and attenuate proinflammatory cytokine responses in the nasal fluids of exposed mice [29]. The exact mechanisms are unknown; however, defensins first start by binding to microbial products attenuating inflammatory-inducing capacity. Here, we showed that also a synthetic peptide comprising the γ-motif of a plant defensin exerts an anti-inflammatory activity *in vitro*.

Moreover, we determined to what extent SolyC spared probiotic bacterial species, considering that intestinal flora represents a defense barrier against pathogens [30]. Whereas gentamicin killed the totality of the probiotics tested (see methods), SolyC killed a minority of each bacterial species (Table 3). In addition, we observed a general lack of human red blood cells hemolysis, the nontoxicity of SolyC towards eukaryotic cells *in vitro* and reduced synthesis of NO_2^- in cells treated with LPS. These additional properties make SolyC a feasible candidate as a new generation drug.

In conclusion, the results from this study suggest an analogy between endogenous AMPs and SolyC, a peptide of plant origin. Both display a twofold role, rapidly acting against pathogens and reducing inflammation. These findings demonstrate how the γ-core of plant defensins represents a potential source of antimicrobial molecules and may provide new opportunities in the field of therapeutic drug design and of plant biotechnology.

References

1 Silva ON, Mulder KCL, Barbarosa AED, Otero-Gonzalez AJ, Lopez-Abarrategui C, Rezende TMB, Dias SC, Franco OL. Exploring the pharmacological potential of promiscuous host-defense peptides: from natural screenings to biotechnological applications. *Front. Microbiol.* 2011; **2**: 232.

2 Capparelli R, Ventimiglia I, Palumbo D, Nicodemo D, Salvatore P, Amoroso MG, Iannaccone M. 2007. Expression of recombinant puroindolines for the treatment of staphylococcal skin infections (acne vulgaris). *J. Biotechnol.*; **128**(3): 606–614.

3 Lehours P, Vale FF, Bjursell MK, Melefors O, Advani R, Glavas S, Guegueniat J, Gontier E, Lacomme S, Alves Matos A, Menard A, Megraud F, Engstrand L, Andersson AF. Genome sequencing revels a phage in *Helicobacter pylori*. *MBio* 2011; **2**(6): e00239-11.

4 Yokota S, Okabayashi T, Rehli M, Fujii N, Amano K. *Helicobacter pylori* lipopolysaccharides upregulate toll-like receptor 4 expression and proliferation of gastric epithelial cells via the MEK1/2-ERK1/2 mitogen-activated protein kinase pathway. *Infect. Immun.* 2010; **78**(1): 468–476.

5 Jakobsson HE, Jernberg C, Andersson AF, Sjolund-Karlsson M, Jansson JK, Engstrand L. Short-term antibiotic treatment has differing long-term impacts on the human throat and gut microbiome. *PLoS One* 2010; **5**: e9836.

6 Carvalho AO, Gomes VM. Plant-defensins-prospects for the biological functions and biotechnological properties. *Peptides* 2009; **30**: 1007–1020.

7 Aerts AM, Thevissen K, Bresseleers SM, Sels J, Wouters P, Cammue BP, Francois IE. *Arabidopsis thaliana* plants expressing human-beta-defensin-2 are more resistant to fungal attack: functional homology between plant and human defensins. *Plant Cell Rep.* 2007; **26**: 1391–1398.

8 Ghacomo EW, Jimenez-Lopez JC, Kayode APP, Baba-Moussa L, Kotchoni SO. Structural characterization of plant defensin protein superfamily. *Mol. Biol. Rep.* 2011; **39**(4): 4461–4469.

9 Giacommelli L, Nanni V, Lenzi L, Jun Z, Della Serra M, Banfield MJ, Town CD, Silverstein KA, Baraldi E, Moser C. Identification and characterization of the defensin-like gene family of grapevine. *Mol. Plant Microbe. In.* 2012. http://dx.doi.org/10.1094/MPMI-12-11-0323

10 Yount NY, Yeaman MR. Multidimensional signatures in antimicrobial peptides. *Proc. Natl. Acad. Sci. U.S.A.*. 2004; **101**(19): 7363–7368.

11 Yeaman MR, Yount NY. Unifying themes in host defence effector polypeptides. *Nat. Rev. Microbiol.* 2007; **5**(9): 727–740.

12 The Tomato Genome Consortium. Tomato genome sequencing and comparative analysis reveal two consecutive triplications that spawned genes influencing fruit characteristics. *Nature* 2012; **485**: 635–641.
13 Punta M, Coggill PC, Eberhardt RY, Mistry J, Tate J, Boursnell C, Pang N, Forslund K, Ceric G, Clements J, Heger A, Holm L, Sonnhammer EL, Eddy SR, Bateman A, Finn RD. The Pfam protein families database. *Nucleic Acids Res.* 2012; **40**: D290–D301.
14 Hammami R, Ben Hamida J, Vergoten G, Fliss I. PhytAMP: a database dedicated to antimicrobial plant peptides. *Nucleic Acids Res.* 2009; **37**: D963–D968.
15 Larkin MA, Blackshields G, Brown NP, Chenna R, McGettigan PA, McWilliam H, Valentin F, Wallace IM, Wilm A, Lopez R, Thompson JD, Gibson TJ, Higgins DG. ClustalW and ClustalX version 2. *Bioinformatics* 2007; **23**(21): 2947–2948.
16 Romanelli A, Moggio L, Montella RC, Campiglia P, Iannaccone M, Capuano F, Pedone C, Capparelli R. Peptides from Royal Jelly: studies on the antimicrobial activity of jelleins, jelleins analogues and synergy with temporins. *J. Pept. Sci.* 2011; **17**: 348–352.
17 Becker K, Roth R, Peters G. Rapid and specific detection of toxigenic *Staphylococcus aureus*: use of two multiplex PCR enzyme immunoassays for amplification and hybridization of staphylococcal enterotoxin genes, exfoliative toxin genes, and toxic shock syndrome toxin 1 gene. *J. Clin. Microbiol.* 1998; **36**: 2548–2553.
18 Bubert A, Hein I, Rauch M, Lehner A, Yoon B, Goebel W, Wagner M. Detection and differentiation of Listeria spp. by a single reaction based on multiplex PCR. *Appl. Environ. Microbiol.* 1999; **65**: 4688–4692.
19 Hong Y, Liu T, Lee MD, Hofacre CL, Maier M, White DG, Ayers S, Wang L, Berghaus R, Maurer JJ. Rapid screening of *Salmonella enterica* serovars Enteritidis, Hadar, Heidelberg and Typhimurium using a serologically-correlative allelotyping PCR targeting the O and H antigen alleles. *BMC Microbiol.* 2008; **8**: 178.
20 Ananias M, Yano T. Serogroups and virulence genotypes of *Escherichia coli* isolated from patients with sepsis. *Braz. J. Med. Biol. Res.* 2008; **41**: 877–883.
21 Tomasini ML, Zanussi S, Sozzi M, Tedeschi R, Basaglia G, De Paoli P. Heterogeneity of cag genotypes in *Helicobacter pylori* isolates from human biopsy specimens. *J. Clin. Microbiol.* 2009; **41**(3): 976–980.
22 Capparelli R, Romanelli A, Iannaccone M, Nocerino N, Ripa R, Pensato S, Pedone C, Iannelli D. Synergistic antibacterial and anti-inflammatory activity of temporin A and modified temporin B in vivo. *PLoS One* 2009; **4**(9): e7191.
23 Orsine JVC, da Costa RV, da Silva RC, Santos MFMA, Novaes MRCG. The acute cytotoxicity and lethal concentration (LC50) of Agaricus sylvaticus through hemolytic activity on human erythrocyte. *Int. J. Nutr. Metab.* 2012; **4**(11): 19–23.
24 Cardile V, Proietti L, Panico A, Lombardo L. Nitric oxide production in fluoro-edenite treated mouse monocyte-macrophage cultures. *Oncol. Rep.* 2004; **12**(6): 1209–1215.
25 Rozalska B, Wadstrom T. Interferon-γ, interleukin-1 and tumor necrosis factor-α synthesis during experimental murine staphylococcal infection. *FEMS Immunol. Med. Microbiol.* 1993; **7**: 145–152.
26 Lay FT, Anderson MA. Defensins-components of the innate immune system in plants. *Curr. Protein Pept. Sci.* 2005; **6**(1): 85–101.
27 Silverstein KA, Graham MA, Paape TD, VandenBosch KA. Genome organization of more than 300 defensin-like genes in Arabidopsis. *Plant Physiol.* 2005; **138**(2): 600–610.
28 Sagaram UK, Pandurangi R, Kaur J, Smith TJ, Shah DM. Structure- Activity determinants in antifungal plant defensins MsDef1 and MtDef4 with different modes of action aginst *Fusarium graminearum*. *PLoS One* 2011; **6**(4): e18550.
29 Kohlgraf KG, Pingel LC, Dietrich DE, Brogden KA. Defensins as anti-inflammatory compunds and mucosal adjuvant. *Future Microbiol.* 2010; **5**(1): 99–113.
30 Norhagen GE, Engstrom PE, Hammarstrom L, Smith CI, Nord CE. Oral and intestinal microflora in individuals with different immunoglobulin deficiencies. *Eur. J. Clin. Microbiol. Infect. Dis.* 1990; **9**: 631–633.

Capparelli et al. BMC Immunology 2012, 13:61
http://www.biomedcentral.com/1471-2172/13/61

BMC Immunology

RESEARCH ARTICLE Open Access

New perspectives for natural antimicrobial peptides: application as antinflammatory drugs in a murine model

Rosanna Capparelli[1*], Francesco De Chiara[1], Nunzia Nocerino[1], Rosa Chiara Montella[1], Marco Iannaccone[1], Andrea Fulgione[1], Alessandra Romanelli[2], Concetta Avitabile[2], Giuseppe Blaiotta[3] and Federico Capuano[4]

Abstract

Background: Antimicrobial peptides (AMPs) are an ancient group of defense molecules. AMPs are widely distributed in nature (being present in mammals, birds, amphibians, insects, plants, and microorganisms). They display bactericidal as well as immunomodulatory properties. The aim of this study was to investigate the antimicrobial and anti-inflammatory activities of a combination of two AMPs (temporin B and the royal jellein I) against *Staphylococcus epidermidis*.

Results: The temporin B (TB-KK) and the royal jelleins I, II, III chemically modified at the C terminal (RJI-C, RJII-C, RJIII-C), were tested for their activity against 10 different *Staphylococcus epidermidis* strains, alone and in combination. Of the three royal jelleins, RJI-C showed the highest activity. Moreover, the combination of RJI-C and TB-KK (MIX) displayed synergistic activity. In vitro, the MIX displayed low hemolytic activity, no NO_2^- production and the ability to curb the synthesis of the pro-inflammatory cytokines TNF-α and IFN-γ to the same extent as acetylsalicylic acid. In vivo, the MIX sterilized mice infected with *Staphylococcus epidermidis* in eleven days and inhibited the expression of genes encoding the prostaglandin-endoperoxide synthase 2 (COX-2) and CD64, two important parameters of inflammation.

Conclusion: The study shows that the MIX – a combination of two naturally occurring peptides - displays both antimicrobial and anti-inflammatory activities.

Background

Coagulase-negative staphylococci (CoNS) are highly abundant on the human skin, already a few hours after birth. The CoNS *Staphylococcus epidermidis* is an ubiquitous and permanent colonizer of human skin and the first cause of nosocomial infections [1]. Most infections with high morbidity and mortality are caused by methicillin-resistant strains of *Staphylococcus epidermidis* (MRSE) [2,3]. In addition, many MRSE strains form a capsule which favors biofilm development, where the pathogen can persist protected from antibiotics and invisible to the immune system [4,5].

New, unconventional antimicrobials are therefore urgently needed [6,7]. In this context, antimicrobial peptides (AMPs), in their natural form or after chemical modification, display interesting features as candidates to become new antimicrobials. They have a broad spectrum of activity against Gram-positive and Gram-negative bacteria, can be easily synthesized in laboratory and have limited toxicity for eukaryotic cells [8,9]. As innate immune components, AMPs lack specificity and immune memory, with the consequence that the pathogens rarely develop resistance to them [10]. Importantly, AMPs rapidly intercept and kill pathogens [11]. AMPs differ each other by size, sequence and secondary structure (α-helix or β-sheet) [12]. Most of them are hydrophobic and amphipathic [13]. AMPs can exert their activity by disrupting the membrane [14] or passing through the bacterial membrane [15]. Molecules belonging to the former class of AMPs permeabilize the membrane phospholipids bilayer and kill the bacterial cell; those belonging to the latter class pass through the bacterial membrane and

* Correspondence: capparel@unina.it
[1]Faculty of Biotechnology, University of Naples "Federico II", Naples 80134, Italy
Full list of author information is available at the end of the article

interacts with variable intracellular components, much as traditional antibiotics. AMPs, in addition to the antimicrobial activity, display also immune-modulatory properties (such as chemiotaxis, which contributes to bacterial elimination) and interact with natural and adaptive immunity [16,17]. Thus, in view of the above properties, AMPs represent one of the most promising future strategies for combating infections and microbial drug resistance. The present study describes two chemically modified AMPs - an analogue of the temporin B (TB-KK) secreted by the granular glands of the European red frog (*Rana temporaria*) [18] and an analogue of the royal jellein I (RJI-C) secreted by the mandible and hypopharyngeal glands of honeybees (*Apis mellifera*) [9,19]. These two peptides behave differently towards the bacterial membrane. RJI-C folds into beta sheets and aggregates onto the membrane; TB-KK folds into an alpha helix and does not aggregate onto the membrane [8,9].

Recent data demonstrate that hydrophobic peptides, when mixed with peptides possessing a net positive charge, give origin to a mixture with potential antibacterial activity [20,21]; second, that the combination of antimicrobial peptides derived from different organisms are highly active against Gram positive bacteria [9]. In agreement with these results, here we show that a mixture of TB-KK and RJI-C – two AMPs derived from different sources - displays strong antimicrobial activity against Gram-positive bacteria - modulates pro-inflammatory cytokines and nitric oxide production, in vitro and in vivo. The two peptides, following chemical modification, potentially can be made available in large quantities and in a homogeneous and highly pure form.

Results

Characterization of *Staphylococcus epidermidis* strains

To establish the clonal origin of the *Staphylococcus epidermidis* strains used in the study, the strains (10) were characterized phenotypically - with respect to their antibiotic resistance pattern and molecularly with respect to their Restriction Endonucleases Analysis (Pulse Field Gel Electrophoresis - REA-PFGE) pattern. All strains resulted resistant to aztreonam (30 μg; ATM30), bacitracin (10 μg; B2), cloxacillin (1 μg; CX1) and metronidazole (80 μg; M80) and sensitive to imipenem (10 μg; IPM10). The remaining 25 antibiotics displayed a strain specific pattern (Table 1). Also, with one exception (the strain SE), the strains displayed all different macro-restriction patterns, when analyzed by Sma I REA-PAGE (Figure 1). Thus, the strains used in this study belong to different clonal lineages.

In vitro antimicrobial activity of TB-KK and RJI-C

To evaluate the antimicrobial activity of RJI-C, RJII-C, RJIII-C and TB-KK (Table 2) these AMPs were tested in vitro [8,9], individually and in combination, against 10 *Staphylococcus epidermidis* strains. Among the three royal jelleins, RJI-C showed the highest activity (MIC: 30 μg/ml) (Table 3). Tested in various combination (RJI-C at 20 μg/ml and RJII-C at 5–20 μg/ml ; RJI-C at 20 μg/ml and RJIII-C at 5–20 μg/ml; RJII-C at 20 μg/ml and RJIII-C at 5–20 μg/ml), the royal jelleins did not display synergistic effects. Only RJI-C was thus tested for synergism with TB-KK. The combination of the two antimicrobials – RJI-C at 9 μg/ml and TB-KK at 6 μg/ml (MIX) – displayed a fractional inhibitory concentration index ≤ 0.5, which is evidence of synergism [20] (Table 3). The strains of *Staphylococcus epidermidis* were all sensitive to the MIX, but not its components (Table 4). This conclusion is supported by the larger inhibition ring of the MIX, compared to that of the individual components (Figure 2A).

Interestingly, the antibacterial activity of the MIX against probiotics bacteria (*Lactobacillus plantarum*, *Lactobacillus Paracasei*, *Bifidobacterium animalis*) was five-fold lower than that of gentamicin (Table 5).

In vitro hemolytic and cytotoxic activities of the MIX

To test the cytotoxic activity of the MIX, we used the hemolytic and the LC50 assays. The MIX lysed less than 12% of the murine erythrocytes (data not shown) and the LC50 value was 143,8 mg/ml versus 58.5 μg/ml of TB-KK and 64.6 μg/ml of RJI-C (Additional file 1: Table S1). The MIX was not toxic towards the macrophage J774 cells, which remained vital at 72 hours (Figure 2B).

In vitro the MIX does not induce synthesis of NO_2^-

The MIX (RJI-C at 9 μg/ml and TB-KK at 6 μg/ml) did not induce NO_2^- synthesis in J774 cells. Rather, when these cells were stimulated with LPS (10 μg/ml/well for 3 hours) and then treated with the RJ-IC, TB-KK and MIX reduced NO_2^- synthesis (Table 6), one of the parameters to determine the cellular toxicity.

In vitro anti-inflammatory activity of the MIX

To investigate whether the MIX, in addition to the antimicrobial activity, also displays anti-inflammatory activity, J774 cells (10^6 cells/well) were stimulated with either LPS or LTA (0.1, 1 or 10 μg/ml) for 3 hours. The results show that LPS stimulates inflammation in the J774 cells better than LTA (Figure 3A). Later, J774 cells were treated with gentamicin (5 μg/ml), acetylsalicylic acid (ASA, 5 μg /ml) or MIX (RJI-C 9 μg/ml + TB-KK 6 μg/ml) for 3 hours. In the absence of the agent causing inflammation (LPS), the MIX, gentamicin and ASA do not induce inflammation (Figure 3B). In J774 cells (10^6 cells/well) stimulated with LPS for 3 hours, the MIX curbs the synthesis of the pro-inflammatory cytokines TNF-α

Table 1 Results of antibiotic susceptibility tests of ten *Staphylococcus epidermidis* strains

	Antibiotics tested																													
Strain	**FD10**	**P120**	**AMX25**	**AM10**	**ATM30**	**B2**	**CB100**	**CD30**	**FOX30**	**CAZ30**	**A30**	**CX1**	**K15**	**FF50**	**GM10**	**IPM10**	**MY2**	**M80**	**MZ75**	**NET30**	**FM300**	**NB30**	**T30**	**P10**	**PIP100**	**RF30**	**SP100**	**RL100**	**TE30**	**VA30**
SE	R	R	R	R	R	R	R	R	I	S	I	R	R	S	R	S	R	R	R	R	R	R	I	R	R	R	R	R	R	R
3/28	R	I	S	S	R	R	R	S	S	I	I	R	R	R	R	S	R	R	S	I	S	S	S	R	S	S	S	R	I	I
2/2	S	R	R	R	R	R	R	R	R	I	S	R	R	R	I	S	R	R	R	I	S	S	S	R	R	I	R	R	I	I
5/6	I	R	I	R	R	R	I	R	I	S	I	R	R	R	I	S	I	R	R	I	S	S	S	R	R	S	I	R	I	I
5/8	S	R	I	R	R	R	I	R	I	I	R	R	R	S	R	S	R	R	R	I	S	S	R	R	R	S	S	R	S	S
12/14	S	R	R	R	R	R	I	R	S	S	R	R	R	R	R	S	S	R	R	I	S	S	R	R	R	R	I	R	R	I
9/1	S	R	R	R	R	R	I	R	S	I	S	R	S	S	I	S	S	R	R	S	S	S	S	R	R	S	I	R	S	I
10/28	S	I	R	R	R	R	R	R	S	I	R	R	R	S	R	S	S	R	R	I	S	S	R	R	R	S	I	R	I	I
12/26	S	R	R	R	R	R	R	R	S	I	S	R	S	S	R	S	S	R	R	I	S	S	S	R	R	S	I	R	S	I
5/25	S	R	R	R	R	R	R	R	S	I	S	R	R	I	I	S	R	R	R	I	S	S	S	R	R	S	I	R	S	S

R= strain resistant to the antibiotic.
S= strain sensitive to the antibiotic.
I= intermediate strains sensitive to the antibiotic.

and IFN-γ more efficiently than gentamicin and at the same extent of the ASA (Figure 3C).

These experiments demonstrate that the MIX exerts anti-inflammatory as well as antimicrobial activities, while the single components of the MIX have no anti-inflammatory activity (Additional file 2: Figure S1). Since COX-2 is a well-established parameter of inflammation [22] , the J774 cells were stimulated with LPS (10 μg/ml) and 1 hour later treated with the MIX, RJII-C (non-active peptide), acetylsalicylic acid (ASA), gentamicin or vehicle (PBS) for 3 hours. The level of the COX-2 protein was then detected by western blot. The MIX-treated cells, displayed a COX-2 protein level comparable to that of the cells treated with ASA or gentamicin, and much lower than that of the cells treated with RJII-C or the vehicle (Figure 3D). The above results demonstrate that the MIX curbs inflammation to the same extent as ASA [23].

In vivo anti-inflammatory activity of the MIX in mice stimulated with LPS

To investigate further the property of the MIX to curb inflammation in vivo, LPS (250 μg, ~10 mg/Kg) was administrated to four groups of mice (3 mice/group). After 3 hours, the groups were treated respectively with the MIX (RJI-C 9 μg/mouse + TB-KK 6 μg/mouse), gentamicin (5 μg in 100 μl/mouse) or ASA (5 μg in 100 μl/mouse). The last group received 100 μl of saline buffer as control. After 3 hours, the mice that received the MIX showed a reduced level of both the pro-inflammatory cytokines TNF-α and IFN-γ, when compared to gentamicin-treated group, but an higher expression level of IFN- γ, when compared to the ASA group (Figure 3E). In conclusion,

Table 2 Peptide sequences and mass analysis of the royal jelleins (RJ) and temporin (TB) used in the study

Peptide	Sequence	Calc. mass (DA)	Meas. mass (DA)
RJI-C	PFKIDIHLGGY-NH_2	1230.46	1231.02
RJII-C	TPFKISIHLGGY-NH_2	1331.56	1331.90
RJIII-C	EPFKISIHLGGY-NH_2	1359.57	1360.10
TB	YLLPIVGNLLKSLL-NH2	1391.80	1391.20
TB-KK.	KKYLLPI VGNLLKSLL-NH2	2295.40	2294.30

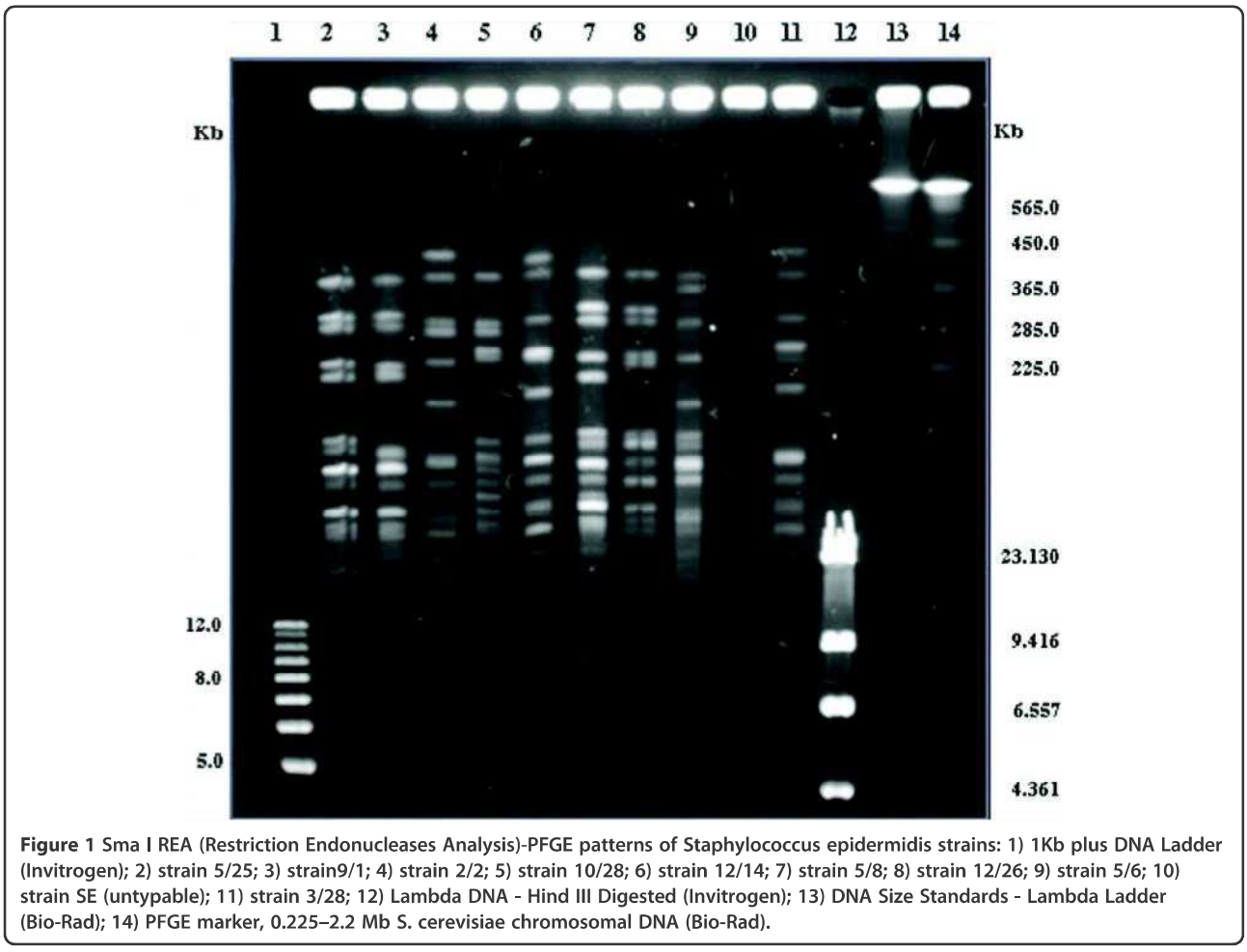

Figure 1 Sma I REA (Restriction Endonucleases Analysis)-PFGE patterns of Staphylococcus epidermidis strains: 1) 1Kb plus DNA Ladder (Invitrogen); 2) strain 5/25; 3) strain9/1; 4) strain 2/2; 5) strain 10/28; 6) strain 12/14; 7) strain 5/8; 8) strain 12/26; 9) strain 5/6; 10) strain SE (untypable); 11) strain 3/28; 12) Lambda DNA - Hind III Digested (Invitrogen); 13) DNA Size Standards - Lambda Ladder (Bio-Rad); 14) PFGE marker, 0.225–2.2 Mb S. cerevisiae chromosomal DNA (Bio-Rad).

Table 3 The FIC index against Staphylococcus epidermidis strains: ≤ 0.5, synergy ; >0.5, no interaction

Antimicrobial peptides	MIC_{100}	Fic index
RJI-C	30 μg/ml (24 μM)	
RJII-C	200 μg/ml (150 μM)	
RJIII-C	300 μg/ml (220 μM)	
TB-KK	7 μg/ml (3 μM)	
Gentamicin	5 μg/ml (10 μM)	
RJI-C + TB-KK	9 μg/ml + 6 μg/ml (7.3 μM + 2.6 μM)	0.5

the MIX performs better than gentamicin, but worse than ASA.

In vivo antimicrobial efficacy of the MIX given intravenously at 12 hours post infection

To evaluate the efficacy of the MIX to contrast microbial infection, four groups of mice (15 mice/group) were infected with lethal dose (10^8 CFU/mouse) of *Staphylococcus epidermidis* (SE). This strain was chosen since it is resistant to the majority of the antibiotics tested (Table 1).

One group did not receive any treatment (control group); a second group received sterile PBS (100 μl/mouse) (placebo group – data not shown); the third group received the MIX (RJI-C 9 μg/mouse + TB-KK 6 μg/mouse); the fourth group received gentamicin (5 μg/mouse). PBS, MIX and gentamicin were administered intravenously at 3 hours post infection. In both, placebo and control groups, the bacterial load of kidneys and spleens increased progressively, while it decreased in the groups treated with gentamicin or the MIX (Additional file 3: Figure S2). Upon treatment of the mice with the MIX, the acute phase proteins, which represent important markers of inflammation [24], were evaluated (Additional file 4: Table S2). The SAA (Serum amyloid A), haptoglobin and fibrinogen were within normal ranges in the mice treated with the MIX or with gentamicin, while significantly high in the control mice (infected but not treated) (Additional file 4: Table S2).

In vivo anti-inflammatory efficacy of the MIX given intravenously at 12 hours post infection

The four groups of mice described before have been used also to evaluate the anti-inflammatory activity of the MIX. For this purpose, the expression levels of the TNF-α , IFN-γ, IL-10 cytokine genes were measured at 3, 6 and 9 hours after treatment in the kidney samples (Figure 4A-C, respectively). In the group treated with the MIX, the TNF-α and IFN-γ were under expressed (at 6, 9 hours from treatment), as compared to the group treated with gentamicin (Figure 4A-C). This result suggests that the MIX controls inflammation better than gentamicin.

Also CD64 and COX-2 markers of inflammation in vivo were evaluated. Blood samples were collected 3, 6, or 9 hours after the treatments. CD64 was measured by flow cytometry (Figure 5A). Six and nine hours after the treatment with gentamicin or the MIX, the mice displayed a decreased expression of the CD64 marker (Figure 5A). The level of COX-2, was evaluated by RT-PCR on the mRNA extracted from kidney samples. In control mice displayed a significantly higher expression level of COX-2, compared to the mice treated with MIX or gentamicin. In the control mice COX-2 peaked 3 hours after the treatment. In the mice treated with gentamicin or the MIX, COX-2 expression level returned to the normal level nine hours after the treatment (Figure 5B).

To verify whether the MIX affected granulocytic infiltration in the kidneys of infected mice, hematoxylin-eosin staining was performed. As expected, kidneys of control mice displayed granulocytic infiltration within the lumen of the cortical convoluted tubules and hence lymphocytic infiltration, vessel activation and glomerular hyperplasia (Figure 6 panel 1, 5). Instead, kidneys of MIX-treated mice showed a dramatic reduction in the number of granulocytic cells localized in the cortical

Table 4 Antimicrobial activity of the MIX and its components against different strains of *Staphylococcus epidermidis*

Strains	% inhibition of bacterial growth RJI-C 9 μg/ml (7.3 μM)	% inhibition of bacterial growth TB-KK 6 μg/ml (2.6 μM)	% inhibition of bacterial growth RJI-C 9 μg/ml + TB-KK 6 μg/ml (RJI-C 7.3 μM + TB-KK 2.6 μM) (MIX)
3/28	17 ± 2	19 ± 2	91 ± 1
2/2	18 ± 1	23 ± 0.5	96 ± 2
5/6	4 ± 3	10 ± 1	100 ± 0
5/8	12 ± 2	21 ± 2	95 ± 2
12/14	11 ± 0.5	20 ± 3	92 ± 1
9/1	18 ± 0	26 ± 2	96 ± 2
10/28	0	4 ± 1	100 ± 0
12/26	19 ± 2	14 ± 2	100 ± 0
5/25	15 ± 1	21 ± 1	90 ± 2

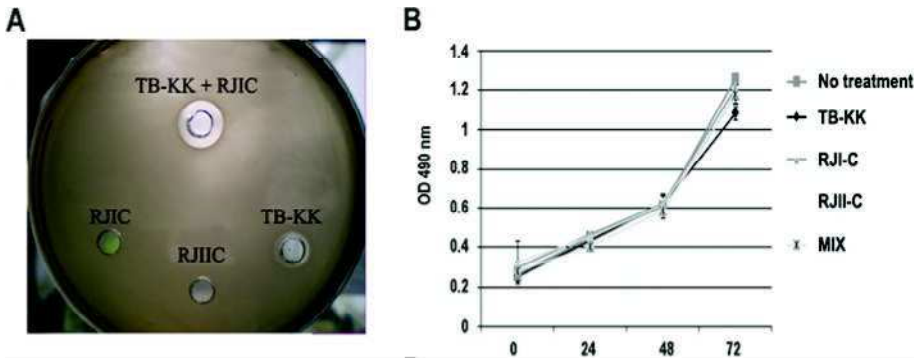

Figure 2 (A) Antimicrobial activity of the single peptides (RJI-C 9 μg/ml; RJII-C 15 μg/ml; TB-KK 6 μg/ml) and of MIX (RJI-C at 9 μg/ml and TB-KK at 6 μg/ml) are shown as inhibition zone assay. A larger zone of inhibition is evident around the MIX compared to the single components. (**B**) J774 cell line treated with the single peptides (RJI-C 9 μg/ml; RJII-C 15 μg/ml; TB-KK 6 μg/ml) or the MIX (RJI-C at 9 μg/ml and TB-KK at 6 μg/ml) maintain the same growth rate compare to the untreated control.

convoluted tubules, less glomerular hyperplasia, and no lymphocyte infiltration (Figure 6 panel 2–4).

In vivo antimicrobial efficacy of the MIX for the period of 12 days

To test the antimicrobial activity of the MIX in vivo for a longer period, mice were infected with a sub-lethal dose (10^7 CFU/mouse) of *Staphylococcus epidermidis* and then treated with the MIX. Four groups of mice (24 mice/group) were infected with the bacterial strain (SE). One group of mice did not receive any treatment (control group); a second group received sterile PBS (100 μl/mouse) (placebo group); the third group received the MIX (RJI-C: 9 μg/mouse + TB-KK: 6 μg/mouse); the fourth group received gentamicin (5 μg/mouse). PBS, MIX and gentamicin were administered intravenously in three boosts 3, 6 and 9 days post infection. In the placebo and the control groups, the bacterial load of kidneys and spleens (the target organs of the pathogen) increased progressively, while the load was significantly lower in the groups treated with gentamicin or the MIX. Eleven days after the infection, the mice treated with gentamicin were still infected, while those treated with the MIX were already sterile (Figure 7A-B).

Table 5 Antimicrobial activity of the MIX or gentamicin on probiotic bacteria

Strains	MIX RJI-C 9 μg/ml +TB-KK 6 μg/ml (RJI-C 7.3 μM +TB-KK 2.6 μM)	Gentamicin 5 μg/ml (10 μM)
Bifidobacterium animalis	29% ± 3	96% ± 4
Lactobacillum plantarum	23% ± 2	97% ± 4
Lactobacillum paracasei	25% ± 2	96% ± 3

Four days after the infection, in addition to spleen and kidneys (10^6 CFU/gr and 10^7 CFU/gr respectively), the bacterium was also detected (at a threshold level: 10^2 CFU/g) in the liver (data not shown). Thus, the MIX is slightly more effective than gentamicin (Figure 7A-B). In all four groups, bacteria were no longer detected in the blood circulation within 2 h from infection (Additional file 5: Figure S3).

In vivo anti-inflammatory efficacy of the MIX for the period of 12 days

To evaluate the anti-inflammatory activity of the MIX, the expression levels of the TNF-α, IFN-γ, IL-10 cytokines genes were measured in the kidneys. The experiment was carried out on the same four groups of mice described in the previous paragraph. For this purpose, the expression levels of the cytokines were measured 24 and 48 hours after each treatment with MIX (or 4, 5, 7, 8,10 and 11 days post infection). In the group treated with the MIX, compared to the group treated with gentamicin, the TNF-α and IFN-γ levels were under expressed (at 7 days) while the IL-10 levels were over expressed (at 10 days) (Figure 7C). This result suggests that the MIX controls inflammation better than gentamicin.

Discussion

Recently we demonstrated that new antimicrobials are more effective than traditional antibiotics against *Staphylococcus epidermidis* [25,26]. The present study extends these results, providing evidence that the MIX – a mixture of a royal jellein modified at the C-terminal (RJI-C) and an analogue of temporin B (TB-KK) – is a valid alternative to the use of gentamicin against skin infections caused by *Staphylococcus epidermidis*.

In vivo, endogenous antimicrobial peptides (such as human defensins and cathelecidins) are known to be pleiotropic: they act as antimicrobials [27]; neutralize

Table 6 NO_2^- production of J774 cells: Mouse macrophages untreated, treated with RJI-C, TB-KK or the MIX, stimulated with LPS, stimulated with LPS and treated with RJI-C, TB-KK or the MIX

Treatment	Time of incubation (h)		
	24	48	72
No treatment	0.25 ± 0.04	0.69 ± 0.02	0.92 ± 0.2
RJI-C (15 μg/ml) (12 μM)	0.42 ± 0.03	0.75 ± 0.01	1.02 ± 0.3
TB-KK (15 μg/ml) (6.5 μM)	0.82 ± 0.05	1.25 ± 0.2	1.34 ± 0.2
MIX (RJI-C 9 μg/ml + TB-KK 6 μg/ml) (RJI-C 7.3 μM + TB-KK 2.6 μM)	0.72 ± 0.3	0.85 ± 0.3	1.06 ± 0.2
LPS (10 μg/ml)	2.93 ± 0.2	10.96 ± 0.4	12.16 ± 0.5
LPS + RJI-C (15 μg/ml) (12 μM)	2.85 ± 0.3	8.42 ± 0.1	10.21 ± 0.2
LPS + TB-KK (15 μg/ml) (6.5 μM)	3.12 ± 0.6	9.75 ± 0.1	11.45 ± 0.2
LPS + MIX (RJI-C 9 μg/ml + TB-KK 6 μg/ml) (RJI-C 7.3 μM + TB-KK 2.6 μM)	2.63 ± 0.4	7.25 ± 0.3	8.26 ± 0.1

Data are expressed as micromoles of NO2- for 106 input cells, and are means ± standard deviation of three different experiments each performed in triplicate.

bacterial components (LTA and LPS), which otherwise would induce an excess of inflammation and tissue damage [28,29]; attract inflammatory cells to the wound site and promote wound healing.

The two exogenous components of the MIX also behave in a pleiotropic fashion: they control the bacterial load (Figure 7A-B and Additional file 3: Figure S2), inhibit the synthesis of pro-inflammatory cytokines (Figures 4 and 7C) and control the expression of COX-2 (Figures 3D and 5B), the acute phase proteins (Additional file 4: Table S2) and the expression of the CD64 receptor (Figure 5A). At the histological level, the MIX reduces kidney lymphocyte infiltration (Figure 6).

Mice infected with a sub-lethal dose of *Staphylococcus epidermidis* and three days later treated with the MIX (RJI-C: 9 μg/mouse + TB-KK: 6 μg/mouse), within 11 days from treatment, displayed sterile kidneys and spleen – the organs targeted by the bacterial strain used in this study (Figure 7A-B). Samples collected at 15 min intervals from infection showed that bacteria leave the blood circulation within 2 h (Additional file 5: Figure S3). These results are clinically relevant since they suggest that the MIX can potentially be used in humans, where infection is generally caused by a small initial inoculum and treatment is therefore initiated several days after infection (Figure 7A-B).

The MIX is not toxic for eukaryotic cells, in vitro and in vivo (Figure 2B); its components act synergistically (Figure 2A) and becomes moderately hemolytic (12%). In addition, the MIX reduces the synthesis of NO_2^- in cells infected with *Staphylococcus epidermidis* (Table 6). These additional properties make the MIX a candidate for a new generation drug.

In vitro and in vivo experiments demonstrate that the MIX down regulates the level of the pro-inflammatory cytokines TNF–α and IFN-γ while enhancing the expression of the anti-inflammatory cytokine IL-10. This effect is comparable to that of gentamicin, a well-known antimicrobial drug. These results confirm that the MIX, in addition to an antibacterial activity, also exerts – in vivo and in vitro - an anti-inflammatory activity.

The intestinal flora represents a defense barrier against pathogens [30]. We therefore also investigated whether the MIX spared probiotic bacterial species in vitro. While gentamicin killed the totality of the probiotics tested (*Lactobacillus plantarum*, *Lactobacillus Paracasei*, *Bifidus animalis*), the MIX killed a minority of each bacterial species (29%-23%-25%, respectively) (Table 5).

The influence of the MIX on the major cell signaling pathways was also studied. CD64 and COX-2 warn about the cell exposure to inflammatory stimuli [31,32]. The MIX reduced the expression level of COX-2 (Figures 3D and 5B) and CD64 (Figure 5A), proofing that the MIX exerts also anti-inflammatory activity. The CD64 levels are high in the mice infected. In the mice infected and then treated with MIX at both 3, 6 and 9 hours from treatment, levels of CD64 are reduced (Figure 5A). This last result provides evidence that the MIX has effects on mechanisms of both innate and adaptive immunity.

Conclusions

This study provided evidence which suggests an analogy between endogenous AMP and the MIX, consisting of exogenous and chemically modified AMPs. Both display a two-fold role, rapidly recognizing the presence of a pathogen and preventing an excess of inflammation.

Methods

Bacteria

List and origin of *Staphylococcus epidermidis* used in this study is reported in Additional file 6: Table S3. All strains were isolated from patients hospitalized at the Medical School of the University of Naples Federico II. All strains were molecular identified by means of *kat*

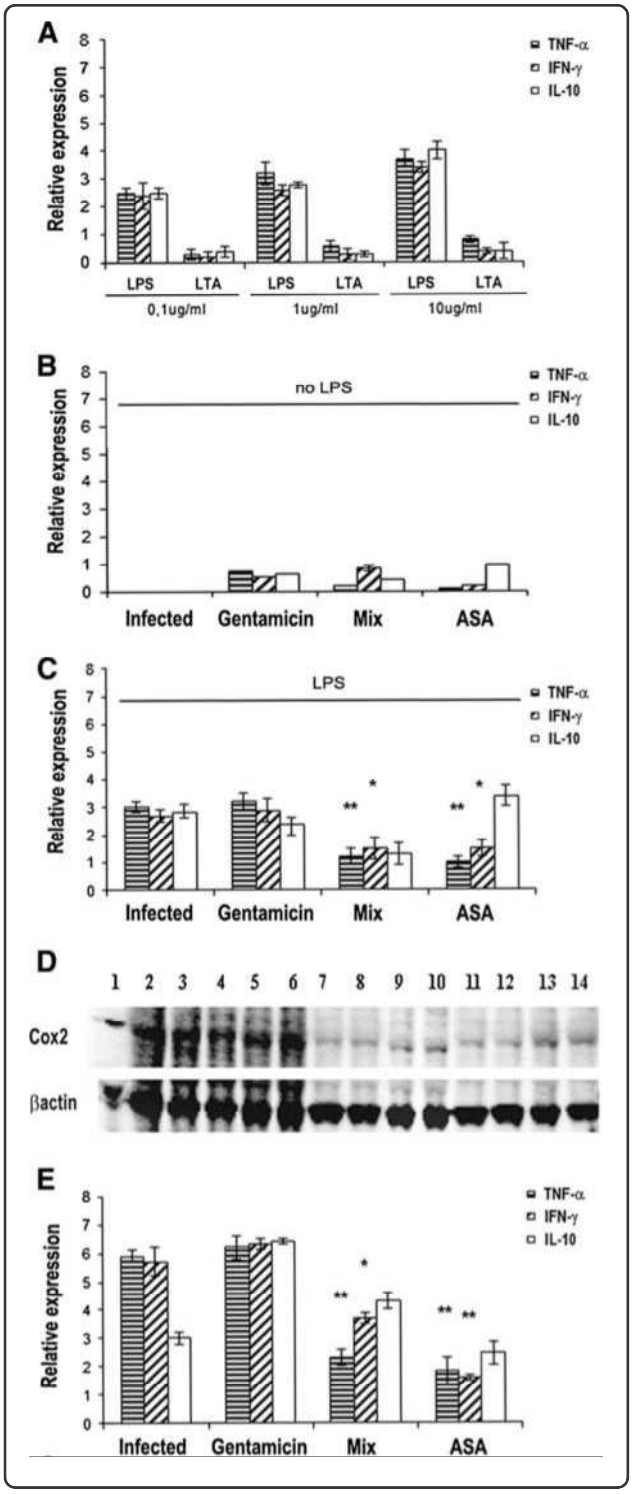

Figure 3 (A) TNF-α, IFN-γ, IL-10 mRNA expression levels in J774 cells stimulated with LPS or LTA (0,1,1 or 10 μg/ml) for 3 hours. (**B**) J774 cells treated with gentamicin (5 μg/ml) or MIX (RJI-C 9 μg/ml + TB-KK 6 μg/ml) or ASA (5 μg/ml) for 3 hours. (**C**) J774 cells stimulated with LPS (10 μg/ml) for 3 hours and treated with gentamicin (5 μg/ml) or MIX (RJI-C 9 μg/ml + TB-KK 6 μg/ml) or ASA (5 μg/ml) for further 3 hours. (**D**) Western blot analysis of COX-2 in J774 cell line. **Lane 1–3**: J774 cells + LPS(10 μg/ml); **Lane 4–6**: J774 cells + LPS (10 μg/ml) + inactive peptide (RJII-C 15 μg/ml); **Lane 7–9**: J774 cells + LPS (10 μg/ml) + ASA (5 μg/ml); **Lane 10–12**: J774 cells + LPS (10 μg/ml) + MIX (RJI-C 9 μg/ml + TB-KK 6 μg/ml; **Lane 13–14**: J774 cells + LPS (10 μg/ml) + gentamicin (5 μg/ml). (**E**) TNF-α, IFN-γ, IL-10 mRNA expression levels in kidney of mice (3mice/group) stimulated with LPS (250 μg, ~10 mg/Kg) for 3 hours; stimulated with LPS (250 μg, ~10 mg/Kg) for 3 hours and treated with gentamicin (5 μg/mouse) or MIX (RJI-C 9 μg/mouse + TB-KK 6 μg/mouse) or ASA (5 μg/mouse) for 3 hours. Values were normalized with GAPDH and compared to untreated control. *P <0.05, **p < 0.01; ***p < 0.001, Student's *t* test gentamicin vs MIX and gentamicin vs ASA.

A-RFLP analysis technique described by Blaiotta et al. [33].

The study does not investigate clinical aspects of the disease, nor it uses human specimen. The study therefore does not require the Ethic Committee approval.

Antibiotic susceptibility of *Staphylococcus epidermidis* strains

The antibiotic-susceptibility profile of strains was tested using the disk diffusion method on Mueller-Hinton agar, according to the NCCLS guidelines (2002) [34]. The antibiotics used and their concentrations were as follows: amoxicillin (25 μg; AMX25), ampicillin (10 μg; AM10), aztreonam (30 μg; ATM30), bacitracin (10 μg; B2), carbenicillin (100 μg; CB100), ceftazidime (30 μg; CAZ30), cefoxidin (30 μg; FOX30), cephaloridine (30 μg; CD30), cloxacillin (1 μg; CX1), erythromycin (15 μg; E15), fosfomycin (50 μg; FF50), fusidic acid (10 μg; FD10), gentamicin (10 μg; GM10), imipenem (10 μg; IPM10), lincomycin (2 μg; MY2), metronidazole (80 μg; M80), mezlocillin (75 μg; MZ75), netilmycin (30 μg; NET30), nitrofurantoin (300 μg; FM300), novobiocin (30 μg, NB30), oxytetracycline (30 μg, T30), penicillin-G (10 μg; P10), piperacillin (100 μg, PIP100), rifampicin (30 μg; RF30), chlorotetracycline (30 μg; A30), spiramycin (100 μg; SP100), sulfamethoxazole (100 μg; SP100), tetracycline (30 μg; TE30), and vancomycin (30 μg; VA30). All antibiotics were provided by BioMérieux SA, (Marcy l'Etoile, France).

Pulsed-field electrophoresis of *Staphylococcus epidermidis* strains

The procedure adopted was that described [35]. Briefly, inserts of intact DNA were digested in 200 μl of appropriate buffer supplemented with 40 U of *Sma* I (Promega, Milan). Pulsed field gel electrophoresis (PFGE) of the restriction digests was performed by using the CHEF system (Bio-Rad Laboratories, Hercules, CA, USA) with 1% (wt/vol) agarose gels and 0.5 x TBE as running buffer, at 10°C. Restriction fragments were resolved in a single run, at constant voltage of 6 V cm^2 and an orientation angle of 120° between electric fields, by a single phase procedure for 24 h with a pulse ramping between 1 and 50s.

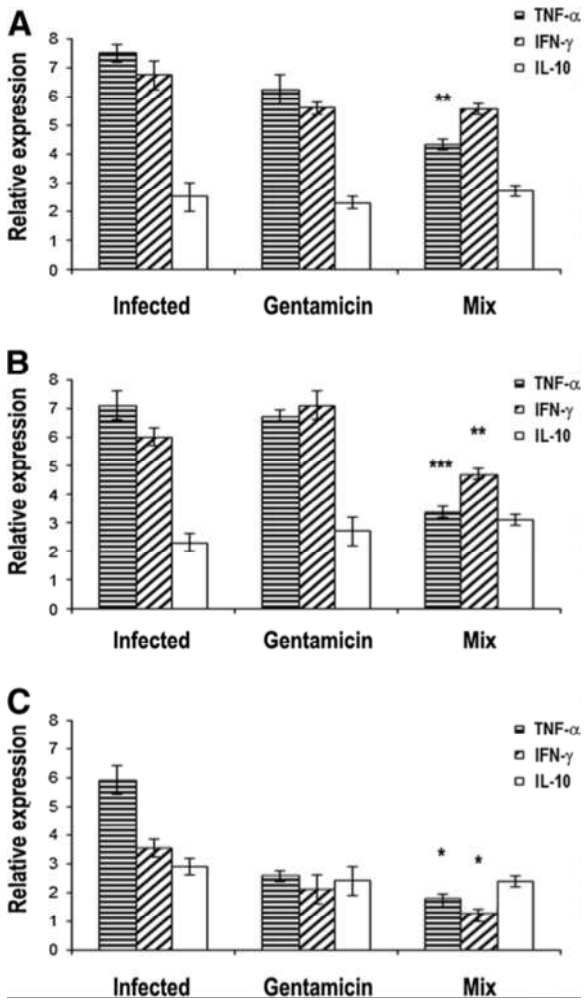

Figure 4 (A-C) TNF-α, IFN-γ, IL-10 mRNA expression levels in infected mice with Staphylococcus epidermidis (108 CFU/mouse) or infected with Staphylococcus epidermidis (108 CFU/mouse) and treated with the MIX (RJI-C at 9 μg/mouse and TB-KK at 6 μg/mouse) or gentamicin (5 μg/mouse) at 3(A), 6 (B) and 9 (C) hours after treatment. Values were normalized with GAPDH and compared to untreated control. *P <0.05, **p < 0.01; ***p < 0.001, Student's *t* test gentamicin vs MIX.

Antibacterial activity of AMPs

Antibacterial activity of the peptides used in this work was evaluated as described previously [8]. A potential synergism (FIC) between TB-KK and RJI-C (MIX) was evaluated by adding combinations of two peptides in a serial two-fold dilutions (RJI-C 5–100 μg, 40 μl/well; TB-KK 5–100 μg, 40 μl/well;) to wells containing 10^5 CFU/well in 60 μl [8]. The fractional inhibitory concentration (FIC) index for combinations of two peptides was calculated according to the equation: FIC index = FICA + FICB = A/MICA + B/MICB , where A and B are the MICs of drug A and drug B in the combination, MICA and MICB are the MICs of drug A and drug B alone, and FICA and FICB are the FICs of drug A and drug B. The FIC indices were interpreted as follows: ≤0.5, synergy; 0.51–4.0, no interaction; > 4.0, antagonism [23].

The growth inhibition percentages of *Staphylococcus epidermidis* and probiotic strains were assessed under the same conditions.

Inhibition zone assay and test of the haemolytic activity of the antimicrobials

The MIX (RJI-C at 9 μg/ml and TB-KK at 6 μg/ml) was tested for its haemolytic activity using mouse red blood cells and for inhibition zone assay test [8]. The MIX was tested for its haemolytic activity using mouse red blood cells. The blood was collected from the tail of the animals and centrifuged ($4x10^2$ g for 3 min). The erythrocytes were washed with saline, suspended at $3x10^6$ erythrocytes/ml, mixed with the peptide combination (RJI-C 9 μg and TB-KK 6 μg in 100 μl saline) and incubated for 1 h at 37°C. The haemolytic activity was measured according to the formula $OD_{peptide} - OD_{negative\ control}/OD_{positive\ control} - OD_{negative\ control}$ X 100 where the negative control (0% haemolysis) was represented by erythrocytes suspended in saline and the positive control (100% haemolysis) was represented by the erythrocytes lysed with 1% triton X100 [36].

The LC50 values relative to the two peptides and the MIX were calculated as described [37].

Cell culture

J774 murine macrophages from the American Tissue Culture Collection (ATCC, Rockville, MD,USA) were cultured in Dulbecco's modified Eagle's medium (DMEM, Cambrex Bio Science, Verviers, Belgium). Culture media contained 10% fetal bovine serum (FBS, Sigma, Milan, Italy), 100 IU/ml penicillin, 100 μg/ml streptomycin (all from Gibco, Paisley, Scotland). Cells were seeded on 96-well plates (Falcon, Milan) for the MTT Assay, and on 24-well plates (Falcon, Milan) for NO_2^- measurements, fluorescence microscopy analysis, and RT-PCR assays. Cell monolayers were grown to adherence before the experiments were started.

Mice

Experiments were carried out on female BALB/c mice (aged 8 to 10 weeks) at the animal facility of the University of Naples. Bacteria (10^7 or 10^8 CFU/mouse) were inoculated by intravenous routes (i.v.). LPS (250 μg, ~10 mg/Kg) (Sigma-Aldrich Milan), or an equivalent volume of sterile 0,9% saline vehicle (250 μl) was administered intraperitoneally. Blood samples were drawn from the tail vein using 0.5 ml syringes. Spleen and kidney were collected at several time points (4,5,7,8,10, 11and 12 days) after the mice infection with a sub-lethal dose of *Staphylococcus epidermidis* (10^7 CFU/mouse). However the same organs were also collected at 3, 6, 9

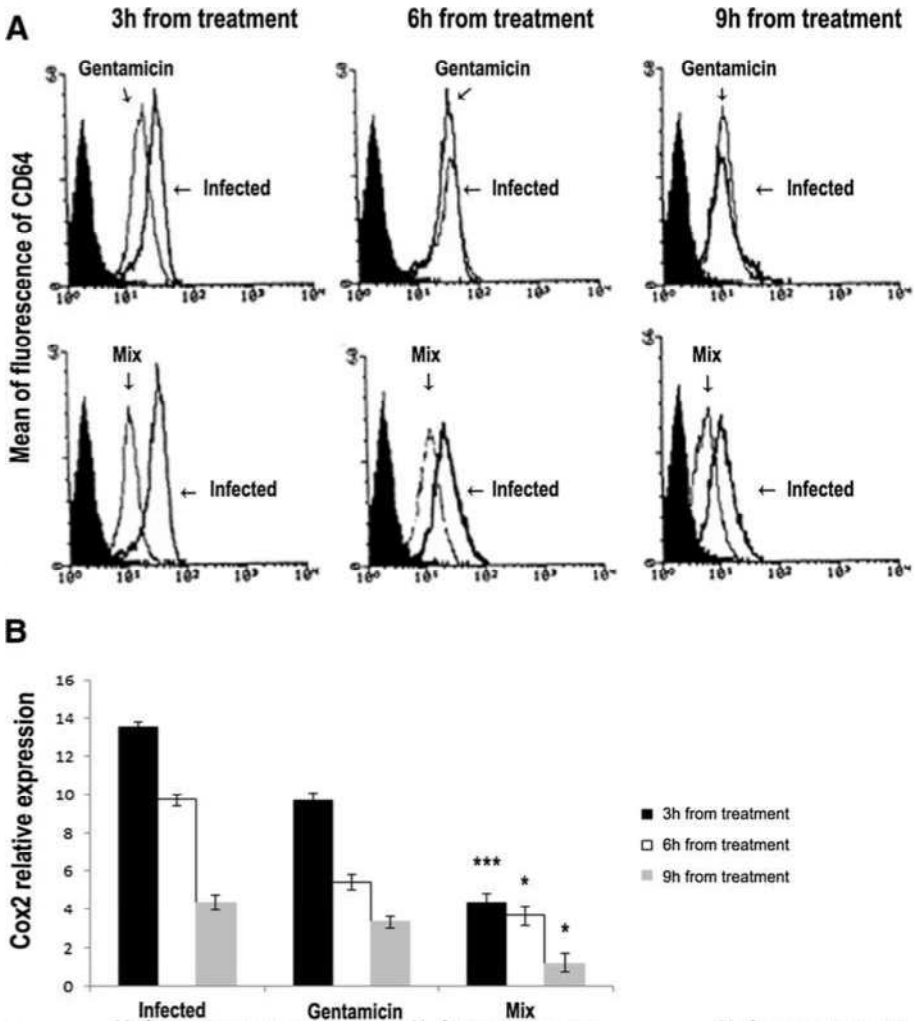

Figure 5 (A) Using flow cytometry, CD64 levels were measured at 3, 6 and 9 hours after treatment in blood samples from mice infected with Staphylococcus epidermidis (108 CFU/mouse), from mice infected with Staphylococcus.epidermidis (108 CFU/mouse) and treated either with MIX (RJI-C at 9 μg/mouse and TB-KK at 6 μg/mouse) or with gentamicin (5 μg/mouse). (**B**) mRNA expression level of COX-2, measured in kidneys of *Staphylococcus.epidermidis* (10^8 CFU/mouse) infected mice and in kidneys of *Staphylococcus epidermidis* (10^8 CFU/mouse) infected mice and treated with MIX (RJI-C at 9 μg/mouse and TB-KK at 6 μg/mouse) or gentamicin (5 μg/mouse) . *p <0.05, **p < 0.01; ***p < 0.001, Student's *t* test gentamicin vs MIX.

and 12 hours after infection with a lethal dose of *Staphylococcus epidermidis* (10^8 CFU/mouse). Spleens and kidneys were dissected and weighed. One g of each sample was homogenized in 1 ml saline and serially diluted in saline.

Colony forming units (CFU) were evaluated by the plate count assay. Animal experiments were approved by the Animal Care Committee of the University of Naples.

Measurement of cell viability

Analysis of cell viability was performed using the CellTiter 96® AQueous One Solution Cell Proliferation Assay system (MTS assay) (Promega, Madison,WI, USA). J774 cells were seeded at 2500 cells per well in a 96-well plate and incubated at 37°C, in a humidified atmosphere with 5% CO_2. TB-KK 15 μg/ml, RJI-C 15 μg/ml, MIX (TB-KK 6 μg/ml + RJI-C 9 μg/ml) or RJII-C (Control 15 μg/ml) were added to the medium immediately after cell adhesion. At each time point 20 μl of CellTiter 96® AQueous One Solution reagent was added to each well, according to the manufacturer's instructions. Absorbance was recorded at 490 nm after 2 h using an EnVision 2102 multilabel reader (PerkinElmer, Waltham, USA).

Nitrite formation in J774 cells stimulated with LPS and treated with RJI-C, TB-KK, and the MIX

Nitrite accumulation (NO_2^-, μmol/10^6 cells) in the cell culture medium was determined by the Griess reaction [38].

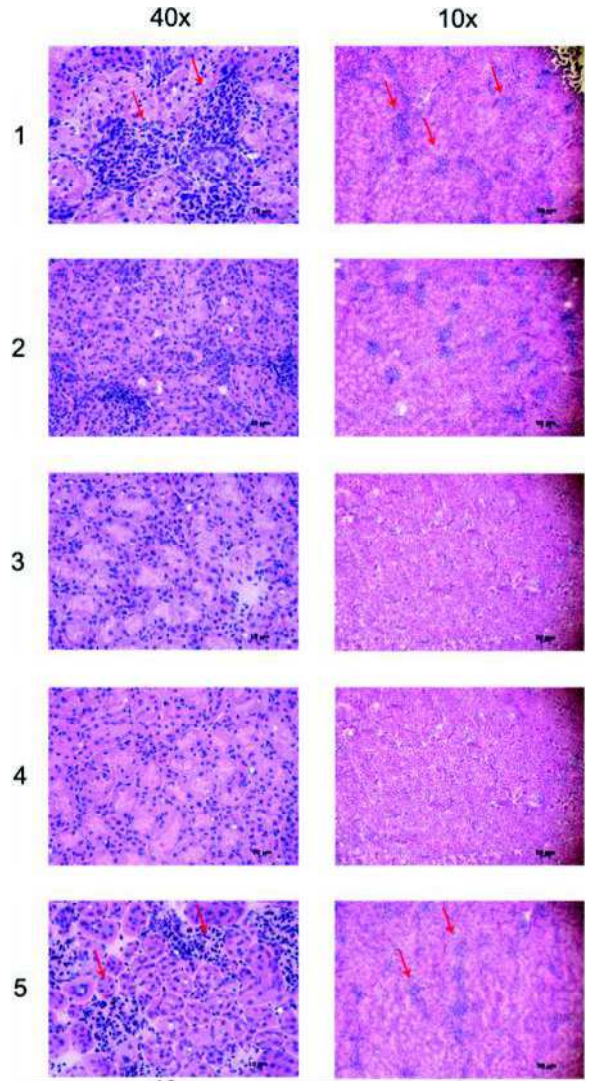

Figure 6 Haematoxylin eosin staining. Kidney sections from *Staphylococcus epidermidis* (10^8 CFU/mouse) infected mice after 3 or 9 hours (panel 1and 5); kidney sections from *Staphylococcus epidermidis* (10^8 CFU/mouse) infected mice after 3 hours and treated with MIX (RJI-C at 9 μg/mouse and TB-KK at 6 μg/mouse) for 3, 6 and 9 hours (panel 2–4).

Western Blot Analysis COX-2

Cell lysates for Western blotting were prepared by washing cells twice with ice-cold phosphate-buffered saline followed by cell lysis in 500 μl of Fastprep lysis buffer (1X protease inhibitor cocktail tablet (Roche EDTA free) resuspended in 1X PBS) on ice and lysed 20s at 6.5 intensity, 2X intervalling with 5–10 minutes on ice. Cell lysates were centrifuged for 10 min at 7800 *g* at 4°C, and the supernatants were collected and stored at −80°C until analysis. Lysate protein concentrations were measured using the Bio-Rad protein assay method, as described in the manufacturer's instructions. Cell lysate volumes corresponding to 20 μg of total protein were diluted 1:1 in Laemmli buffer (Bio-Rad) and boiled for 5 min prior to electrophoresis on a 10% acrylamide gel. The resolved proteins were electroblotted on PVDF membrane (Bio-Rad) by the Bio-Rad semidry transfer method, according to the manufacturer's instructions. Membranes were stained with PonceauRed to verify uniform protein transfer, and then blocked with blocking buffer (1X TBS, 0.1% Tween-20, 5% w/v non-fat dry milk) for 1 h at RT. Blocked membranes were incubated overnight at 4°C with COX-2 mouse monoclonal antibody (diluted 1/2000), β-actin mouse monoclonal antibody (diluted 1/10,000). Blots were washed three times in TBS-Tween before incubation with the appropriate horseradish peroxidase-conjugated secondary antibody (sheep anti-mouse IgG diluted 1/5000) for 1 h at room temperature.

After three washes with TBS-Tween, the signal was developed using standard procedure. Gel image was acquired in Fujifilm LAS-3000 Chemiluminescence system (Fujifilm Life science).

Real time PCR of pro-inflammatory

Total RNA was isolated from the tissue and the cell line after treatment by using Trizol reagent (Invitrogen, Milan, Italy). RNA was suspended in RNase-DNAse free distilled water, assessed for concentration (by measuring the absorbance at 260 nm) and purity (by ascertaining that the A260/A280 ratio was .1.9). RNA (1 μg) was then treated with 1U RNAse-free DNAse (Promega, Madison, WI). DNA contamination of RNA samples was excluded by PCR with primers specific for the gapdh gene. Reverse transcription was carried out with ImProm-II reverse transcriptase (Promega, Madison, WI) and oligo (dT). Real-time PCR was performed on 50 ng cDNA, using 1x master mix SYBRGreen (Applied Biosystem, Milan) in a StepOne Applied Biosystem instrument (Applied Biosystem, Milan). Reactions were performed in 20 μl in triplicate. The primer list is reported in Additional file 7: Table S4.

ELISA test of pro-inflammatory cytokines

In addition, the ELISA test was used to measure the anti-inflammatory activity of the MIX and its components : RJI-C 9 μg/mL e TB-KK 6 μg/mL.

Briefly, J774 cells (10^6 cells/well) were stimulated with LPS (10 μg/ml; 1 hour), treated with RJI-C 9 μg/ml or TB-KK 6 μg/ml or MIX (RJI-C 9 μg/ml + TB-KK 6 μg/ml) in presence or absence of LPS (10 μg/ml). The supernatants from these cells (100 μl/well) were transferred into the wells of a plate previously coated with mouse anti-human TNF-α (BD Pharmingen; 50 μl diluted 2 x 10-3/well) or mouse anti-human IFN-γ (Biosciences, 50 μl diluted 2 x 10-3/well) along with a second dose of anti IFN- γ or TNF- α, HRP-labelled rabbit anti mouse IgG diluted 10^{-3} (100 μl/well) and TMB peroxidase

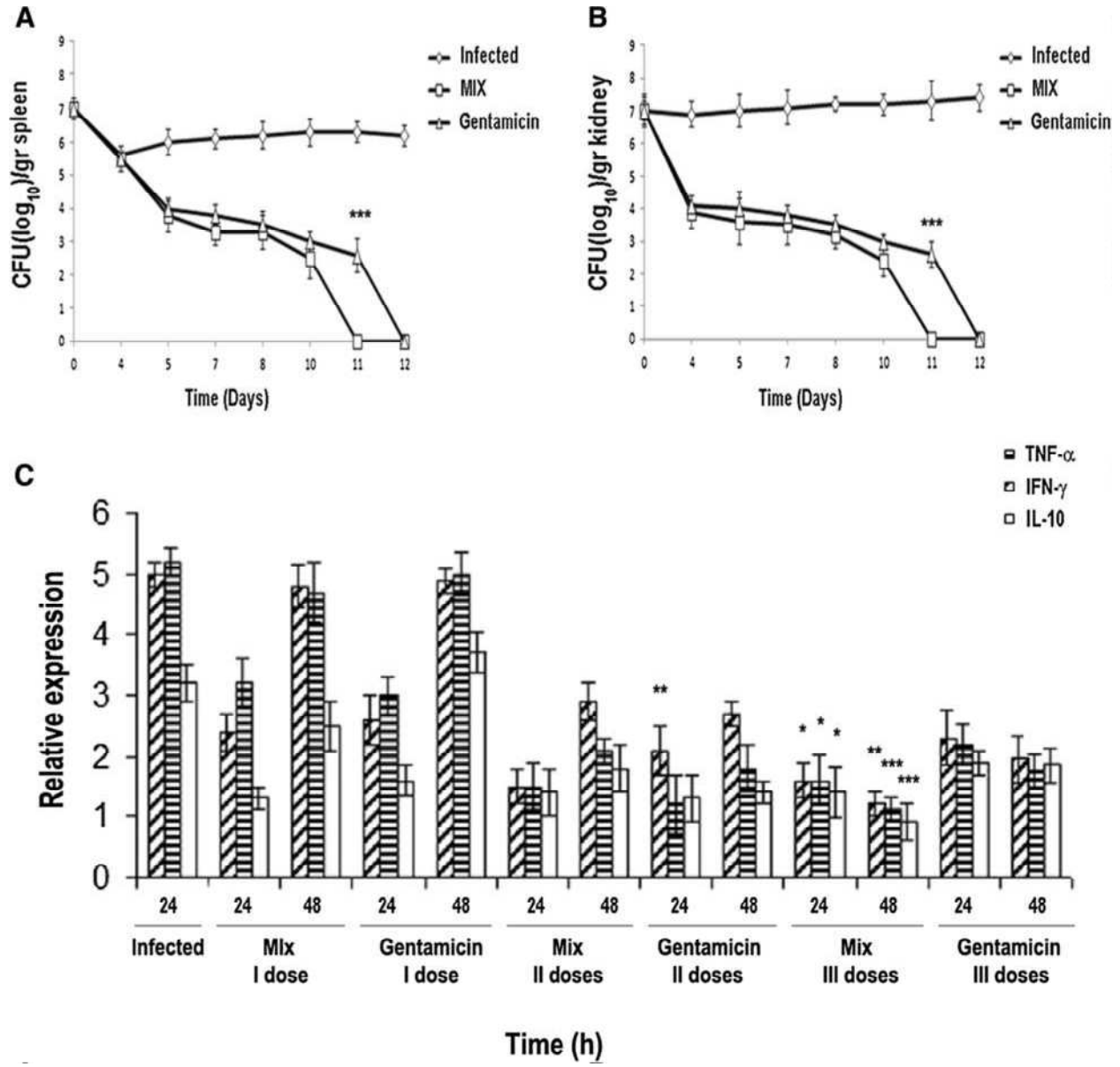

Figure 7 (A-B) Bacterial load in spleen and kidneys of animals (24/groups) infected with Staphylococcus epidermidis (107 CFU/mouse; rumble line); infected with Staphylococcus epidermidis(107 CFU/mouse) and treated with the MIX (RJI-C at 9 μg/mouse and TB-KK at 6 μg/mouse; square line) or gentamicin (5 μg/mouse; triangle line) *P <0.05, **p < 0.01; ***p < 0.001, Student's t test gentamicin vs MIX. (**C**) TNF-α, IFN-γ, IL-10 mRNA expression levels were quantified, at the indicated time points, in mice infected with *Staphylococcus epidermidis* (10^7 CFU/mouse) or infected with *Staphylococcus epidermidis* (10^7 CFU/mouse) and treated with three different doses (I,II,III) of the MIX (RJI-C at 9 μg in 100 μl/mouse and TB-KK at 6 μg in 100 μl/mouse) or gentamicin (5 μg in 100 μl/mouse). Values were normalized with GAPDH and compared to untreated control. *P <0.05, **p < 0.01; ***p < 0.001, Student's *t* test gentamicin vs MIX.

substrate (BIORAD; 100 μL/well), in the order. The optical density of each well was read at 405 nm using a microplate reader (Bio-Rad, Japan). Triplicate positive and negative controls were included in each plate [39].

Cytofluorimetric analysis

CD64 expression in total White Blood Cells was analyzed using a Flow cytometry EPICS Elite (Beckman Coulter, Fullerton, CA). Daily instrument quality control including fluorescence standardization, linearity assessment, and spectral compensation were performed to ensure identical operation from day to day. At least 10.000 events for each sample was analyzed and the data were saved for later analysis on EXPO32 software (Beckman Coulter). Data analysis was performed by using electronic gating on the basis of FSC and SSC excluded

cellular debris and nonviable cells. PE-coniugated anti-mouse CD64 expression was measured using a $\log_{10}$ scale. Briefly, 50 ul of whole blood was incubated for 10 minutes at room temperature with saturating amounts of phycoeritrine- conjugated anti-CD64 murine monoclonal antibody (Becton Dickinson) followed by red blood cell lysis with an ammonium chloride–based red cell lysis solution (Beckman Coulter, Fullerton, CA). Samples were then washed once and resuspended with phosphate-buffered saline at pH 7.4, to a volume of 1 mL.

Other methods

The kidney was fixed in 10% buffered formalin, sectioned (10 μm) and stained with hematoxylin-eosin according to standard protocols. Bacterial counts and cytokine levels were analyzed using Student's *t* test.

Additional files

Additional file 1: Table S1. Lethal concentration (LC_{50}) of Temporin B –KK, Royal jelleins-IC, MIX through their hemolytic activity on mouse erythrocytes.

Additional file 2: Figure S1. Anti-inflammatory activity. The levels of IFN- γ and TNF- α were determined by a sandwich ELISA test in J774 cells untreated; J774 cells infected with *S. epidermidis* for 1 h; J774 cells stimulated with RJI-C (9 μg/ml) for1 h; J774 cells stimulated with TB-KK. (6 μg/ml) for1 h; J774 cells stimulated with MIX (RJI-C 9 μg/ml + TB-KK 6 μg/ml) for1 h; J774 cells infected with *S. epidermidis* for 1 h and stimulated with MIX for 1 h. Results from two representative experiments are presented as mean value ± S.D. *P <0.05, **p < 0.01; ***p < 0.001, Student's *t* test *S. epidermidis* vs *S. epidermidis* + MIX.

Additional file 3: Figure S2 (A-B). Bacterial load in spleen and kidneys of *S. epidermidis* infected mice (rumble line) and subsequently treated with the MIX (square line) or gentamicin (triangle line). Data are representative of 15 animals/group. Student's *t* test gentamicin vs MIX not significant.

Additional file 4: Table S2. Acute phase proteins. Acute phase proteins from blood samples of mice infected with *Staphylococcus epidermidis* and treated with MIX or with Gentamicin.

Additional file 5: Figure S3. Time course (30, 60, 90 and 120 minutes) of bacterial load in blood of *S. epidermidis* infected mice.

Additional file 6: Table S3: Origin of S. epidermidis strains.

Additional file 7: Table S4: Sequences of the primers.

Competing interests

The authors declare that they have no competing interests.

Authors' contributions

RC designed the study and wrote the paper. AR and CA designed and synthesized the peptides. GB carried out the antibiotic resistance test. NN, RCM and MI carried out cell culture and in vivo tests. FDC, AF and FC carried out biochemical, statistical and in vivo tests. All authors read and approved the final manuscript.

Acknowledgements

This study was supported with funds from the Ricerca Finalizzata 2009 (RF-2009-1539461).

Author details

[1]Faculty of Biotechnology, University of Naples "Federico II", Naples 80134, Italy. [2]Department of Biological Sciences, University of Naples "Federico II", Naples 80134, Italy. [3]Department of Food Science, University of Naples "Federico II", Portici 80055, Italy. [4]Department of Food Inspection IZS ME, via Salute 2, Portici 80055, Italy.

Received: 30 July 2012 Accepted: 12 November 2012
Published: 17 November 2012

References

1. Uckay I, Pittet D, Vaudaux P, Sax H, Lew D, Waldvogel F: **Foreign body infections due to Staphylococcus epidermidis.** *Ann Med* 2009, **41:**109–119.
2. Neely AN, Maley MP: **Survival of enterococci and staphylococci on hospital fabrics and plastic.** *J Clin Microbiol* 2000, **38:**724–726.
3. Jamaluddin TZ, Kuwahara-Arai K, Hisata K, Terasawa M, Cui L, Baba T, Sotozono C, Kinoshita S, Ito T, Hiramatsu K: **Extreme genetic diversity of methicillin-resistant Staphylococcus epidermidis strains disseminated among healthy Japanese children.** *J Clin Microbiol* 2008, **46:**3778–3783.
4. Fitzpatrick F, Humphreys H, O'Gara JP: **The genetics of staphylococcal biofilm formation will a greater understanding of pathogenesis lead to better management of device-related infection?** *Clin Microbiol Infect* 2005, **11:**967–973.
5. Folkesson A, Haagensen JA, Zampaloni C, Sternberg C, Molin S: **Biofilm induced tolerance towards antimicrobial peptides.** *PLoS One* 2008, **3**(4):e1891. Apr 2.
6. Levy SB, Marshall B: **Antibacterial resistance worldwide: causes, challenges and responses.** *Nat Med* 2004, **10:**S122–S129.
7. Brogden NK, Brogden KA: **Will new generations of modified antimicrobial peptides improve their potential as pharmaceuticals?** *Int J Antimicrob Agents* 2011, **38**(3):217–225. Sep.
8. Capparelli R, Romanelli A, Iannaccone M, Nocerino N, Ripa R, Pensato S, Pedone C, Iannelli D: **Synergistic antibacterial and anti-inflammatory activity of temporin A and modified temporin B in vivo.** *PLoS One* 2009, **4:**e7191.
9. Romanelli A, Moggio L, Montella RC, Campiglia P, Iannaccone M, Capuano F, Pedone C, Capparelli R: **Peptides from Royal Jelly: studies on the antimicrobial activity of jelleins, jelleins analogs and synergy with temporins.** *J Pept Sci* 2011, **17:**348–352.
10. Peschel A, Sahl HG: **The co-evolution of host cationic antimicrobial peptides and microbial resistance.** *Nat Rev Microbiol* 2006, **4**(7):529–536. Jul.
11. Boman HG: **Peptide antibiotics and their role in innate immunity.** *Annu Rev Immunol* 1995, **13:**61–92.
12. Marshall SH, Arenas G: **Antimicrobial peptides: A natural alternative to chemical antibiotics and a potential for applied biotechnology.** *Electron J Biotechnol* 2003, **6:**271–284.
13. Yount NY, Bayer AS, Xiong YQ, Yeaman MR: **Advances in antimicrobial peptide immunobiology.** *Biopolymers* 2006, **84**(5):435–458.
14. Powers JP, Hancock RE: **The relationship between peptide structure and antibacterial activity.** *Peptides* 2003, **24**(11):1681–1691. Nov.
15. Hancock RE, Rozek A: **Role of membranes in the activities of antimicrobial cationic peptides.** *FEMS Microbiol Lett* 2002, **206**(2):143–149. Jan 10.
16. Ganz T: **The role of antimicrobial peptides in innate immunity.** *Integr Comp Biol* 2003, **43**(2):300–304. Apr.
17. Steinstraesser L, Kraneburg U, Jacobsen F, Al-Benna S: **Host defense peptides and their antimicrobial-immunomodulatory duality.** *Immunobiology* 2011, **216:**322–333.
18. Simmaco M, Mignogna G, Canofeni S, Miele R, Mangoni ML, Barra D: **Temporins, antimicrobial peptides from the European red frog Rana temporaria.** *Eur J Biochem* 1996, **242:**788–792.
19. Fontana R, Mendes MA, de Souza BM, Konno K, César LM, Malaspina O, Palma MS: **Jelleines: a family of antimicrobial peptides from the Royal Jelly of honeybees (Apis mellifera).** *Peptides* 2004, **25**(6):919–928. Jun.
20. Rosenfeld Y, Barra D, Simmaco M, Shai Y, Mangoni ML: **A synergism between temporins toward Gram-negative bacteria overcomes resistance imposed by the lipopolysaccharide protective layer.** *J Biol Chem* 2006, **281**(39):28565–28574.
21. Mangoni ML, Epand RF, Rosenfeld Y, Peleg A, Barra D, Epand RM, Shai Y: **Lipopolysaccharide, a key molecule involved in the synergism between temporins in inhibiting bacterial growth and in endotoxin neutralization.** *J Biol Chem* 2008, **283**(34):22907–22917.
22. Seibert K, Masferrer JL: **Role of inducible cyclooxygenase (COX-2) in inflammation.** *Receptor* 1994, **4**(1):17–23.

23. Chávez E, Castro-Sánchez L, Shibayama M, Tsutsumi V, Pérez Salazar E, Moreno MG, Muriel P: **Effects of acetyl salycilic acid and ibuprofen in chronic liver damage induced by CCl4.** *J Appl Toxicol* 2012, **32**(1):51–59. Jan.
24. Lee DC, Rizer J, Selenica ML, Reid P, Kraft C, Johnson A, Blair L, Gordon MN, Dickey CA, Morgan D: **LPS- induced inflammation exacerbates phospho-tau pathology in rTg4510 mice.** *J Neuroinflammation* 2010, **16**:7–56.
25. Capparelli R, Ventimiglia I, Palumbo D, Nicodemo D, Salvatore P, Amoroso MG, Iannaccone M: **Expression of recombinant puroindolines for the treatment of staphylococcal skin infections (acne vulgaris).** *J Biotechnol* 2007, **128**(3):606–614. Feb 20.
26. Kang M-S, Oh J-S, Lee S-W, Lim H-S, Choi N-K, Kim S-M: **Effect of Lactobacillus reuteri on the proliferation of Propionibacterium acnes and Staphylococcus epidermidis.** *J Microbiol* 2012, **50**(1):137–1426.
27. Lai Y, Gallo RL: **AMPed up immunity: how antimicrobial peptides have multiple roles in immune defense.** *Trends Immunol* 2009, **30**:131–141.
28. Lee SH, Baek DH: **Antibacterial and neutralizing effect of human β-defensins on Enterococcus faecalis and Enterococcus faecalis lipoteichoic acid.** *J Endod* 2012, **38**(3):351–356. Mar.
29. Suzuki K, Murakami T, Kuwahara-Arai K, Tamura H, Hiramatsu K, Nagaoka I: **Human anti-microbial cathelicidin peptide LL-37 suppresses the LPS-induced apoptosis of endothelial cells.** *Int Immunol* 2011, **23**(3):185–193. Mar.
30. Norhagen GE, Engstrom PE, Hammarstrom L, Smith CI, Nord CE: **Oral and intestinal microflora in individuals with different immunoglobulin deficiencies.** *Eur J Clin Microbiol Infect Dis* 1990, **9**:631–633.
31. Nieminen R, Lahti A, Jalonen U, Kankaanranta H, Moilanen E: **JNK inhibitor SP600125 reduces COX-2 expression by attenuating mRNA in activated murine J774 macrophages.** *Int Immunopharmacol* 2006, **6**:987–996.
32. Nuutila J, Hohenthal U, Laitinen I, Kotilainen P, Rajamäki A, Nikoskelainen J, Lilius EM: **Simultaneous quantitative analysis of FcgammaRI (CD64) expression on neutrophils and monocytes: a new, improved way to detect infections.** *J Immunol Methods* 2007, **328**:189–200.
33. Blaiotta G, Fusco V, Ercolini D, Pepe O, Coppola S: **Diversity of Staphylococcus spp. strains based on partial kat (catalase) gene sequences and design of a PCR-RFLP assay for identification and differentiation of coagulase positive species (S. aureus, S. delphini, S. hyicus, S. intermedius, S. pseudintermedius, and S. schleiferi subsp. coagulans).** *J Clin Microbiol* 2010, **48**:192–201.
34. NCCLS: *Performance Standards for Antimicrobial Susceptibility; Seventeenth Informational Supplement*. Wayne, PA: NCCLS; 2002. NCCLS document M100-S17.
35. Blaiotta G, Moschetti G, Simeoli E, Andolfi R, Villani F, Coppola S: **Monitoring lactic acid bacteria strains during "cacioricotta" cheese production by restriction endonucleases analysis and pulsed-field gel electrophoresis.** *J Dairy Sci* 2001, **68**:139–144.
36. Lee J, Choi Y, Woo ER, Lee DG: **Isocryptomerin, a novel membrane-active antifungal compound from Selaginella tamariscina.** *Biochem Biophys Res Commun* 2009, **379**(3):676–680. Feb 13.
37. Orsine JVC, da Costa RV, da Silva RC, de Fátima Menezes Almeida Santos M, Novaes MRCG: **The acute cytotoxicity and lethal concentration (LC50) of Agaricus sylvaticus through hemolytic activity on human erythrocyte.** *Int J Nutr Metab January* 2012, **4**(11):19–23.
38. Cardile V, Proietti L, Panico A, Lombardo L: **Nitric oxide production in fluoro-edenite treated mouse monocyte-macrophage cultures.** *Oncol Rep* 2004, **6**:1209–1215.
39. Rozalska B, Wadstrom T: **Interferon-γ, interleukin-1 and tumor necrosis factor-α synthesis during experimental murine staphylococcal infection.** *FEMS Immunol Med Microbiol* 1993, **7**:145–152.

doi:10.1186/1471-2172-13-61
Cite this article as: Capparelli *et al.*: New perspectives for natural antimicrobial peptides: application as antinflammatory drugs in a murine model. *BMC Immunology* 2012 **13**:61.